

INFORMATION TO USERS

This manuscript has been reproduced from the microfilm master. UMI films the text directly from the original or copy submitted. Thus, some thesis and dissertation copies are in typewriter face, while others may be from any type of computer printer.

The quality of this reproduction is dependent upon the quality of the copy submitted. Broken or indistinct print, colored or poor quality illustrations and photographs, print bleedthrough, substandard margins, and improper alignment can adversely affect reproduction.

In the unlikely event that the author did not send UMI a complete manuscript and there are missing pages, these will be noted. Also, if unauthorized copyright material had to be removed, a note will indicate the deletion.

Oversize materials (e.g., maps, drawings, charts) are reproduced by sectioning the original, beginning at the upper left-hand corner and continuing from left to right in equal sections with small overlaps.

Photographs included in the original manuscript have been reproduced xerographically in this copy. Higher quality 6" x 9" black and white photographic prints are available for any photographs or illustrations appearing in this copy for an additional charge. Contact UMI directly to order.

**Bell & Howell Information and Learning
300 North Zeeb Road, Ann Arbor, MI 48106-1346 USA**

UMI[®]
800-521-0600

**NATURAL CONVECTION HEAT TRANSFER IN A RECTANGULAR
ENCLOSURE
WITH SUSPENSIONS OF
MICROENCAPSULATED PHASE CHANGE MATERIALS:
A PARAMETRIC STUDY.**

by

PARTHA DATTA

DISSERTATION

Submitted to the Graduate School

of Wayne State University,

Detroit, Michigan

**in partial fulfilment of the requirements
for the degree of**

DOCTOR OF PHILOSOPHY

1999

MAJOR: MECHANICAL ENGINEERING

Approved by:

[Signature] 5th June 1999

Advisor

Date

[Signature] 6/7/99

[Signature] 6/7/99

[Signature] 6/7/99

[Signature] 6/8/99

UMI Number: 9954193

**Copyright 1999 by
Datta, Partha**

All rights reserved.

UMI[®]

UMI Microform 9954193

Copyright 2000 by Bell & Howell Information and Learning Company.

**All rights reserved. This microform edition is protected against
unauthorized copying under Title 17, United States Code.**

**Bell & Howell Information and Learning Company
300 North Zeeb Road
P.O. Box 1346
Ann Arbor, MI 48106-1346**

© COPYRIGHT BY

PARTHA DATTA

1999

All Rights Reserved

To my mother, my wife and my daughter Amisha

ACKNOWLEDGEMENTS

I would like to express my indebtedness to Dr. Subrata Sengupta for giving me the opportunity to work with him. His constant guidance and encouragement have been a source of great inspiration. His lucid explanations and understanding of the subject have made all my work with him a great experience. What little I understand of transport phenomenon, I owe to him.

My heartfelt thanks are also due to Dr. Trilochan Singh, for his patience, guidance, help and support over the years. I will always remember his fairness and helpfulness in the projects I undertook at Wayne State.

I would also like to express my gratitude to Dr. Jerry Ku, Dr. Ming Chia Lai, Dr. Robert Piccirelli and Dr. Simon Ng for their invaluable guidance and comments.

A special word of thanks to Dr. Kumar Srinivasan, for all the lengthy discussions and disagreements he had to put up with. Thanks Kumar. Thanks are also due to all my friends and colleagues, Dr. Dhananjay Joshi, Steve Kunze, Sandeep Modi and Dr. Hengchu Han. I would be remiss if I did not express my gratitude to my buddy Kathy Tamborino for always finding a way to encourage me to finish.

Most importantly, I would like to say thank you to three people, without whom, I would probably never have finished. My mother Mrs. Kum Kum Datta, for all her sacrifices, my dear wife, Somlika Datta for her love, support and the many sleepless nights she has endured, my daughter Amisha (the cause of those sleepless nights) whose arrival finally gave me the impetus to finish.

CONTENTS

	Page No.
Dedication	ii
Acknowledgements	iii
Contents	iv
List of Figures	viii
Nomenclature	xii
Chapter 1	
Introduction	1
Chapter 2	
Literature Survey	5
2.1 Free convection in enclosures with pure fluids	5
2.1.1 Experimental studies	5
2.1.2 Numerical studies	8
2.2 Heat transfer using suspensions	10
2.2.1 Non-Phase Change suspensions	11
2.2.1.1 Theoretical studies	11
2.2.1.2 Experimental studies in Laminar forced convection	15
2.2.1.3 Experimental studies in turbulent forced convection	16
2.2.2 Phase Change suspensions	17

2.2.2.1 Forced convection	17
2.2.2.2 Natural convection	20
2.3 Microencapsulation	24
Chapter 3	
Problem Statement	26
3.1 Problem statement	26
3.2 Experimental procedure	29
3.3 Parameters of interest	30
3.3.1 Fluid Parameters	30
3.3.1.1 Particle concentration	30
3.3.2 Natural convection parameter	31
3.3.2.1 The Grashof and Rayleigh numbers	31
3.3.2.2 The Prandtl number	31
3.3.3 Phase Change Parameters	32
3.3.3.1 The Stefan number	32
3.3.3.2 Sub-Cooling ratio	32
3.4 Matrix of Experiments	33
3.5 Scope of Experiments	34
3.6 Numerical Simulations	35
Chapter4	
Physical Properties	38
4.1 Particle properties	38

4.1.1 Particle density	39
4.1.2 Particle specific heat	40
4.1.3 Particle thermal conductivity	40
4.2 Slurry properties	41
4.2.1 Slurry viscosity	42
4.2.2 Slurry density	42
4.2.3 Slurry specific heat	43
4.2.4 Slurry thermal conductivity	43
4.3 Particle specifications	44
Chapter 5	
Results and Discussions	49
5.1 Experimental work	49
5.1.1 Validation runs	49
5.1.2 Enhancement runs	51
5.1.2.1 Experiments with water as the suspending fluid	52
5.1.2.1.1 Variation of Nu with Ra	52
5.1.2.1.2 Variation of Nu with Ste	60
5.1.2.2 Experiments with a silicone oil as the suspending fluid	67
5.1.2.2.1 Variation of Nu with Ra	67
5.1.2.2.2 Variation of u with Ste	77
5.1.2.3 The competing phases	86
5.1.2.4 Idealized estimate of the phase change per capsule	89
5.1.2.5 Estimating the actual phase change in the experiments	97

5.1.2.6 The effective thermal conductivity	99
5.1.2.7 Correlations	99
5.2 Numerical work	104
5.2.1 Assumptions	104
5.2.2 Validation runs	104
5.2.3 Enhancement runs	108
5.2.4 A New Metric	112
Chapter 6	
Conclusions	116
Chapter 7	
References	120
Appendix A	
Properties	128
Appendix B	
Uncertainty Analysis	133
Appendix C	
Numerical Results	135
Abstract	151
Autobiographical Statement	153

LIST OF FIGURES

	Page No.
Fig 1.1 Relative magnitude of heat transfer coefficients for various modes of convection.	3
Fig 1.2 Schematics of a generic electronic coolant system (left) and the immersion cooling system for the CRAY-2.	3
Fig 2.1 Photographs showing different flow regimes	22
Fig 2.2 Photographs showing different flow regimes	23
Fig 2.3 Photographs showing different flow regimes	23
Fig 2.4 Photographs of whole microcapsules	25
Fig 2.5 Photographs of collapsed microcapsules	25
Fig 3.1 Problem statement	26
Fig 3.2 Schematic showing the details of the experimental test section	27
Fig 3.3 Photograph showing the experimental test section	27
Fig 3.4 Close up of the test section used in the experimental work	28
Fig 3.5 Virtual test section showing the computational domain	36
Fig 4.1 Schematic of a microcapsule showing the cell wall and capsule core	38
Fig 4.2 Variation of particle wall thickness with particle diameter.	39
Fig 4.3 Shows the variation of the viscosity with the particle	

concentration	42
Fig 4.4 Myristic acid micro-capsules (100 microns). (X~50)	46
Fig 4.5 Myristic acid micro-capsules 100 microns (X~50)	46
Fig 4.6 30 micron Palmitic acid micro-capsules (X~200)	47
Fig 4.7 Palmitic acid microcapsules (30 microns) (X~200)	47
Fig 4.8 Results from the work of Datta (1992)	48
Fig 5.1 Validation curves for the apparatus.	50
Fig 5.2 Variation of the Nusselt number with the Rayleigh number.	55
Fig 5.3 Variation of the Nusselt number with the Rayleigh number	56
Fig 5.4 Variation of the Nusselt number with the Rayleigh number	57
Fig 5.5 Nu Vs Ra showing the heat transfer detriment at low concentrations (high Stefan number)	58
Fig 5.6 Nu Vs Ra showing the heat transfer detriment at low concentrations (high Stefan number)	59
Fig 5.7 Variation of the Nusselt number with the Stefan number.	61
Fig 5.8 Variation of the Nusselt number with the Stefan number	62
Fig 5.9 Variation of the Nusselt number with the Stefan number	63
Fig 5.10 Variation of the Nusselt number with the Stefan number	64
Fig 5.11 Variation of the Nusselt number with the Stefan number	65
Fig 5.12 Variation of the Nusselt number with the Stefan number	66
Fig 5.13 Variation of the Nusselt number with the Rayleigh number for the silicone oil slurry.	70
Fig 5.14 Variation of Nu Vs Ra showing heat transfer enhancement	71

Fig 5.15 Variation of Nu Vs Ra for high concentration case	72
Fig 5.17 Variation of the Nusslet number with Rayleigh number	73
Fig 5.18 Variation of Nu Vs Ra for lower SCR and high concentrations	74
Fig 5.19 Nu Vs Ra plot for concentrations around 2%	75
Fig 5.20 Variation of the Nusslet number with Rayleigh number at a SCR of 0.69	76
Fig 5.21 Variation of Nu with concentration (Stefan number)	78
Fig 5.22 Variation of Nu with concentration (Stefan number)	79
Fig 5.23 Variation of Nu with concentration (Stefan number)	80
Fig 5.24 Variation of Nu with concentration (Stefan number)	81
Fig 5.25 Variation of Nu with concentration (Stefan number)	82
Fig 5.26 Variation of Nu with concentration (Stefan number)	83
Fig 5.27 Variation of Nu with concentration (Stefan number)	84
Fig 5.28 Variation of Nu with concentration (Stefan number)	85
Fig 5.29 Material property contours showing the property variation through the capsule and the fluid	87
Fig 5.30 Contour plots showing the heat flux (w/m²) entering the capsules	87
Fig 5.31 Schematic of a microcapsule melting (Bejan 1995)	89
Fig 5.32 Schematic of the test section showing the melt and freeze zones	92
Fig 5.33 Free body diagram showing the forces acting on the particle	93
Fig 5.34 Plot showing rise of the capsule as PCM core melts (100μm Myristic acid capsule in Siloxane)	95
Fig 5.35 Plot showing rise of the capsule as PCM core melts	

(30μm Palmitic acid capsule in water)	96
Fig 5.36 Curve fit for the data obtained using the silicone oil slurry	100
Fig 5.37 Curve fit for the data obtained using the silicone oil slurry (SCR ~ 0.95)	101
Fig 5.38 Curve fit for the data obtained using the water slurry (SCR ~ 0.45)	102
Fig 5.39 Curve fit for the data obtained using the water slurry (SCR ~ 0.9)	103
Fig 5.40 Steady state numerical results compared to those of previous investigators	107
Fig 5.41 Plot showing the variation of C_p over the melting temperature for different concentrations	110
Fig 5.42 Nu Vs Ra results for enhancement runs with the PCM effect modeled as a C_p pulse	111

NOMENCLATURE

C_p	:	Specific heat
D	:	Enclosure depth
d_p	:	Particle diameter
g	:	gravitational constant
t	:	time
L	:	Length of the enclosure
D	:	Cavity depth
K	:	Thermal conductivity
L_f	:	Latent heat of fusion
N	:	Number of microcapsules per unit volume
q	:	heat flux
r	:	Interface location in the particle during melting/freezing
r_p	:	Particle radius
S	:	Source term due to PCM melting
T	:	Dimensional temperature
u, v	:	x & y-direction velocity components
W	:	Z-direction velocity component
SCR	:	Sub-cooling ratio
Greek Characters		
α	:	Thermal diffusivity

β	:	Coefficient of thermal expansion
μ	:	Dynamic viscosity
ν	:	Kinematic viscosity

Subscripts, superscripts

b	:	bulk
c	:	cold wall
f	:	fluid
l	:	liquid (PCM)
m	:	melting
p	:	particle
s	:	solid (PCM)
scr	:	sub-cooling ratio
ΔT	:	based on the temperature gradient

Wall, Shell : Capsule wall

m	:	melting
c	:	cold wall
h	:	hot wall
p,part	:	particle
f	:	fluid
b	:	bulk
eff	:	effective
*	:	Indicates non-dimensional quantity

CHAPTER

1

INTRODUCTION

The last century has witnessed an unprecedented surge in the fields of electricity and electronics. In depth understanding of solid state physics at the atomic level, has greatly helped scientists break new frontiers in electronics. With the rapid advances in miniaturization and VLSI technologies and the dramatic reduction in the size of electronic circuitry, module level heat fluxes have increased manifold.

In addition to this, applications wherein thermal energy can be stored, have also been gaining ground. There is a need for, working fluids which have advanced heat transfer properties and high thermal capacitances. Such fluids would reduce operating temperatures, keep from sudden transient temperature surges and store heat for later utilization. The use of these techniques encompasses fields such as, solar energy storage, waste heat utilization (Kasza and Chen (1984) and residential heating and cooling systems (Colvin and Mulligan (1989)).

While it is natural to try and find single phase fluids with better heat transfer properties, this approach would be unsuccessful in the case of electronic coolants. Electrical and thermal properties are analogous and closely related at the atomic level. As such, almost all substances be they liquid or solid, have poor thermal properties if they have poor electrical properties. Since it is imperative that an electronic coolant have good

insulating properties (electrically), it is often observed that they also have extremely poor thermal properties (good insulators). It is very difficult if not altogether impossible to obtain a single phase fluid, which while being a good electrical insulator, would possess good thermal conductive properties.

One solution to the problem therefore, is the use of thermal-property-enhancing additives, which retain the fluid's electrical inertness. In the recent past, a new technique involving the use of phase change materials has been studied (Kasza and Chen (1984)). In this technique a phase change material (PCM) is encapsulated in a resinous shell, thus forming a phase change capsule. These capsules are then suspended in a suitable heat transfer fluid. The resulting slurry is termed as a "phase change suspension or slurry". They can be used as the working fluid in devices operating in both the natural and forced convection devices (Datta (1992), Goel (1992)).

Passive heat exchangers are inherently more reliable and are easy to use because, they work on naturally occurring phenomenon and do not require the use of any kind of prime mover to impart energy to the working fluid. The heat removal rate of a passive heat exchanger is typically an order of magnitude lower than the heat removal rate of an active one. Therefore if the heat removal rate can be raised by an order of magnitude, passive heat exchangers could replace active ones thereby offering a great reduction in weight and cost.

The use of efficient passive heat removal techniques for microelectronic cooling has been receiving a fair amount of attention in the industry in the past decade. 3M manufactures flexible bags filled with Fluorinert (FC-77), an electrically inert liquid.

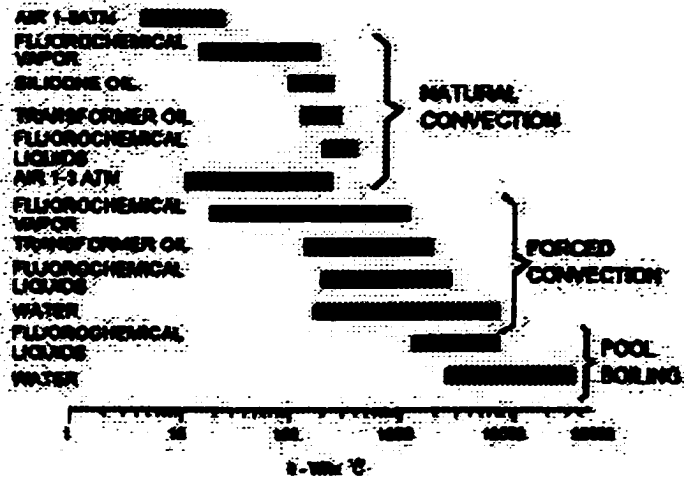


Fig 1.1 Relative magnitude of heat transfer coefficients for various modes of convection.

these bags are inserted between the circuitry, they act as heat sinks presenting no danger to the circuitry. Modern day electronic circuits have such large heat fluxes, that some situations even necessitate immersion cooling, wherein, a whole electronic circuit is immersed into a bath of a suitable coolant (Fig 1.2).

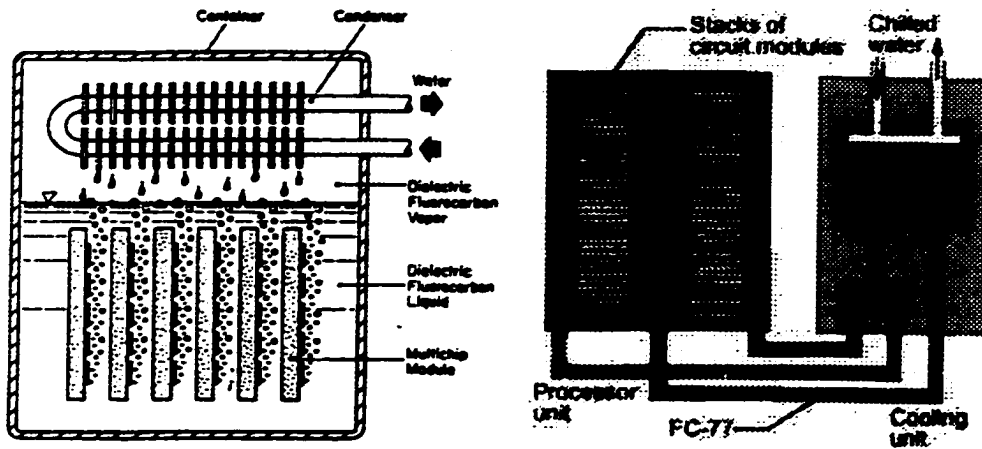


Fig 1.2 Schematics of a generic electronic coolant system (left) and the immersion cooling system for the CRAY-2.

The use of phase change slurries as potential 'enhanced heat transfer fluids' and also thermal energy storing fluids has been studied in the past (Kasza and Chen (1984), Colvin and Mulligan (1989), Datta (1992), Goel (1992), Harhira (1992)). However, no study encompasses a definitive range of the parameters involved and most studies have been preliminary in nature (atleast quantitatively). This is especially true in the field of natural convection heat transfer using phase change suspensions.

Natural convection or buoyancy driven flows, and in particular flows inside cavities and enclosures have been a subject of great scientific interest for many decades (Bejan (1995)). These flows are complex and are often encountered in many engineering applications like microelectronic cooling, flame stabilization with baffles, ventilation flows in rooms, crystal growth, etc.,.

The present work will focus on the heat transfer enhancing capability of phase change slurries in natural convection in enclosures and will attempt to quantify the result both experimentally and numerically over wide parameter ranges ($\Delta Ra \sim 10^4$) hitherto not investigated.

No definitive study investigating the enhancement of natural convection heat transfer using PCM slurries has been conducted before this. This study will experimentally quantify heat transfer using phase change slurries. Correlations for the variation of Nu with Ra and Ste are to be developed. Thermo-physical parameters which influence the performance of a PCM slurry along with recommendations for designing a heat transfer enhancing PCM slurry will be presented. Numerical work to simulate this phenomenon has also been initiated in this study.

CHAPTER

2

LITERATURE SURVEY

A considerable amount of experimental and numerical work has been completed both in free and forced convection heat transfer, using single phase fluids and suspensions. However, there exists a relative dearth of literature on the subject of heat transfer using microencapsulated phase change suspensions; especially in the realm of free convection.

As such, literature has been surveyed in forced and natural convection heat transfer using single and two phase fluids with and without the use of PCMs.

2.1 Free convection in enclosures with pure fluids

2.1.1 Experimental studies

Dropkin and Somerscales (1965) have investigated the heat transfer in fluids confined in rectangular and circular containers. Their experiments spanned a wide parameter range ($5 \times 10^4 < Ra < 7.17 \times 10^8$ and $0.02 < Pr < 11,560$), they also investigated the effect of inclining the enclosure and suggested the following heat transfer

relation: 'c' is a constant which varies from 0.069 in the horizontal case, to 0.049 for the vertical case.

$$N = c(Ra)^{0.333} (Pr)^{0.074}$$

Garon and Goldstein (197) also conducted similar investigations in which they have measured the vertical component of fluid velocity and the heat transfer for a horizontal layer of water heated from below. Their results suggest the simple power law relationship shown below:

$$Nu = 0.13(Ra)^{0.293}$$

Their study also points towards the possibility of flow transition at relatively high Rayleigh numbers. Chu and Goldstein (1973), Tanaka and Miyata (1980) and many other investigators have also studied heat transfer in enclosures. Some of the most important results are listed in Table 2.1 along with the correlations which resulted from the investigations and the Rayleigh number ranges that they are valid in.

INVESTIGATORS	RESULTS	COMMENTS
Dropkin and Somerscales (1965)	$Nu = cRa^{0.33} Pr^{0.074}$	They studied heat transfer in cavities at high Ra and Pr ranges and the effect of the inclination of the enclosure.
Garon and Goldstein (1973)	$Nu = 0.13 Ra^{0.293}$	Heat Transfer and the vertical component of the velocity. Water layers heated from below.

Heslot et al., (1987)	$Nu = 1 + (0.096 Ra^{0.33})$	Low temp Helium ($Ra = 10^{11}$).
Goldstein et al., (1989)	$Sh = 0.065 Ra^{0.33}$	Heat/Mass Transfer analogy. High Pr variation of Nu - Ra.
Hwang et al., (1988)	$Nu = a \text{Log}(Ra (\cos + \sin)) + b$	High Ra and aspect ratio intensify fluid motion, distort temperature distribution.
Globe and Dropkin (1959)	$Nu = 0.051 Ra^{0.33}$	$2 \times 10^5 < Ra < 3 \times 10^7$ - Hg
Rosby (1969)	$Nu = 0.147 Ra^{0.247}$	$2 \times 10^4 < Ra < 5 \times 10^5$ - Hg
Somerscales and Gazda (1968)	$Nu = 0.196 Ra^{0.283}$	$3 \times 10^7 < Ra < 3 \times 10^8$ - Si oils
Goldstein and Chu (1969)	$Nu = 0.123 Ra^{0.294}$	$6 \times 10^5 < Ra < 1 \times 10^8$ - Air, He

Table 2.1

In similar experiments Hwang et al., have experimentally studied the heat transfer in inclined rectangular cells. They found that a large Rayleigh number coupled with a large aspect ratio tended to intensify the fluid motion and distort the temperature distribution. Heslot et al., 1987 used low temperature gaseous Helium to study natural convection heat transfer at very high Rayleigh number range of the order of 10^{11} . Their study indicates a power law exponent of less than 0.333 even at these high Rayleigh number ranges. The correlations developed by them are also listed in Table 2.1

In 1989, Goldstein et al., reviewed the available literature on natural convection heat transfer in horizontal layers heated from below, in order to determine the asymptotic variation of Nu with Ra. Their study, which was carried out using a heat and mass transfer

analogy, indicates "a high Prandtl number variation of the Nusselt number with the Raleigh number. The correlation they developed is :

$$Sh = 0.065(Ra)^{0.333}$$

Quite clearly, almost all studies conducted thus far indicate a power law exponent of 1/3 or less.

2.1.2 Numerical studies :

Ostrach (1968,78,82,etc.,) has been in the forefront of analytical modeling and scaling for the past two decades. His investigations are numerous and span a wide range of complex problems in thermal convection. His articles Ostrach (1988,83) provide an indepth overview of the research done in bouyancy driven and thermocapillary convection in various configurations. He has also analysed the correct scaling procedures and lists them in these articles.

de Vahl and Jones (1983) have conducted a comparative study on the existing numerical simulations of bouyancy driven thermal convection in cavities. They find that, of all the literature cited the three most accurate results were provided by, a finite element method, a Galerkin method and a finite difference method. As expected, they noticed that higher order methods and those having finer grids tended to be more accurate than the others.

In a related study, de Vahl (1983) compiled a finite difference code and obtained benchmarking numerical solutions for natural convection in a rectangular cavity with air as the working fluid. He used the FTCS (Forward in Time, Centered in Space) scheme for discretizing his equations, coupled with the method of the 'false transient' in which extra terms are included into the equations. As steady state is reached, these terms vanish and the modified equations collapse to the original form. His results indicate that the best representation of the overall heat transport in the cavity is obtained by using $Nu_{1/2}$ which he describes as the average Nusselt number in the vertical midplane of the cavity.

In a recent study Paolucci (1990) performed direct simulation of two dimensional natural convection in a cavity well into the turbulent regime ($Ra \sim 10^{10}$). In his problem setup, the temperature gradient was taken to be orthogonal to the gravity vector (differentially heated side walls). The simulation was allowed to proceed from transience to statistical steady state. His results show a good agreement of the mean quantities with experimental data. Using snapshots from the simulation process, he illustrates the production of turbulence from the initial instability. Some prominent large scale structures of turbulence are seen to persist even during steady state.

Refai (1990) conducted a numerical study of natural convection heat transfer from discrete heat sources in a vertical enclosure. He used the Marker and Cell method (MAC) to obtain the two-dimensional solution for laminar natural convection with discrete heat sources (both isoflux and isothermal), attached to one of the vertical walls. Results have been reported for the following parameter ranges :

$$0 \leq Ra \leq 10^6 ; Pr = 0.72 ; 0.25 \leq \varepsilon \leq 1$$

The numerical results were verified with experimental data and showed good agreement.

Leonard (1983) developed a third order accurate, finite difference method to simulate scalar transport in steady two-dimensional flow. They studied "the laminar driven cavity" problem and achieved high convective stability without sacrificing accuracy, by using an upstream bias in the convective terms. Upson et.al., (1983) used the finite element method to simulate confined Rayleigh Benard convection in three dimensions. A plethora of other investigators (Ostrach (1981), Patankar (1980), Poujol et.al., (1993), Fusegi et.al., (1993), Balaji and Venkatesan (1993)) have all conducted numerical experiments in natural convection in enclosures of various geometries in widely varying Rayleigh and Prandtl number ranges. Most investigators have worked on cavities with a horizontal driving temperature gradient. The effects of conduction and radiation on the convective heat flux have been studied in great detail. The bibliography listed at the end gives a detailed list of many investigations completed in natural convection heat transfer in cavities.

2.2 Heat transfer using suspensions

This section can be broadly divided into non-phase change and phase change suspensions. They are considered separately below.

2.2.1 Non-Phase change suspensions

2.2.1.1 Theoretical studies :

The pioneering investigations into the effective thermal properties of slurries dates back to the works of Maxwell (1873). He obtained relations to predict the thermal conductivity of dilute, stationary dispersions of solid spheres. The relation recommended was:

$$K_b = K_f (1 + 3x\phi + O(\phi^2))$$

where x is defined as the ratio:

$$x = \frac{(K_p - K_f)}{(K_p + 2K_f)}$$

and ϕ as the volumetric concentration of the dispersed phase.

Jeffery (1973,74) then improved on Maxwell's, model by introducing a second order concentration correction term. The expression he developed can be reduced to:

$$K_b = K_f \left(1 + 3x\phi + \phi^2 \left(3x^2 + \frac{3x^3}{4} + \frac{9x^3(\alpha + 2)}{16(2\alpha + 3)} \right) \right)$$

where α has been defined as the ratio of the thermal conductivity of the particulate phase to that of the fluid phase and x is the same as in Maxwell's equation. The above equation can also be written as:

$$\frac{K_b}{K_f} = \frac{2 + \frac{K_p}{K_f} + 2c \left(\frac{K_p}{K_f} - 1 \right)}{2 + \frac{K_p}{K_f} - c \left(\frac{K_p}{K_f} - 1 \right)}$$

The effective thermal conductivity for suspensions, is in fact a function of the local shear rate. As a consequence, the effective conductivity of a suspension could increase inspite of the suspending and the suspended phases having identical physical properties.

Keller (1971) conducted a qualitative study to prove the dependence of the effective thermal conductivity on the bulk shear rate. Using an approach conceptually analogous to the mixing length theory of turbulent diffusion, he reasoned that the dispersed phase could be expected to logically enhance the conduction or diffusion mode of transport for heat or mass.

Rocha and Acrivos (1973) have conducted a theoretical study to investigate the stationary thermal conductivity of dilute suspensions. In a similar study, Thovert and Acrivos (1988), have studied the effective thermal conductivity of dilute-polydispersed-random-but statistically homogeneous suspension of spheres to the second order. They used the Jefferies model and another approximate method proposed by Chang and Acrivos (1986). The overall bounds for the effective thermal conductivity has been computed for well mixed suspensions.

In a later investigation Goldshmit and Acrivos (1989), investigated the effective conductivity of a dilute suspension at moderate Peclet number. Their results emphasize the

increasing importance of the convective fluxes when the two phases have similar thermal properties. They also observe that the enhancement in heat transfer increases with increasing concentration of the dispersed phase.

Leal (1973) studied flow contribution to the effective thermal conductivity in dilute suspensions of neutrally buoyant spherical droplets in the low particle Peclet number regime. Taking into consideration the conductive and flow contributions of the dispersed phase, the effective thermal conductivity can be given by :

$$K_e = K_f \left[1 + \phi \left\{ 3x + (1.176x^2 + y(0.12y - 0.028x))Pe^{\frac{3}{2}} + 9(Pe^2) \right\} \right]$$

Where

$$y = \frac{2\mu_f + 5\mu_p}{\mu_f + \mu_p} \quad \& \quad Pe = \frac{\alpha^2 \chi \rho C_p}{K_f}$$

Chen and Sohn (1979,81) have conducted thorough experimental and analytical investigations on the effective thermal conductivity of disperse two phase mixtures in shear flows. They considered the microconvective effects of shear, which make the particles rotate and reinforce the idea that the effective thermal conductivity is a strong function of the shear and not a material property alone. They observed that thermal conductivity enhancement factor is a function of the 1/3 power of the Peclet number in the range $10 < Pe < 300$.

In yet another (predominantly experimental) study, Sohn and Chen (1984) predict Thermal conductivity enhancements as high as 15 times for flows in circular tubes of 1 cm diameter having velocities of 10cm/s. This study indicates that, for Peclet numbers above 300 upto 2500, the enhancement factor is a function of the 1/2 power of the Peclet number.

Nir and Acrivos (1976) derived expressions for the effective thermal conductivity of randomly dispersed suspensions undergoing shear in the limit $Pe \rightarrow \infty$. They proved that in the limiting case the presence of high shear can significantly affect the first order contribution of the particle concentration $O(\phi)$ in the expression for effective thermal conductivity K , which now becomes independent of the thermal conductivity of the dispersed phase.

Soo (1990) points out that most studies based on the conductivity of the mixture, neglect non equilibrium between the two phases. He observes that the studies based on the non-equilibrium multiphase transport by diffusion of energy carrying particles are applicable to both dilute and dense suspensions wherever the effects of particle collision are important. General expressions for multiphase heat fluxes (over a wide range of concentrations) he points out are still insufficient if at all existent. His study includes general modeling of the transport phenomenon including the effect of particle to particle interactions due to binary collisions and random motion of the particles.

Rhazi (1993) studied the effect of neutrally buoyant solid particles on the stability of a fluid layer heated from below. After obtaining an exact solution to the eigenvalue

problem, for both the perfectly conducting and perfectly insulating cases, he showed that the critical Rayleigh and wave numbers increase due to the presence of particles.

2.2.1.2 Experimental studies in Laminar Forced convection :

One of the pioneering works investigating heat transfer enhancement in suspensions was conducted by Ahuja (1975a,b) He observed that the thermal conductivity increased with an increase in the Reynolds number. Ahuja took care to ensure Newtonian behavior by making sure that the concentration of the dispersed phase never exceeded 25%. His results show an increase in thermal conductivity by a factor of 140% when he used a neutrally buoyant suspension of Polystyrene spheres in water.

Chung and Leal (1980) studied the effective thermal conductivity of a sheared suspension of rigid spheres to verify the theoretical correlation of Leal (1973) in the limit of low particle Peclet number. They suggest the following correlation for the thermal conductivity enhancement.

$$R = 3Pe^{\frac{1}{2}}$$

$$\text{where } R = \frac{K_{eff} - K_{bulk}}{\phi K_{fluid}}$$

Chen and Sohn (1979,81) carried out tests in a low velocity couette flow apparatus with neutrally buoyant particles at very low rayleigh numbers. They observed that the thermal conductivity increased by a factor of 5 and that the particle concentration

affected the conductivity. As mentioned before, their most recent correlation ($300 < Pe < 2000$) was that the enhancement in conductivity was proportional to the root of the particle Peclet number.

Charunyakorn (1990), used the results Chung and Leal (1980), Chen and Sohn (1979) and Nir and Acrivos (1976) to obtain a general expression correlating the thermal conductivity enhancement to the particle Peclet number. His analysis indicates that the enhancement falls into three main regimes low, high or moderate. In a private communication, the present author reexamined the data and found that the thermal conductivity of suspensions can be better modeled as falling into four broad regimes - low, low-medium, high-medium and high - the general correlation is for the enhancement R can be given as follows:

$$R = \frac{K_s - K_b}{\phi K_b} = BPe^m + Q$$

where B , m and Q are all constants which depend on the Peclet number range.

2.2.1.3 Experimental studies in turbulent forced convection

Investigations by Salamone and Newmann (1955) using slurries of copper carbon silica and chalk. showed that the effective thermal conductivity increased at low Reynolds numbers and that the specific heat of the dispersed phase had a significant effect on the effective thermal conductivity. Kung and Harriot (1987) studied the heat transfer in

aqueous suspensions of polystyrene beads and sand. They also observed a significant heat transfer enhancement and the heat transfer coefficient increased by as much as 50%.

Other investigators who have studied turbulent forced convection in non-phase change suspensions are Hishida et.al., (1992) studied the effects of soft magnetic particles on local heat transfer coefficients, Ishima et.al., (1993) who studied the effect of particle residence time on particle dispersion in a plane mixing layer.

2.2.2 Phase Change Suspensions

2.2.2.1 Forced Convection

Kasza and Chen (1982,85,87) were amongst the very first people to consider the possibility of using phase change materials for applications related to heat transfer augmentation and thermal storage at the Argonne National Laboratory. Their tests show an order of magnitude increase in the heat transfer even without the use of phase change materials. The use of phase change materials further increased the enhancement in heat transfer. MacMohan Harlowe and Mangold (1982), have done similar work at the Southwest Research Institute.

Colvin and Mulligan (1975,85,87,88) have done considerable work using phase change materials and microencapsulated phase change materials for enhanced heat transport and thermal storage. Their studies encompass a large variety of applications ranging from, use of phase change slurries for residential climate control, to energy

storage in spacecraft systems and space suit liner thermal control. A large body of their work is inaccessible and hard to come by because it is in the form of confidential reports.

Mulligan et al have evaluated the winter time operation of a heat-pump/storage device on its ability to supply NTP heating with minimum power requirement, for residential use in North Carolina. Their device consisted of a phase change unit wherein they packed a PCM in a honeycomb fitted in a rectangular box. They observe that the heat pump storage unit had a reduced COP compared to the heat pump unit acting alone. They conclude that inspite of the theoretical potential which might be expected of a phase change unit, the integrated systems are actually less efficient. They further observe that great care should be taken in adding heat storage devices to standard equipment. Such efforts are expected to damage the equipment. The potential for energy savings exist, they add, only in very special circumstances.

Charunyakorn (1990) numerically studied forced convection heat transfer -flow between flat plates and flow in a circular tube- using microencapsulated phase change slurries. He also studied the effect of the concentration on the heat transfer. His analysis includes a thorough derivation of the governing equations, in which he has included a source term in the energy equation to account for the heat released during the change of phase. His results indicate that there is a 2-4 times increase in the overall heat transfer compared to a single phase fluid. The local Nusselt number increased in the upstream direction and was maximum at the entrance where, the temperature was assumed to be the melting point of the PCM.

Goel (1992), has investigated the effect of microencapsulated phase change materials in laminar forced convection heat transfer in circular tubes. The experimental method was fraught with difficulty; he observed that because of structural unsoundness of the capsules, the high shear stress in the flow and the constant thermal cycling, a large percentage of the particles broke. In spite of this, the results showed a significant increase in the heat transfer (Nu). Even with the increased bulk viscosity, his results predict a substantial decrease in the pumping power.

Choi (1993) has completed an extensive study on the use of phase change slurries in large scale heat exchangers (district cooling). His experiments suggest that since the science of microencapsulation is in its stages of infancy, the capsules are prone to break when used in forced convection systems. In his study Choi realized that using microencapsulated phase change materials in large volumes was not feasible for large scale operation and worked around the problem by using an emulsifier to produce phase change slurries with particles smaller than 0.1 mm. The carrier fluid in his case was water. He found that the local convective heat transfer coefficient and the effective thermal capacity of the PCM slurry varied significantly along the heating test section. The local convective heat transfer coefficient increased in the region where the bulk mean temperature was below the melting point of the PCM, decreased sharply where the phase change occurred and increased again further downstream.

2.2.2.2 Natural Convection

Natural convection heat transfer using microencapsulated phase change slurries is a relatively recent topic of interest and very little work has been completed. Katz (1968) was the first investigator to investigate the potential of using encapsulated phase change materials in passive heat exchangers. He conducted an order of magnitude study on horizontal layers heated from below to estimate the expected increase in heat transfer. His apparatus consisted of a cubical enclosure with two conducting side walls, two insulated side walls and copper plates making the upper isothermal and lower constant heat flux boundaries.

Katz's results indicate that he observed fivefold increases in heat transfer in the laminar range and over an order of magnitude increase in the turbulent range. He observed that there existed five distinct regimes of heat transfer.

- (i) At low heat input, the primary mode of transport was conduction and the particles stuck to the hot wall.
- (ii) On increasing the heat input, Katz observed that, as the wax in the particles began to melt, some of the cells began to rise into the body of the fluid and participate in the heat transfer.
- (iii) On continued increases in the heat flux, a point was reached when all particles actively participated in the transport. This would be the ideal regime for operation.

(iv) Further increases in the heat flux what can be termed as the "runaway" condition.

The heat loss at the cold wall no longer matched the heat input at the hot wall.

The particles began to migrate to the cold wall.

(v) For heat fluxes above the "runaway" heat flux, the cells just stuck to the hot wall and no longer participated in the heat transfer.

In his experiments he used Katz used low concentrations of relatively large disc shaped cells, lack of technical expertise in microencapsulation at the time made it impossible for him to perform definitive work.

Harhira (1992,93) was the only numerical work in natural convection heat transfer using microencapsulated phase change suspensions that has been uncovered thus far. He investigated the heat transfer in the boundary layer formed on a heated vertical plate placed in a suspension of microencapsulated phase change spheres in water. He has developed a code based on an implicit scheme which simulates the transport phenomenon. His results indicate a heat transfer augmentation (in theory) by factors as high as 17. Increases in the concentration also resulted in substantial increases in the heat transfer.

Datta (1992), the present author, conducted an order of magnitude parametric study on natural convection heat transfer using much smaller "micro"-capsules of phase change material. The study was experimental and the test section was based on the one used in Katz's analysis. A number of exciting physical occurrences in the transport phenomenon became clear.

It was observed that the best enhancements in heat transfer could be expected for concentrations as low as 0.5 to 1% in volume. As the concentration was increased, particle-particle interactions increased and clumps of particles formed. In spite of immense care in matching the density of the microcapsules to the suspending fluid, clumping increased the sedimentation rates by almost two orders of magnitude and fewer particles could participate in the convection.

For concentrations of 10 and 20%, the sedimentation rate became so high that a layer of particles formed on the hot plate at all times. This reduced the depth wherein convection was the mode of transport and hence resulted in an effective decrease in the Rayleigh number (a strong function of the depth). The results indicated that there were three important flow regimes which were called 'A', 'B' and 'C' going from the best heat transfer regime (A) to the worst (C). However, due to experimental constraints, the study

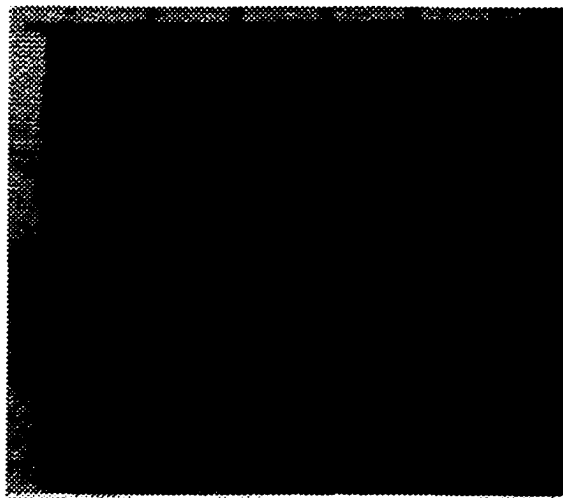


Fig 2.1 Class A regime (1% concentration)

had to be confined to a rather low Rayleigh number range (about 1 order of magnitude) and was thus not quantitatively definitive. The class A flow regime is the ideal flow regime where all particles seem to participate in the transport.

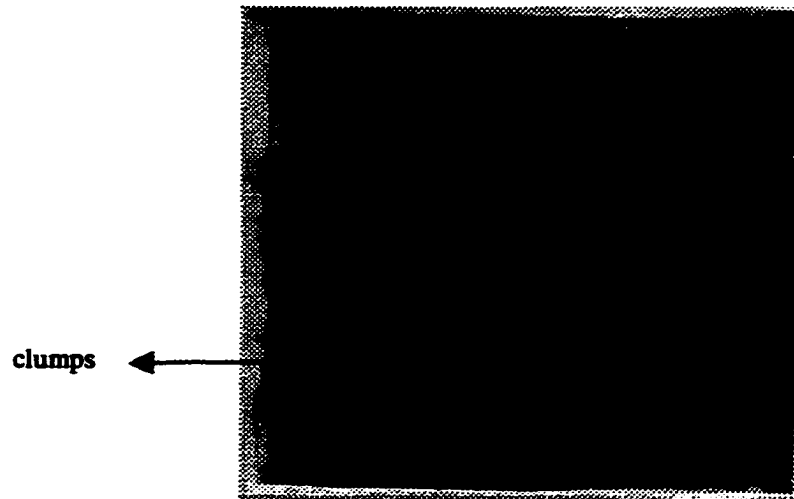


Fig 2.2 Class B regime (5% concentration)

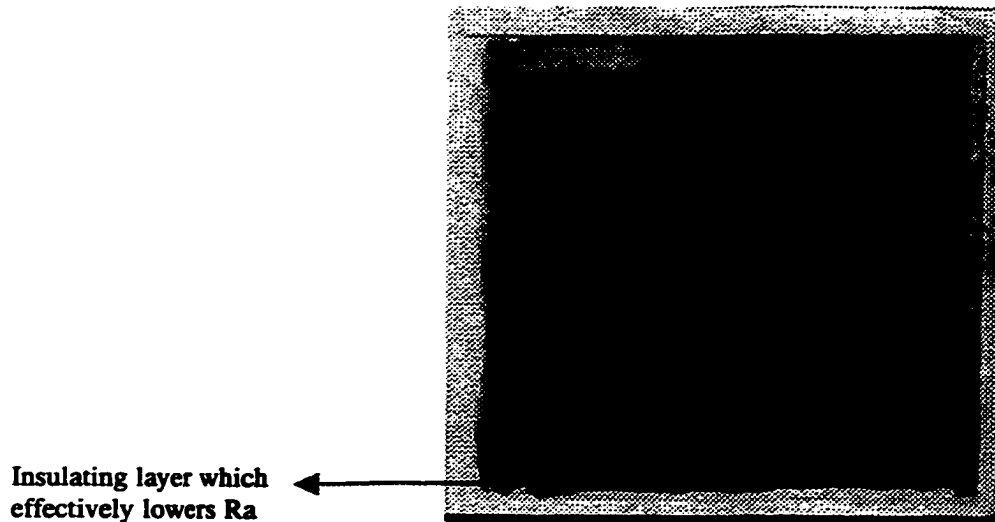


Fig 2.3 Class C regime (20% concentration)

Figs 2.1 – 2.3 Photographs showing the different flow regimes

2.3 Microencapsulation

Microencapsulation is commonly used in the food, drug and fertilizer industries for various purposes. Microcapsules are useful and important in many facets of engineering technology and their salient uses are listed below.

- § Toxic additives can be segregated from the carrier fluid.**
- § Microcapsules can be manufactured to specifications for a timed triggered release of the encapsulated material. Microencapsulation has been used for the triggered release of chemicals in medicinal drugs**
- § Sticky and gluey substances can be converted to free flowing powders.**
- § Liquid - Solid blending can be attained.**
- § Microcapsules are regularly used in food technology to mask taste and for the triggered release of preservatives.**
- § Microcapsules of phase change materials can be added to a suspending liquid, forming a two phase fluid which has enhanced heat transfer properties.**

Each application uses a different set of microcapsules and there exist innumerable methods of microencapsulation (Sparks (1981), Gutcho (1976)). Coacervation is one of the commonly used techniques and the microcapsules used in the present study have been formed using this technique.

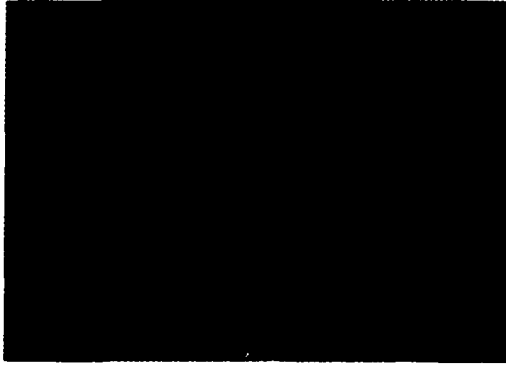


Fig 2.4 Photograph of whole microcapsules

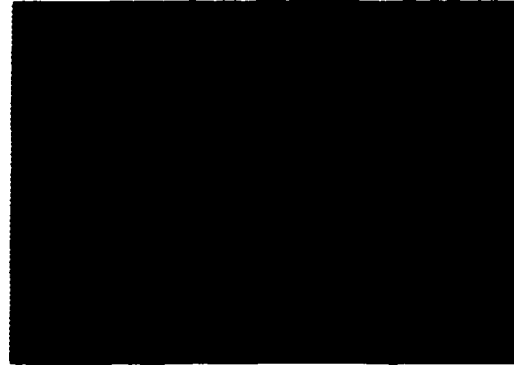


Fig 2.5 Photograph of collapsed microcapsules

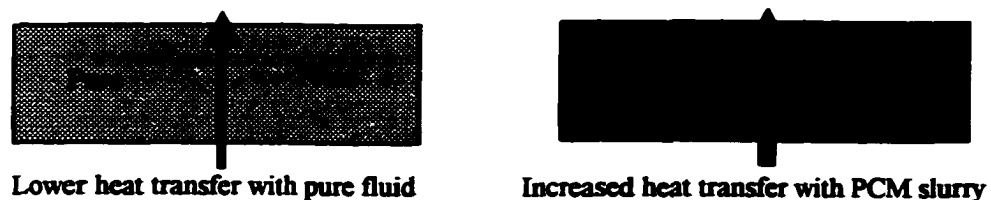
Microencapsulation can be carried out in a variety of ways; coacervation, complex coacervation, injection methods, etc., The process used in the manufacture of particles that are to be used in the present study was coacervation.

The capsules typically consist of a resinous cell wall which makes up about 30% of the weight of the particles. The use of the microcapsules in passive heat exchangers greatly depends on the ability of the resinous shell to withstand the repeated expansions and contractions encountered during thermal cycling.

Roy and Sengupta (1991) performed a study on the feasibility of using phase change microcapsules by testing the properties and structural soundness of the capsules. Three different capsule sizes (50, 100 and 250 microns) and two wall thicknesses (15% and 30% by particle volume) were tested. The durability of the microcapsules with the 30% walls after repeated thermal cycling, was found to be superior to the ones with the thinner walls. Figs 2.4 and 2.5 show typical micro-capsules before and after collapse.

PROBLEM STATEMENT

In this investigation natural convection flow in a cavity, using phase change suspensions is to be studied. Fig 3.2 shows a schematic of the test section to be used in the study. The cavity is a rectangular (cuboid) enclosure with a heated (horizontal) bottom plate, insulated side walls and a (horizontal) top plate being maintained at a constant temperature below that of the hot plate. The working fluid is a suspension of phase change microcapsules in a suitable suspending fluid. The enclosure is free of any obstacles that might interfere with the flow. Property definitions quantifying the working fluid and a detailed problem statement are listed in the following sections.

3.1 The problem statement**Fig 3.1 The problem statement**

The present work investigates the enhancement in natural convection heat transfer, (in rectangular enclosures heated from below), that results due to the use of Phase Change Slurries in place of single phase fluids.

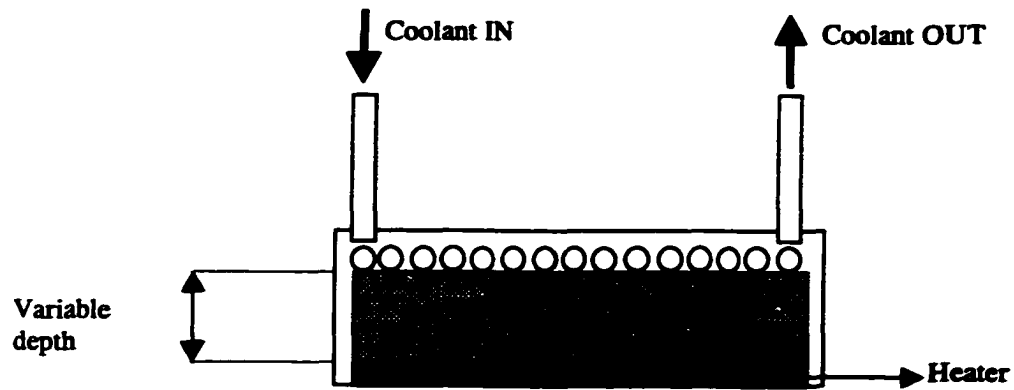


Fig 3.2 Schematic showing the details of the experimental test section

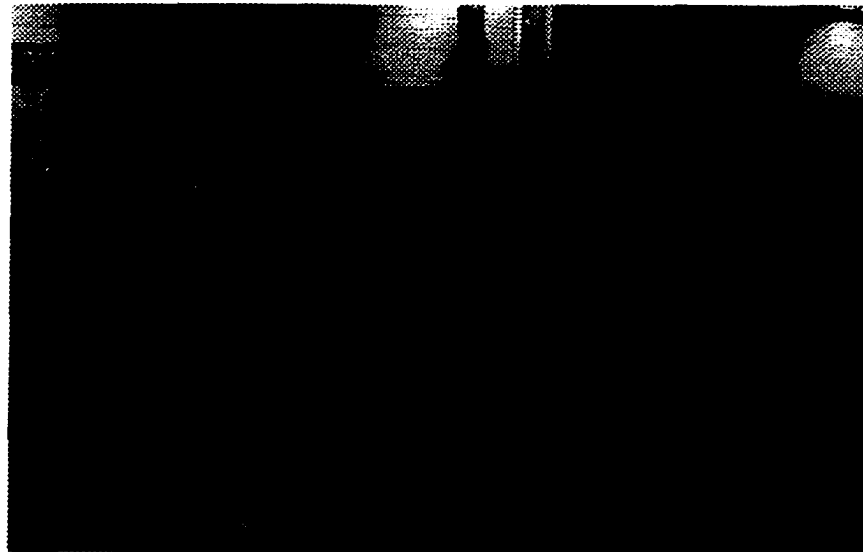


Fig 3.3 Photograph showing the experimental set-up.



Fig 3.4 Close up of the test section used in the experimental work

A close up of the test section used in the present study is shown above. The experiments were carried out in a double walled enclosure made of lexan. The air gap between the walls helps keep the heat losses from the cavity down to a minimum. There is no insulation or guard heater required for the heater since the area below the heater is in essence a cavity heated from above with air as the working fluid. This is a very stable configuration with little possibility of a convective augmentation and hence a very minor heat loss.

The experimental study was conducted on the set-up shown in Fig 3.3. The apparatus consisted of the upper and lower copper plates instrumented with type T thermocouples. The analog outputs from these thermocouples are digitized using a A-D convertor (Acromag temperature measuring unit). The digitized data is routed to and stored on a personal computer. The A-D convertor is unique in that the electronics of each

of its channels are isolated from each other. This helps reduce the interference that can result between the analog outputs of each channel. In view of the tiny voltages that thermocouples put out, this reduces the uncertainty in the data.

3.2 Experimental procedure

The experiments were conducted as follows:

1. A certain volume of water was poured into a measuring cylinder (approximately 10-15 ml).
2. Microcapsules were then added to the water till the increase in volume corresponded to the volume of particles needed.
3. The mixture was then filtered and dried.
4. The capsules were transferred to a beaker to which a small amount (~ 10 ml) of the suspending fluid was added. The slurry was shaken to form a homogeneous mixture.
5. More of the suspending fluid was added to form a slurry with the volume equal to that of the box for the particular experiment.
6. The top of the cavity was removed and the mixture added to the cavity.
7. The upper plate was then eased back into the cavity with care to ensure that no trapped air remained between the cold wall and the upper surface of the fluid.
8. Leveling rods and spirit levels were used to ensure that both the bottom and the top of the cavity remained perfectly horizontal.

9. The recirculating cooler was started to maintain the cold wall at a predetermined value.
10. The heater was powered on to a value (from experience) which would result in a predetermined hot wall temperature.
11. The system was monitored and data recorded till steady state.

3.3 PARAMETERS OF INTEREST

A number of different parameters affect the heat transfer and the fluid flow in natural convection. Non-dimensional parameters such as Ra, Ste etc., govern the flow. They can be classified under different categories as follows

3.3.1 Fluid parameters

3.3.1.1 Particle concentration

Previous studies on natural convection heat transfer using microencapsulated phase change materials (Datta et.al., (1992)) show that at low concentrations there is an improvement in the heat transfer. However, for concentrations above 5% the enhancement falls off and for concentrations of 10% or more the heat transfer is actually less than in the case of a single phase fluid. The most important reason for this phenomenon is, at high concentrations, the inter-particulate distance is so small that the particles coalesce into clumps. These clumps have sedimentation rates much higher than the heat diffusion rate into the particle. Clearly, the volumetric (or gravimetric) particle concentration determines the extent of participation in the energy transport by the dispersed phase.

3.3.2 Natural Convection parameters

3.3.2.1 The Grashof and Rayleigh numbers

$$Gr_{\Delta T} = \frac{g \beta \Delta T D^3}{\nu_b^2}$$

$$Ra_{\Delta T} = \frac{g \beta \Delta T D^3}{\nu_b \alpha_b}$$

Both the Grashof and the Rayleigh numbers are important parameters in the transport phenomenon as indicated by the governing equations. Investigations by Datta et.al., (1992) proved that at higher Rayleigh numbers there was an increase in the heat transfer. However due to the limited range that the study had been conducted in (most of the experiments fell into the 10^8 range), a reliable quantification of the effect of the Rayleigh number was not possible. In the present study, the Rayleigh number was varied over a much higher range (10^4 to 10^9). This better quantifies the enhancement of the heat transfer in microencapsulated phase change suspensions. The Rayleigh number was varied by increasing the enclosure height ($Ra \propto D^3$).

3.3.2.2 The Prandtl number $Pr = \frac{\nu_f}{\alpha_b}$

The Prandtl number is the ratio of the momentum to thermal diffusivities. While it is extremely difficult to design an experiment in which all parameters except the fluid Prandtl numbers are held constant, in the present study, two slurries having very different

suspending fluids have been used. Since these are steady state studies and the thermal masses do not figure into the solution, the Prandtl numbers variation is an indication of the effect of the thermal conductivities of the background fluid on the transport. The higher the Prandtl number the lower the thermal conductivity contribution, (ignoring the effect of the thermal mass of the background fluids).

3.3.3 Phase Change Parameters

3.3.3.1 Stefan number

$$Ste = \frac{(C_p)_b \Delta T}{cL(\frac{\rho_p}{\rho_b})}$$

The stefan number characterizes the effect of increasing the concentration and thereby the amount of the phase change material in the suspension. It also quantifies the effect of the amount of latent heat relative to the sensible heat of the slurry. The Stefan number range is dependent on the value of the latent heat of fusion of the phase change material and the particle *concentration* in the suspension. Since the former is a constant for any chosen PCM, the Stefan number range in this study is dictated by the particle concentration.

3.3.3.2 The sub cooling ratio

$$\theta_{sc} = \frac{(T_m - T_c)}{(T_h - T_c)}$$

In this study an attempt was made to study the effect of the subcooling ratio in isolation by keeping the concentration and the enclosure height constant (this would keep Ste and Ra constant). The sub cooling ratio was varied over a very small range (less than

an order of magnitude). This is because, both T_m and T_h are constrained by material properties such as, the melting point of the PCM. Too high a T_h , would result in the second instability point and the melting point of the Acrylic walls being reached. T_c is also limited to around 1°C (freezing point of water).

3.4 MATRIX OF EXPERIMENTS

$D \longrightarrow$ $C\% \downarrow$	¼ inch $Ra \sim 10^4$	½ inch $Ra \sim 10^5$	1 inch $Ra \sim 10^6$	2 inch $Ra \sim 10^7$	4 inch $Ra \sim 10^8$
0.5 %	ΔT T_{c_1}, T_{c_2}	ΔT T_{c_1}, T_{c_2}	ΔT T_{c_1}, T_{c_2}	ΔT T_{c_1}, T_{c_2}	ΔT T_{c_1}, T_{c_2}
1 %	ΔT T_{c_1}, T_{c_2}	ΔT T_{c_1}, T_{c_2}	ΔT T_{c_1}, T_{c_2}	ΔT T_{c_1}, T_{c_2}	
2 %	ΔT T_{c_1}, T_{c_2}	ΔT T_{c_1}, T_{c_2}	ΔT T_{c_1}, T_{c_2}		
4 %	ΔT T_{c_1}, T_{c_2}	ΔT T_{c_1}, T_{c_2}			

3.5 Scope of the experiments

Slurry I Water + Micro-capsules with a Palmitic acid core

Range of parameters -

1. **Rayleigh number 1×10^5 to 1×10^9 (approx)**
2. **Stefan number based on the Concentration 0% to 4%**
3. **Sub - cooling ratio 0.45 to 1.0 (approx)**
4. **Prandtl Number 3**
5. **Total number of experiments - 28**
6. **Particle size - 30 microns.**

Slurry II PolyDimethyl Siloxane + Micro-capsules with a Myristic acid core

Range of parameters -

1. **Rayleigh number 1×10^4 to 1×10^8 (approx)**
2. **Stefan number based on the Concentration 0% to 4%**
7. **Sub - cooling ratio 0.7 to 1.0 (approx)**
8. **Prandtl Number 660**
9. **Total number of experiments - 28**
10. **Particle size - 100 microns.**

Besides these, some experiments were conducted with water and Myristic acid capsules and Polydimethyl Siloxane with Palmitic acid capsules.

3.2 Numerical Simulations

The computational domain utilized for the present study is shown in Fig 3.5. The grid has been refined close to the lateral walls to capture the larger gradients in velocities and temperatures (wall effect).

It was proposed to use a source term to include the effect of the phase change. The source term was to be of the following form based on Harhira's (1993) work:

$$S^* = \frac{3C}{1-(1-\beta_p)r^*} \left(\frac{D}{r_p}\right)^2 \left(\frac{K_p}{K_b}\right) (\Theta_{scr} - \Theta)$$

The intent was to convert a time derivative (quantifying the melt rate in the particle) to a spatial derivative of the following form (similar to Harhira (1994)). The radius of the solid-liquid melt interface "r" at any instant of time was to be calculated using the following expression:

$$r = \sqrt[3]{1 - 3C \left(\frac{Ste}{Pr}\right)_b \left(\frac{K_p}{K_b}\right) \left(\frac{D}{r_p}\right)^2 \int_0^{x^*} \left(\frac{r^*}{u^*}\right) \frac{(\theta_{scr} - \theta)}{(1-(1-\beta_p)r^*)} d(x^*)}$$

However, for the above expression to be valid, it is imperative that the flow is predominantly uni-directional. In the case of passive heat transfer in a cavity, that is not the case. Hence the above formulation is inappropriate. In fact it is extremely difficult (if not impossible) to formulate a source term from an Eulerian point of view. A Lagrangian approach where every particle or group of particles is tracked would be required.

In view of this difficulty, it was decided to use FLUENT as the solver and to model the heat transfer augmentation using a single phase approach. This meant that all properties of the virtual working fluid, would be the bulk properties of the suspension and

the effect of the phase change would be modeled as an effective specific heat augmentation. In fact, C_p was modeled as a pulse which incorporated the concentration effect by varying the strength of the pulse. This approach is further explained in the section on Results and Discussions (Chapter 5).

The study is restricted to equivalent single phase, 3D, laminar, steady state analyses, (3D transient analyses were too expensive). The domain consisted of adiabatic side walls, an isothermal upper boundary and an isoflux lower wall.

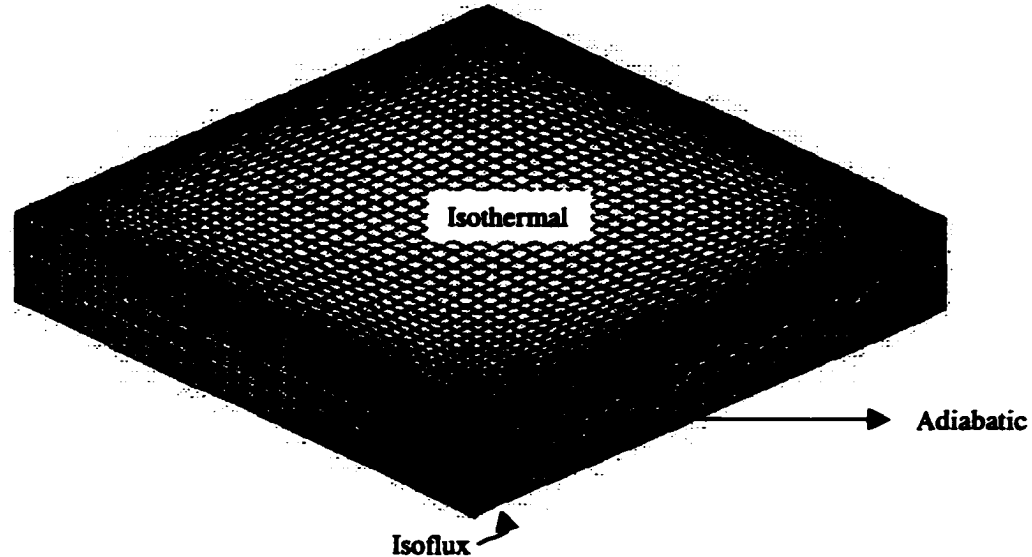


Fig 3.5 Virtual test section showing the computational domain

The fluid was assumed to be isotropic and the Boussinesq assumption for buoyancy driven flow, (which states that all properties of the working fluid are constant at the bulk temperature value, except in the body force term) was invoked. A uni-block structured solver from FLUENT (structured version), was used for the CFD runs. The

runs were conducted with a special set of units designed to scale the velocity output by a factor of a 1000¹ and thereby decrease the sensitivity to roundoff error (for studies in passive heat transfer, this can be an especially irksome hurdle when using dimensional solvers).

¹ This is further discussed in chapter 5.

4.1 Particle properties

The microcapsules used in this investigation are made of a PCM core with a resinous outer shell. The PCMs used in this investigation were Palmitic Acid and Myristic Acid with chemical formulae $\text{CH}_3(\text{CH}_2)_{14}\text{COOH}$ and $\text{C}_{14}\text{H}_{28}\text{O}_2$ respectively, both of which are organic acids with melting points of -63 and 58 deg C. The material properties of the cell wall material, the PCMs and the suspending fluid are all listed in the Appendix.

The figure shown below is a schematic of a typical microcapsule. Roy and Sengupta (1990) have performed some feasibility studies on the structural soundness of the particles with different cell wall thicknesses and concluded that particles with wall thicknesses of 30% or greater are indeed structurally sound. In the present study, the particles used have wall thicknesses between 30 and 40% by weight.

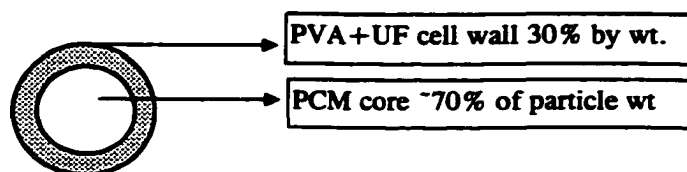


Fig. 4.1 Schematic of a microcapsule showing the cell wall and capsule core

In a previous study, Datta (1992), the present author explains how it would be erroneous to neglect the cell wall properties since the wall makes up about 30% of the microcapsule by weight and hence the particle properties are actually an ensemble of the core and the wall material.

Discussions with the manufacturer of the microcapsule (Ronald T. Dodge Co.) revealed that for all practical purposes, the thermophysical properties of the wall may be closely approximated as those of Urea-Formaldehyde. The properties of U-F are listed in Appendix - A.

4.1.1 Particle Density

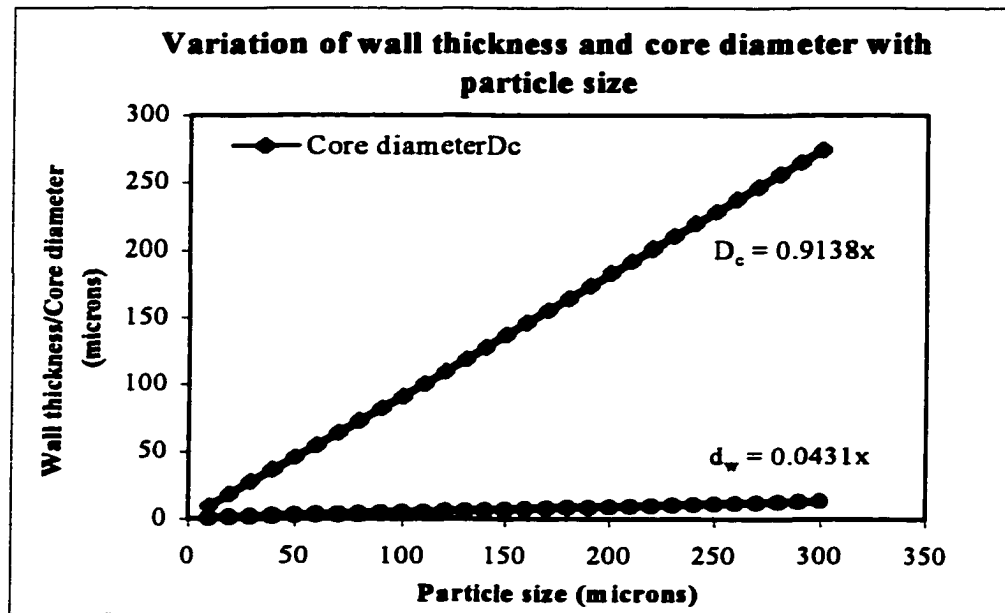


Fig 4.2 Variation of particle wall thickness with particle diameter.

An expression for the capsule density can be easily obtained by taking the ratio of the particle mass to volume and using the fact that the shell wall makes up a certain % of mass of the capsule. The final expressions are given below.

$$\left[\frac{\rho_w(d_p^3 - d_c^3)}{\rho_p d_p^3} \right] = 0.3 \Rightarrow \rho_p = \left[\frac{\rho_w c}{0.3} \left(1 - \frac{d_c^3}{d_p^3} \right) \right] \quad (4.1)$$

$$\text{where } \frac{d_p^3}{d_c^3} = \left[1 + \frac{3 \rho_c}{7 \rho_w} \right]$$

Since both the particle core density and the particle wall density are known, the overall particle density can be calculated.

4.1.2 Particle Specific Heat

The particle specific heat is obtained by taking the weighted mean specific heat of the wall and core. The following formula can be derived for the particle specific heat

$$C_p = \frac{\rho_c V_c C_c + \rho_w V_w C_w}{\rho_c V_c + \rho_w V_w} = 0.7 C_c + 0.3 C_w \quad (4.2)$$

4.1.3 Particle Thermal Conductivity

Datta (92) and Goel (92) developed equations for the thermal conductivity of a microcapsule. However, it was observed that the thermal conductivity of the wall had a

negligible effect (1-2%) on the overall particle thermal conductivity. In view of this, the particle's thermal conductivity has been approximated here to be that of the PCM core.

4.2 Slurry properties

The properties of the PCM slurry are a combination of the properties of the microcapsules and the background (suspending) fluid. Expressions for the thermophysical properties such as the viscosity, the specific heat, the thermal conductivity are :

4.2.1 Slurry Viscosity

The viscosity of solid in liquid suspensions has been studied by many researchers (Einstein (1908), Rutgers (1962), and Vand(1945)). The expressions developed by Einstein and Vand have been listed below. Einstein's prediction deviates from experimental results for concentrations above 10%. However in this study the particle concentrations are to be held less than 10% and as such, both expressions are valid. The expressions for the bulk viscosity are given in equation 4.3.

The interesting observation is that the bulk viscosity is only a function of the volumetric concentration and not the particle size. This was first proved by Rutgers (1962). The viscosity of the suspension is always higher than the background fluid and this becomes especially important for medium and high concentrations since the effective Rayleigh number falls and with it the heat transfer. Rhazi (1994) also observed that the critical Ra increases with the addition of the a second particulate phase.

$$\begin{aligned} \left(\frac{\mu_b}{\mu_f}\right) &= (1 - c - 1.16c^2) && \text{Vand (1945)} && \text{valid for all } c \\ \left(\frac{\mu_b}{\mu_f}\right) &= (1 - 2.5c) && \text{Einstein (1906)} && 0 < c < 10\% \end{aligned} \quad (4.3)$$

The variation has been plotted for viscosities upto and below 25%, and holds true

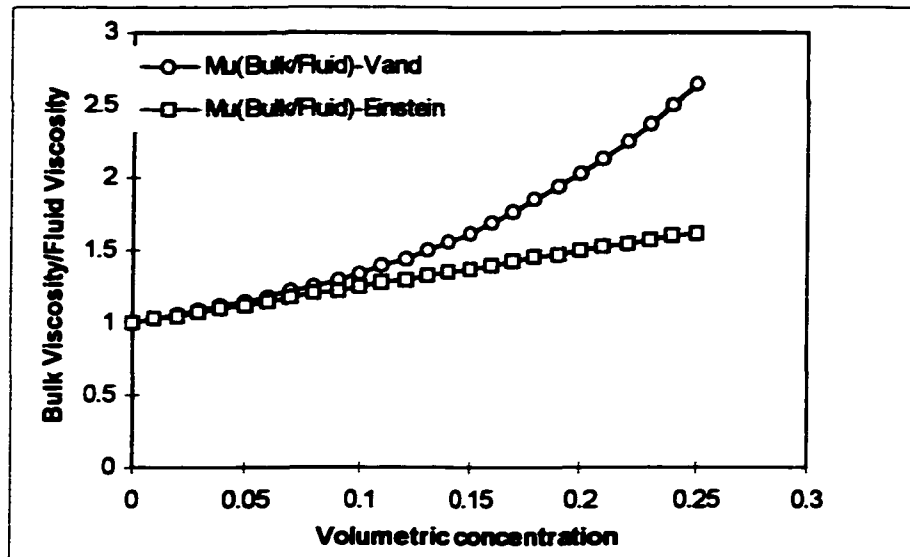


Fig. 4.3 shows the variation of the viscosity with the particle concentration.

only for Newtonian liquids. Clearly, both predictions are almost identical for concentrations below 10%. For concentrations above this, Vand's expression is more accurate.

4.2.2 Slurry Density

As in the case of the particle density, the slurry density is simply a weighted mean of the particulate and dispersing phase. The expression therefore is:

$$\frac{\rho_b}{\rho_f} = c \left(\frac{\rho_p}{\rho_f} - 1 \right) + 1$$

4.2.3 Slurry Specific heat:

Just as in the case of the bulk slurry density, the weighted mean expression for the specific heat is:

$$\frac{C_{pb}}{C_{pf}} = \frac{c \left(\left(\frac{C_{pp}}{C_{pf}} \right) \left(\frac{\rho_p}{\rho_f} \right) \right) + 1}{c \left(\frac{\rho_p}{\rho_f} - 1 \right) + 1}$$

4.2.4 Slurry Thermal conductivity

The thermal conductivity of the slurry can be effectively treated as a combination of the following factors:

- (1) ***The conductive contribution:*** This is the effect of simply altering the properties of the working fluid by virtue of the disparity in the thermal properties of the dispersed and dispersing phases. For instance, adding metallic filings to water would increase the effective thermal conductivity of the water because of the higher thermal conductivity of the metal. Physically, it is akin to increasing the thermal conductivity of the base fluid by embedding material of higher conductivity in it. The increase in thermal conductivity, obviously depends on the amount (or concentration) of the additive. The following expression for the bulk thermal conductivity, quantifies this effect:

$$\frac{K_b}{K_f} = \frac{2 + \frac{K_p}{K_f} + 2c \left(\frac{K_p}{K_f} - 1 \right)}{2 + \frac{K_p}{K_f} - c \left(\frac{K_p}{K_f} - 1 \right)}$$

- (2) ***The flow contribution:*** As mentioned in Chapter 2, previous investigations show that inspite of similar, or identical thermophysical properties for both the dispersed and dispersing phases, it is possible that the effective thermal conductivity of the slurry is actually higher than either of the possible phases. This is due to the “micro-convective” effect. This effect refers to the tiny eddies that are formed around the suspended particles of the additive phase. The strength of these eddies clearly depends on the local Reynolds number (more appropriately, the shear and thus the local Peclet number). As a result, the effective thermal conductivity of a slurry is a function of the local shear rate.

In the case of natural convection however, in view of the fairly low velocities in the cavity, the micro-convective effect would have an insignificant contribution on the overall thermal conductivity enhancement. Hence for the scope of the present study, the thermal conductivity shall be calculated using the expression for the bulk thermal conductivity given above.

4.3 Particle specifications

The microcapsules are manufactured to user specified diameters and wall thicknesses, expressed as a weight percentage of the payload. Ideally, the particles would

all have uniform diameters, or be monodispersed. However, they are actually polydispersed and have a range of diameters.

The particles have been obtained from two sources, Ronald T. Dodge Co. and a Japanese manufacturer. Unfortunately, the quality of the capsules varied considerably. some of the differences were :

- a) The 30 micron capsules with Palmitic acid as the core, had been manufactured with many capsules having coalesced into clumps. Figs. 4.4 and 4.5 bear testimony to this fact. In fact many of the clumps are as large as 250 microns in diameter.
- b) The above mentioned capsules also show exhibited inconsistency in their shape (Figs 4.4 and 4.5). This resulted in capsules of uneven structural soundness and it was observed that many of them had broken during the thermal cycling they experienced in the experiments.
- c) Figs 4.3 and 4.4 show 100 micron particles with a Myristic acid core, manufactured in Japan these particles show a more consistent shape and are devoid of clumping. While being polydispersed, they have a low standard deviation and have a mean diameter of 108 microns!



Fig 4.4 Myristic acid micro-capsules (100 microns). (X~50)

In view of the trends observed in the preliminary work by Datta ('92), the present



Fig 4.5 Myristic acid micro-capsules 100 microns (X~50)

study restricts itself to experiments with relatively low concentrations. The highest concentration to be used is 4% by volume.



Fig 4.6 30 micron Palmitic acid micro-capsules (X~200)

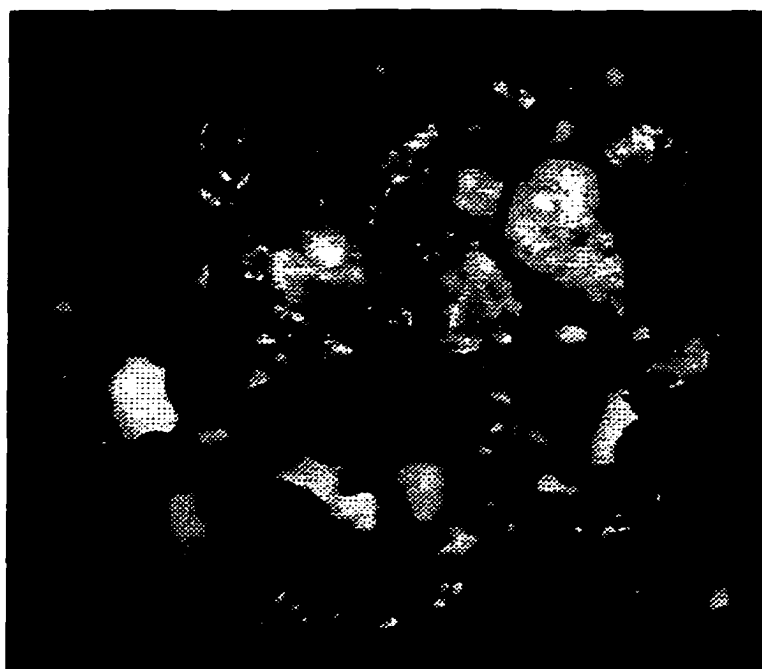


Fig 4.7 Palmitic acid microcapsules (30 microns) (X~200)

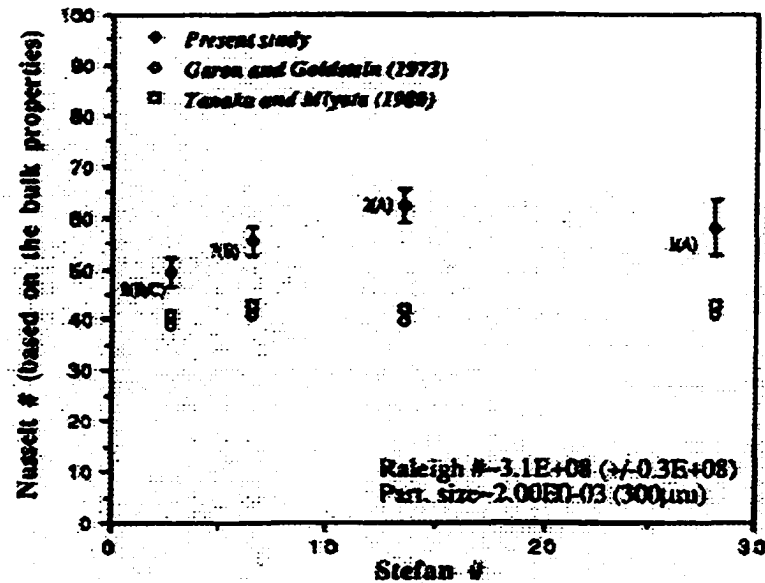


Fig 4.8 Results from the work of Datta (1992)

Fig 4.8 from the results of Datta ('92), illustrates that clumping has a significant effect on the heat transfer rate. The data point labels indicate the kind of regime observed in the cavity (class A, B or C flow regime). With increasing concentrations, one would intuitively expect that, there would be corresponding increases in the heat transfer rate. However, the experimental results point to other mechanisms which impede this and in extreme cases even cause a detriment of heat transfer rate. The primary mechanisms that result in the decrease of the enhancement, (and ultimately increase in the detriment of heat transfer), are *Clumping* and *Sedimentation* (initiated by excessive Clumping).

RESULTS AND DISCUSSIONS**5.1 EXPERIMENTAL WORK****5.1.1 VALIDATION**

Temperature data from the upper and the lower copper plates, was obtained using thermocouples. The average temperature of the upper and lower copper plates, was used to find the driving temperature difference and the bulk fluid temperature. The overall Nusselt and Rayleigh numbers were then calculated using the following formulae, which took into account the height “D” of the enclosure.

$$\text{Nu} = \frac{hD}{K} ; \text{Ra} = \frac{g\beta \Delta T D^3}{\alpha \nu}$$

All properties were calculated at the bulk mean temperature of the fluid.

Initially, the apparatus was validated by running experiments distilled water as the working fluid. Results from the runs are presented in the Nu-Ra plot of Fig 5.1 Clearly, the results follow the trends of data obtained by previous investigators (Goldstein et. al., (1992)). While enough to validate the apparatus, it should be pointed out that the data did follow the lower bound of the predicted results of previous investigators. However, in view of the fact that there is a significant (about

Validation curves

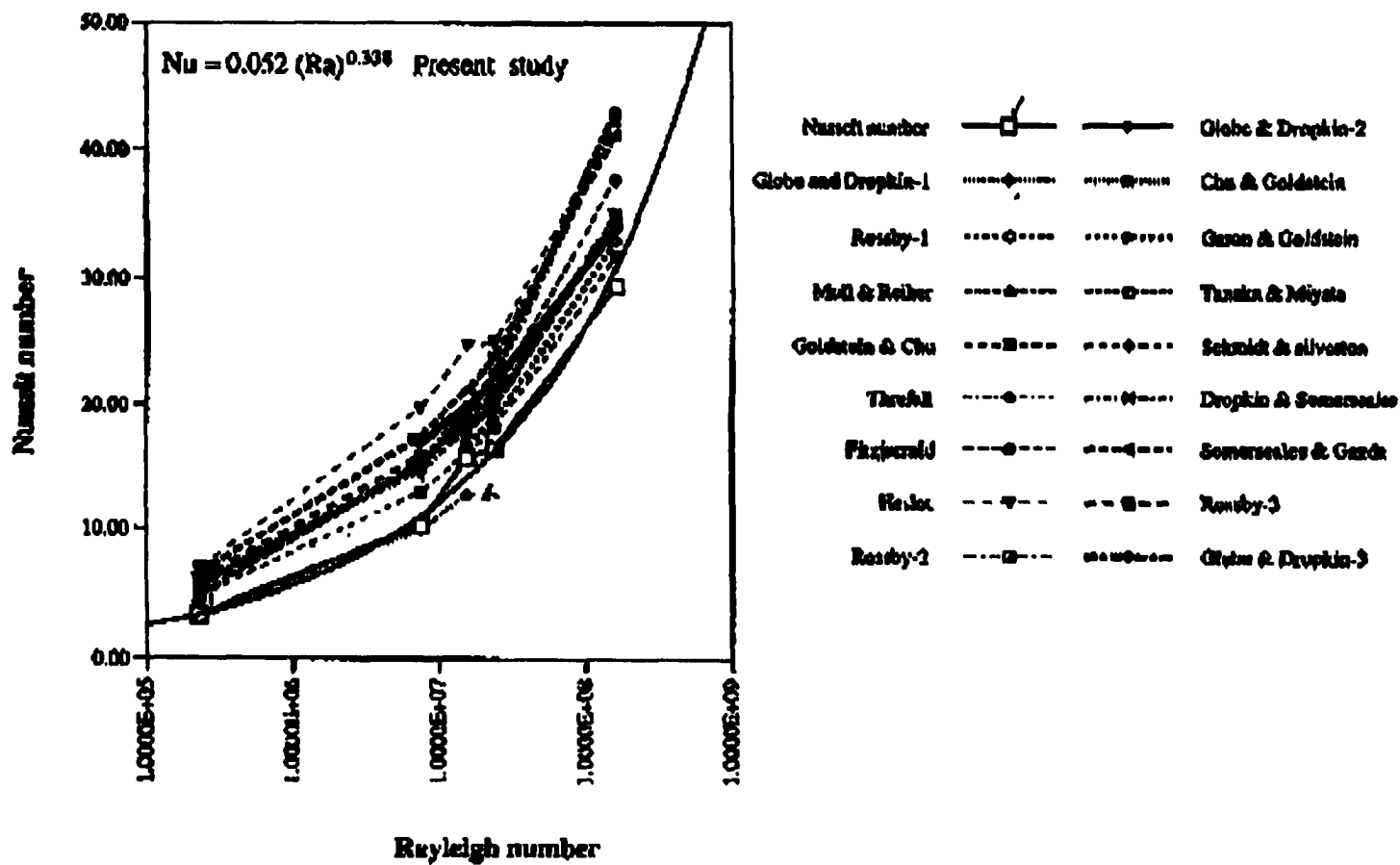


Fig 5.1 Validation curves for the apparatus. Note the variation in the results of previous investigators.

20%) variation between predictions of the previous investigators, and the fact that aspect ratios of many of the studies varied, the results were not deemed suspect.

5.1.2 ENHANCEMENT RUNS

After the apparatus was validated, experiments studying the enhancement characteristics of micro-encapsulated phase change materials were initiated. The calculations performed to study the overall heat transfer (the overall Nu number) were the same as explained in the previous section. However, the fluid properties in these experiments were functions of both the dispersed and the suspending phases. The bulk slurry properties were obtained using the expressions presented in chapter 3. These property values were then used to calculate the various non-dimensional parameters like Nu, Ra, Ste, Pr, etc.,

It has been attempted to vary each of the non-dimensional parameters by keeping the others constant. Experimental constraints have made this fairly difficult and in some cases, the parameters being held constant have varied, albeit not substantially.

The total number of experiments conducted were ~60 - with a few trial runs to pin down the dimensional values to be maintained. The experiments were conducted with two different kinds of microcapsules (~30 μm diameter with Palmitic acid cores and ~100 μm diameter capsules with Myristic acid cores), and two different suspending fluids Water and Poly-Dimethyl Siloxane, a silicone oil (trade name M100 manufactured by BAYER Corp). The data collected will be presented in the form of

non-dimensional plots of Nu Vs Ra , Ste and SCR and they will be presented in three sets each with a different combination of microcapsules and suspending fluid.

5.1.2.1 Experiments with water as the suspending fluid

Presented in Figs 5.2 through 5.12, are the results obtained with water as the suspending fluid while the dispersed phase was 30 μm micro-capsules of Palmitic acid.

5.1.2.1.1 Variation of Nu with Ra

Clearly, the experiments showed no significant enhancement for the Ra range ($>10^4$) and actually showing a detriment in the heat transfer. These results are counterintuitive and disagree (at least in the 10^7 - 10^8 range) with the data obtained in preliminary tests (Datta, (1992)).

Figs 5.2 – 5.6 show the variation of the Nusselt number with the Rayleigh number. Clearly, the Nusselt number trend is similar to the prediction from the pure fluid cases. Contrary to expectations however, there is no enhancement in the heat transfer. After repeated experiments resulted in no enhancements in heat transfer, it was clear that this was no aberration and an underlying physical phenomenon was the root cause of this detriment.

Was there truly any phase change? If so how much? In spite of the lower copper plate being at a temperature above the melting temperature of the PCM it is quite clear that the capsules might not be active participants in the energy transport. Datta observed a very significant increase in the heat transfer (about 80%), these experiments pointed to a detriment of over 50% in the heat transfer.

The most striking difference between the preliminary study (Datta ('92)) and the present study was the suspending fluid. The particles, the kinds of phase change materials used, or the experimental regime did not suggest a radical shift in the transport.

Water is an uncommonly good heat transfer liquid. Compared to other non-metallic liquids it has a very high thermal conductivity (~ 0.61) W/mK, a high specific heat and low viscosity. The Prandtl number of water (12.99 - 2), is low compared to most heat transfer oils (>180). This indicates that water has almost as good a thermal diffusivity as it does momentum diffusivity.

The thermal conductivity of most microcapsules with a PCM core ranges from 0.159 - 0.13 (W/mK). It appears that the thermal conductivity disparity between the two phases, gives the suspending phase a strong advantage (more so when it is convecting) in the transport. In short, most of the energy seems to be bypassing the capsules.

Incidentally, had any heat transfer oil (most heat transfer oils have similar conductivities), been used as the background fluid, this would not have been discovered. While accidental, this finding (if borne out), is of utmost importance in the investigation. Clearly, further analysis was warranted. Sections 5.1.2.3 and 5.1.2.4 which follow, explain this phenomenon further.

The following plots show the variation of Nu with Ra at different sub-cooling ratios. In typical phase change slurries, the sub-cooling ratio should vary between 0 (when the cold wall temperature is the same as the melting temperature) and 1 (when the hot wall temperature is the same as the melting point of the PCM). Increased sub-

cooling ratios indicate a colder upper plate and hence a lower bulk fluid temperature.

The data indicates that there is an increased detriment in the heat transfer rate, for the lower sub-cooling ratio cases.

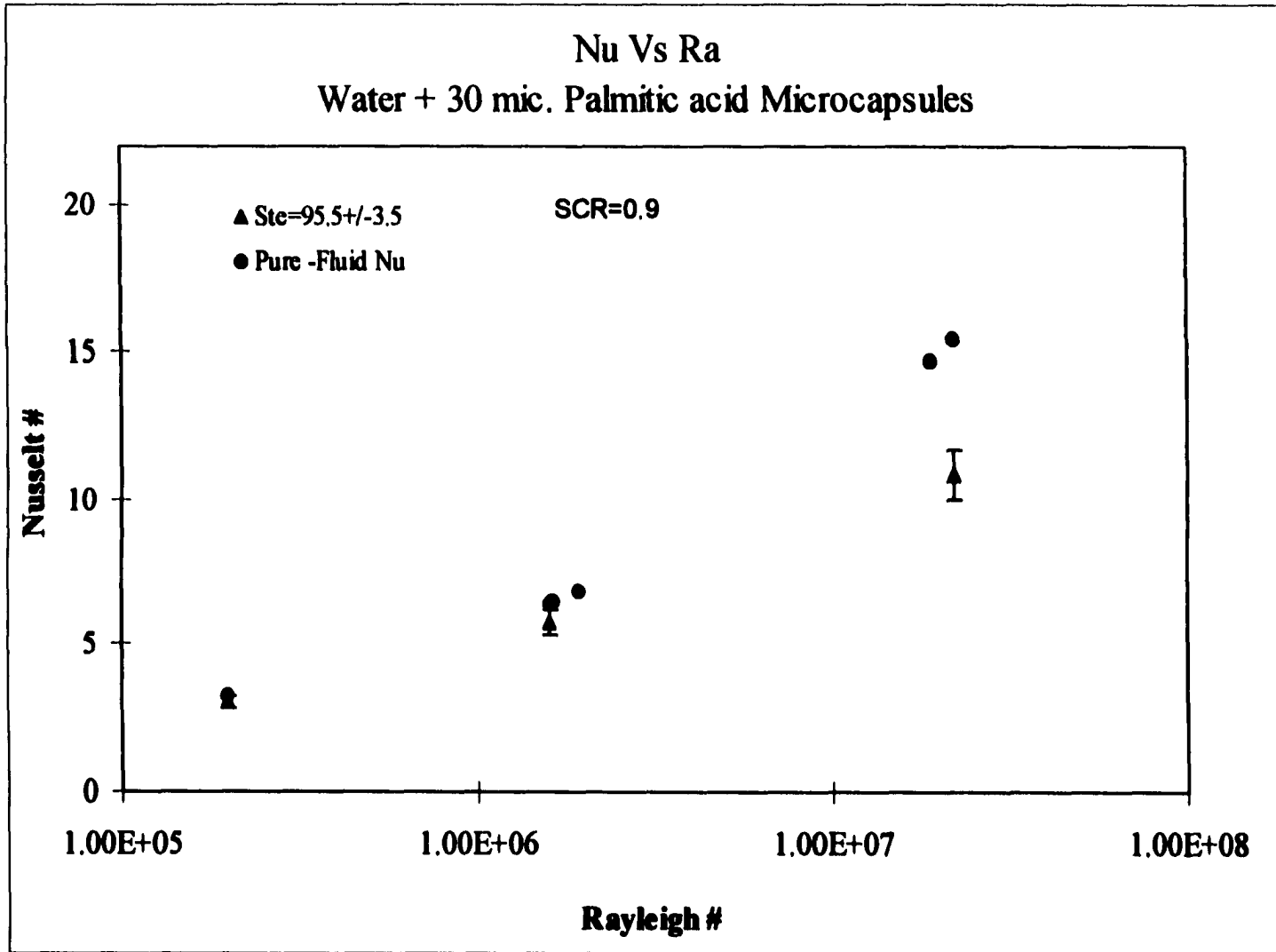


Fig 5.2 Variation of the Nusselt number with the Rayleigh number. Note the detriment in the heat transfer

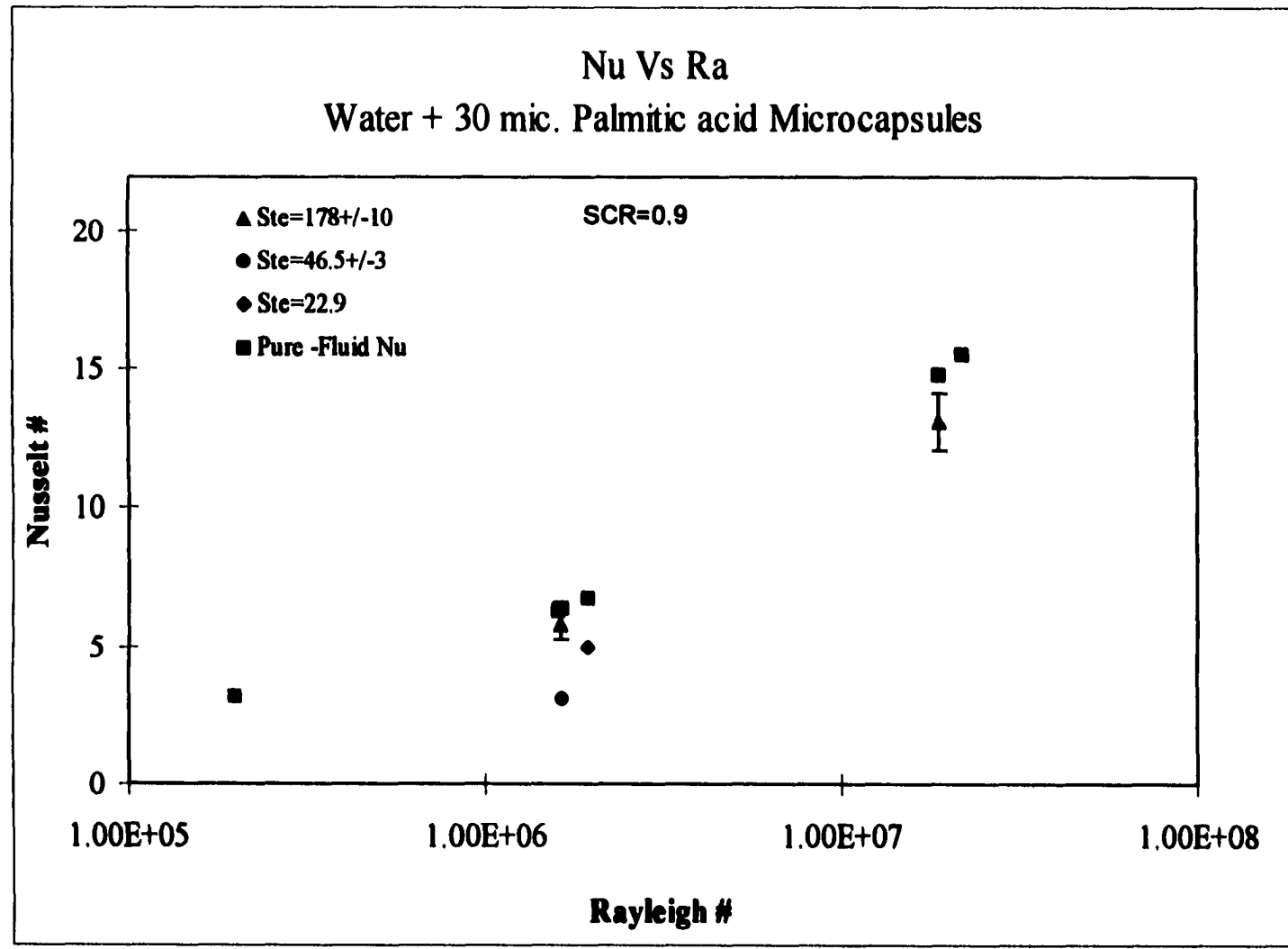


Fig 5.3 Variation of the Nusselt number with the Rayleigh number.

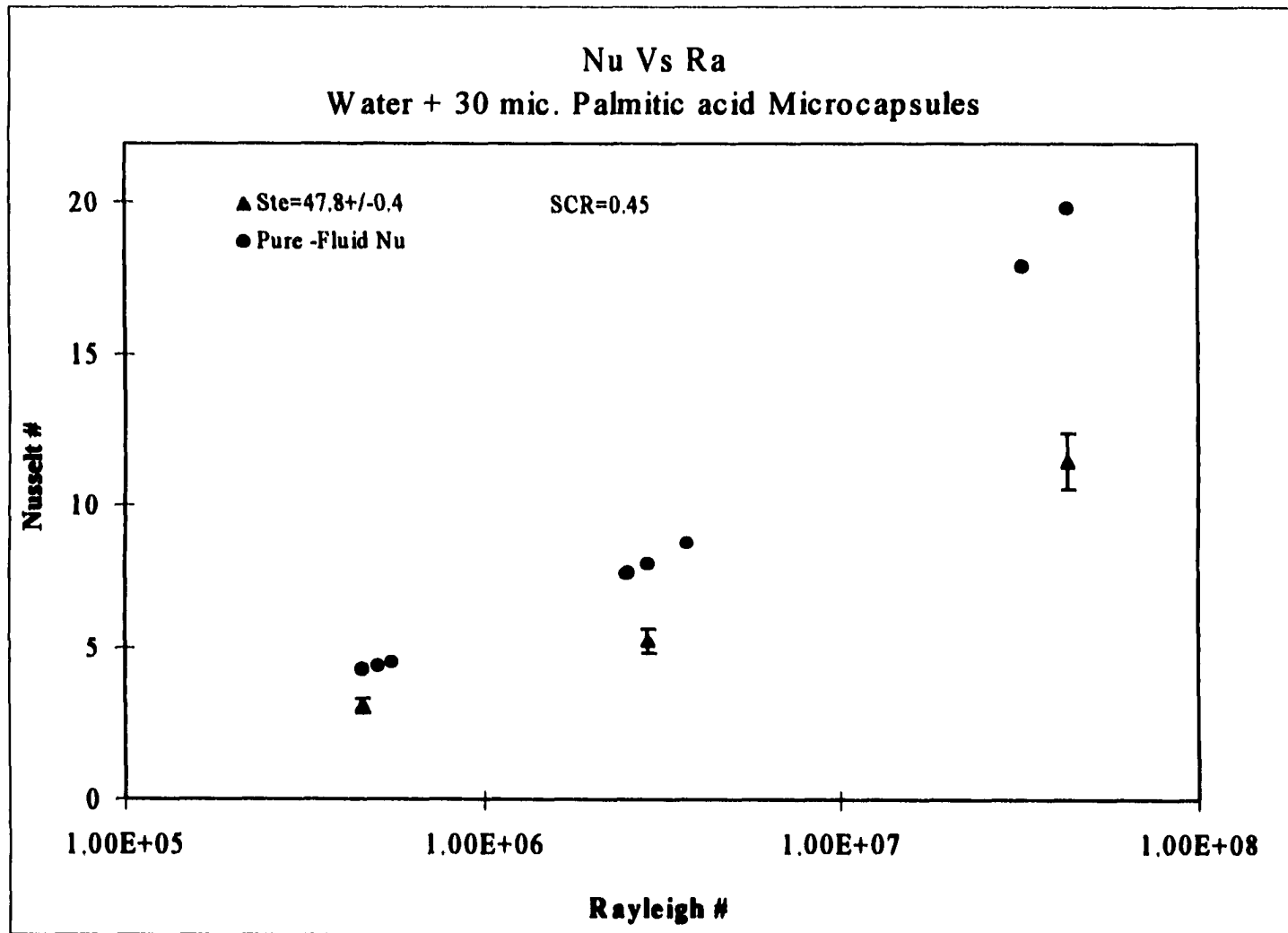


Fig 5.4 Variation of the Nusselt number with the Rayleigh number.

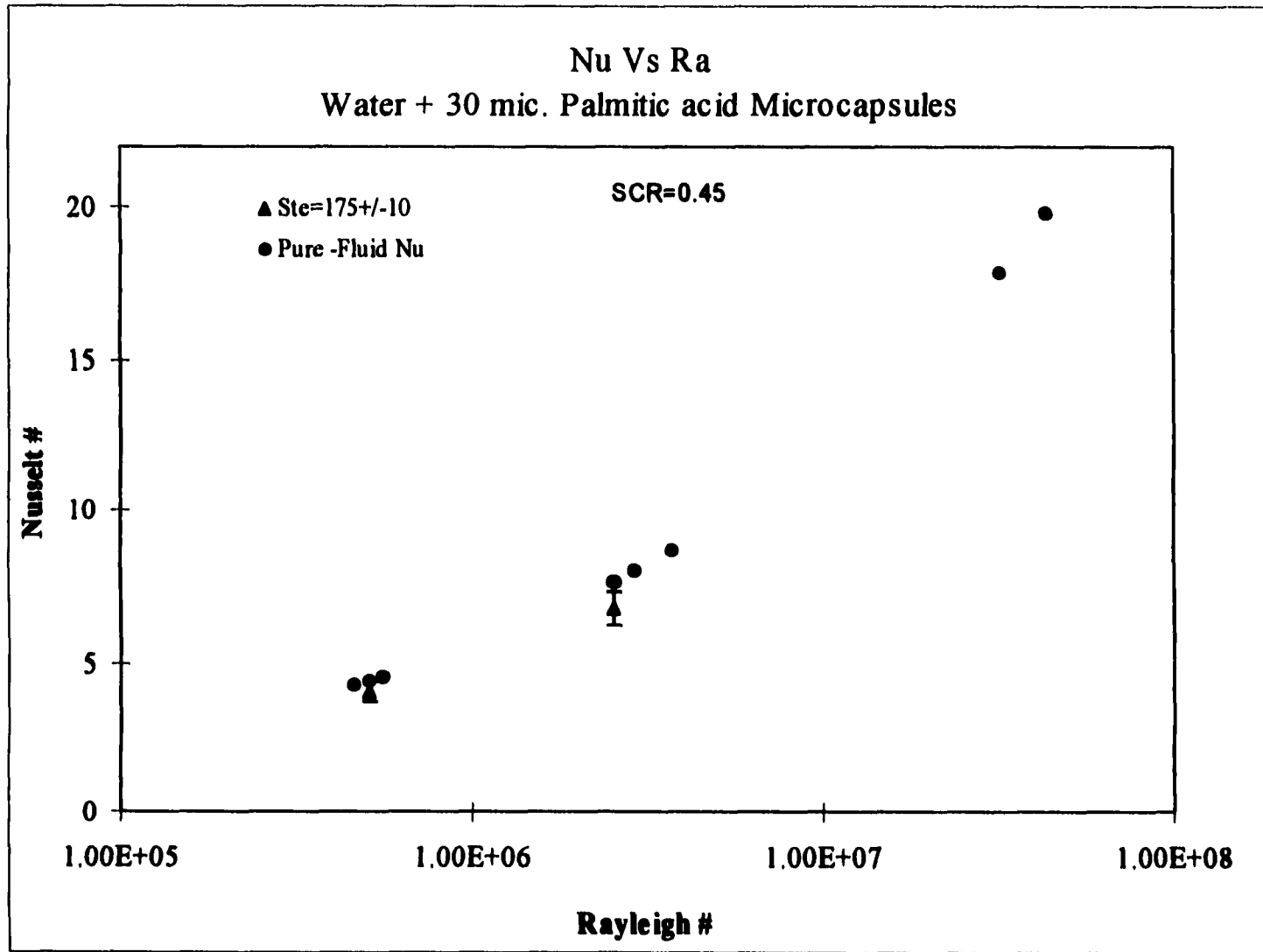


Fig 5.5 Nu Vs Ra showing the heat transfer detriment at low concentrations (high Stefan number)

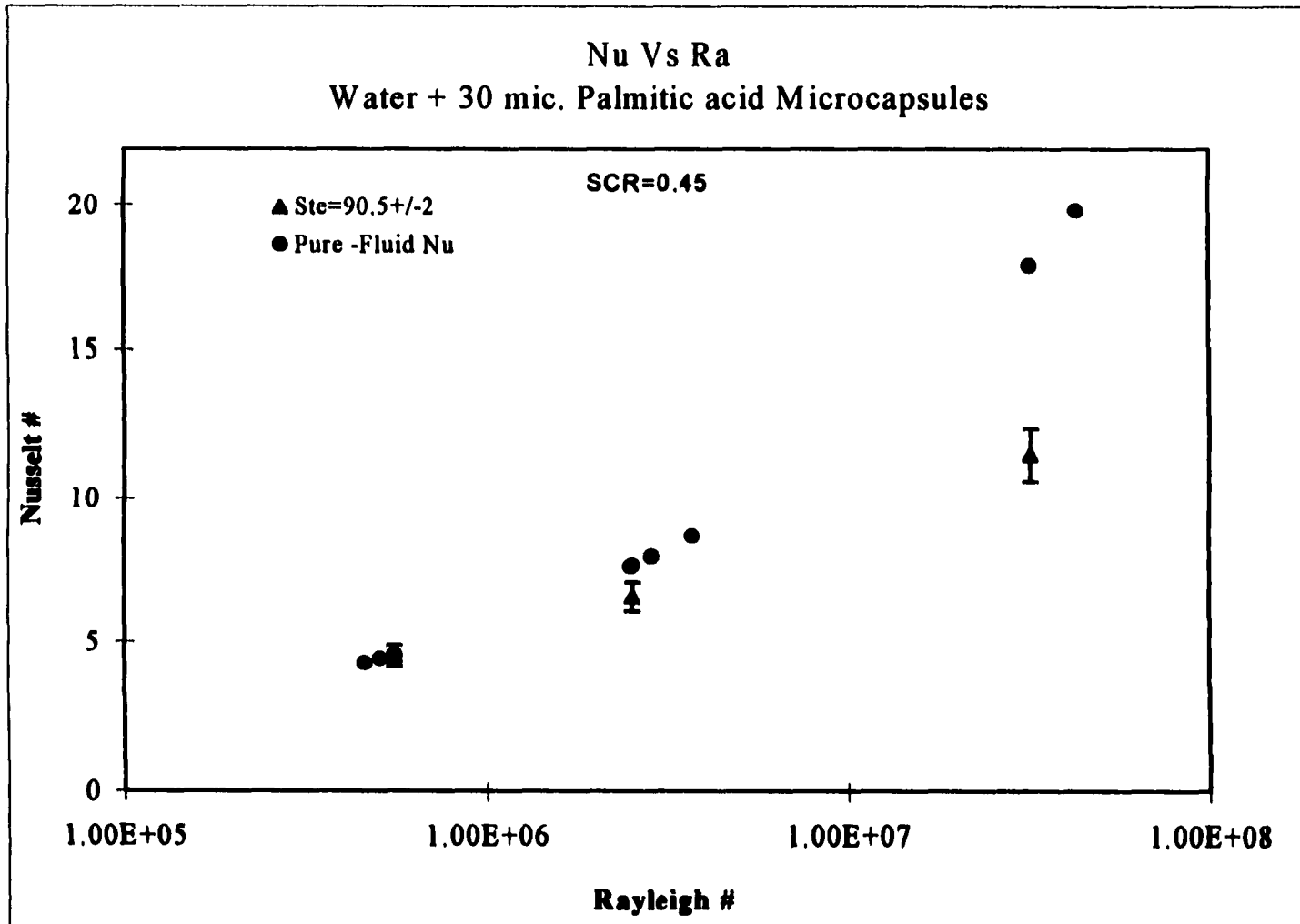


Fig 5.6 Nu Vs Ra showing the heat transfer detriment at low concentrations (high Stefan number)

5.1.2.1.2 Variation of Nu with Ste

The data reveals that none of the experiments showed an increase or an enhancement in the heat transfer rate. Holding Ra constant and varying the Stefan number (by varying the concentration) proved no different. Shown in Figs 5.7 – 5.11, is the data presented as Nusselt number variation with the Stefan number holding Ra constant.

The high Stefan number cases are indicative of low concentrations and vice versa. Experimental constraints prevented the Stefan number from being varied by changing the cold wall temperature holding the concentration constant.

With increases in the concentration, the heat transfer detriment increases. At lower concentrations, the effect of the particles is not as drastically negative. With increased concentration, (if the phase change process is not effective or is non-existent), then the only influence of the non-participating additive phase (the microcapsules) is to increase the viscosity of the working fluid. This contributes to a decrease in the effective Rayleigh number, which in turn leads to a decrease in the heat transfer coefficient, since “h” is governed by Ra.

In addition to these explanations, the photographs of the Palmitic acid microcapsules included in chapter 4 (Figs 4.6 and 4.7) are clear indicators that the slurry was not a “quality” phase change slurry. In fact many “strings” and “clumps” of particles were observed during the experiments. Datta (92) had previously shown using a diffusive time scale analysis, that increased clumping in the suspended phase cause a drop in the heat transfer rate.

The results are echoed for both the sub-cooling ratios tested.

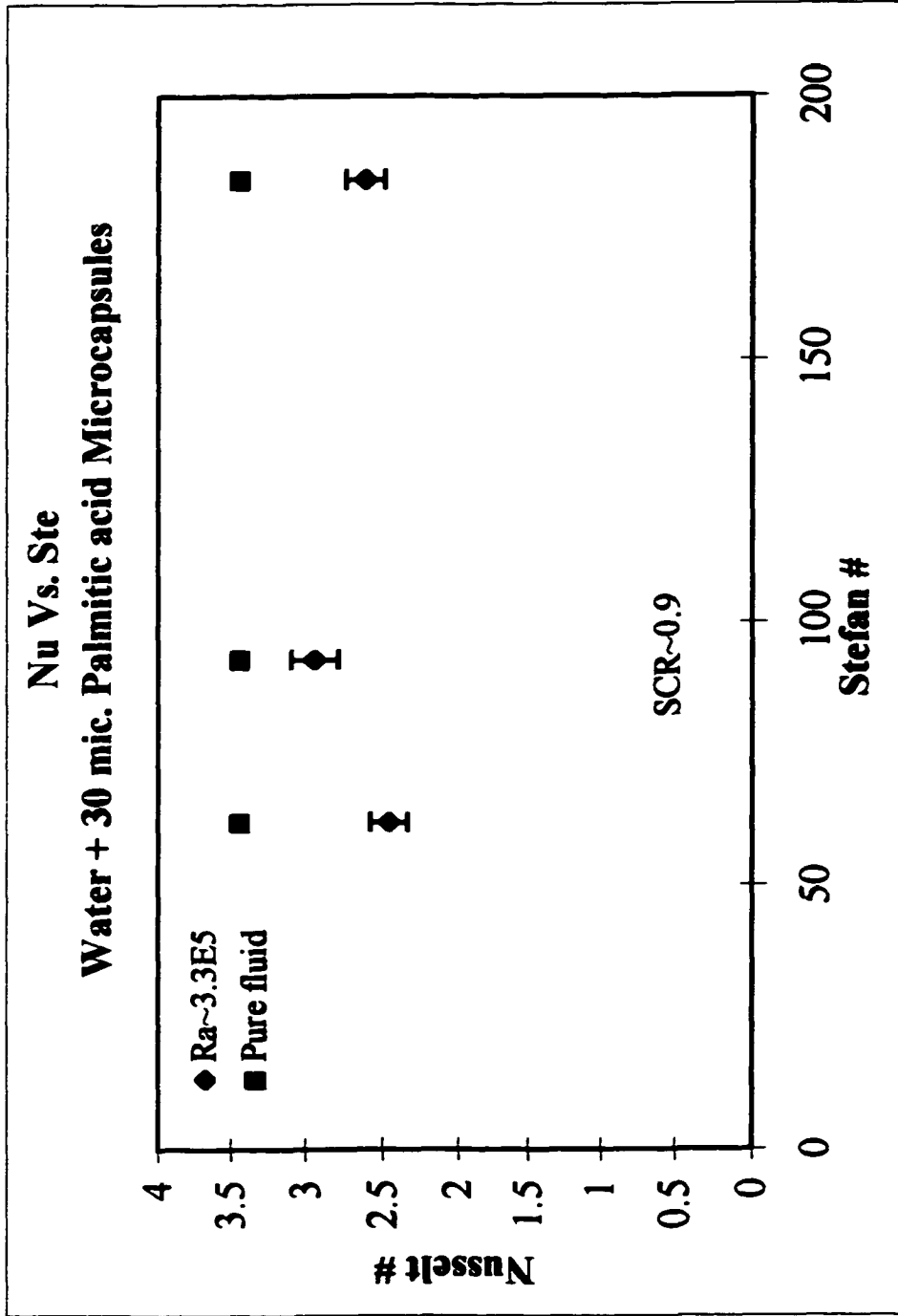


Fig 5.7 Variation of the Nusselt number with the Stefan number.

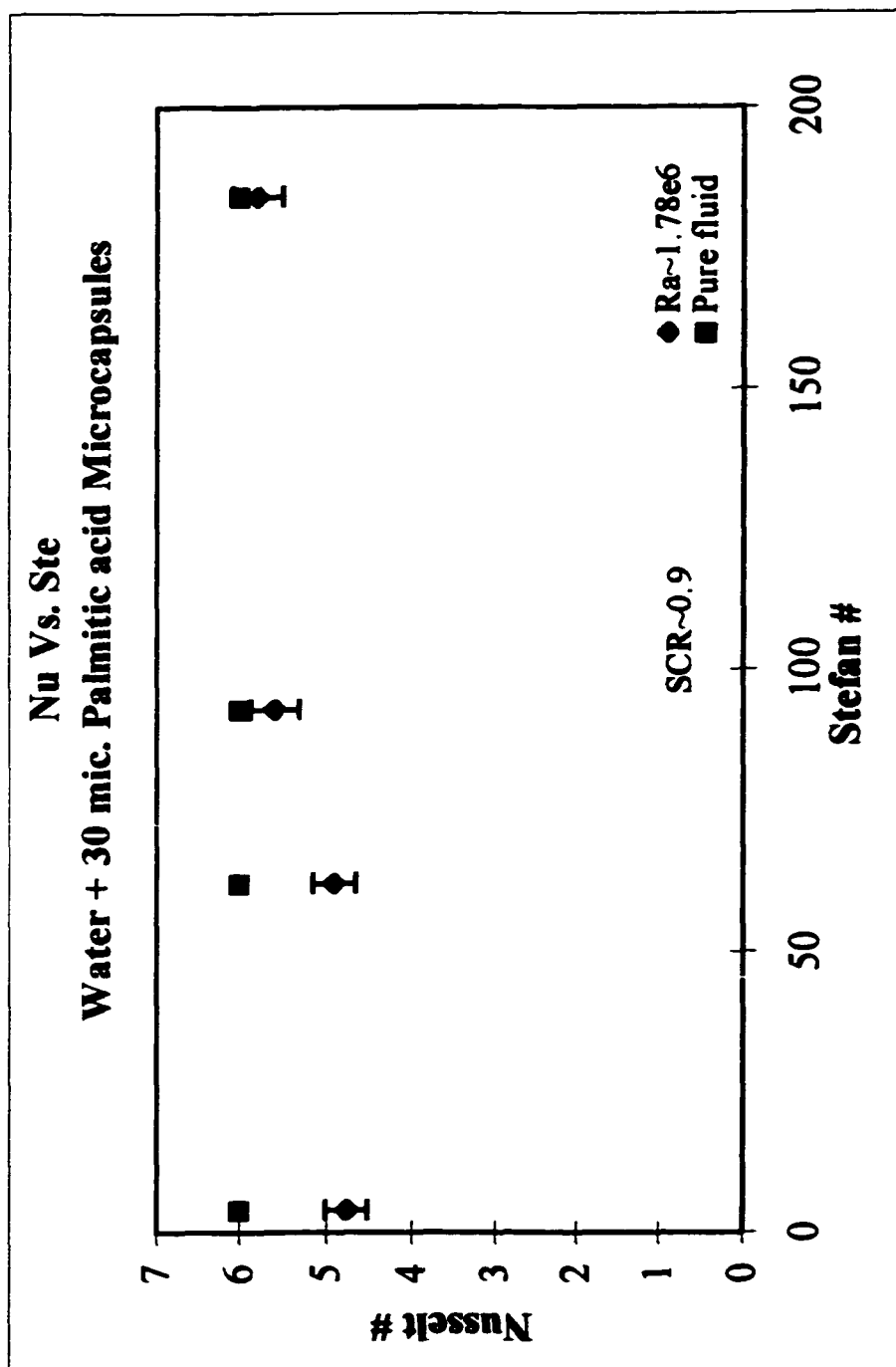


Fig 5.8 Variation of the Nusselt number with the Stefan number

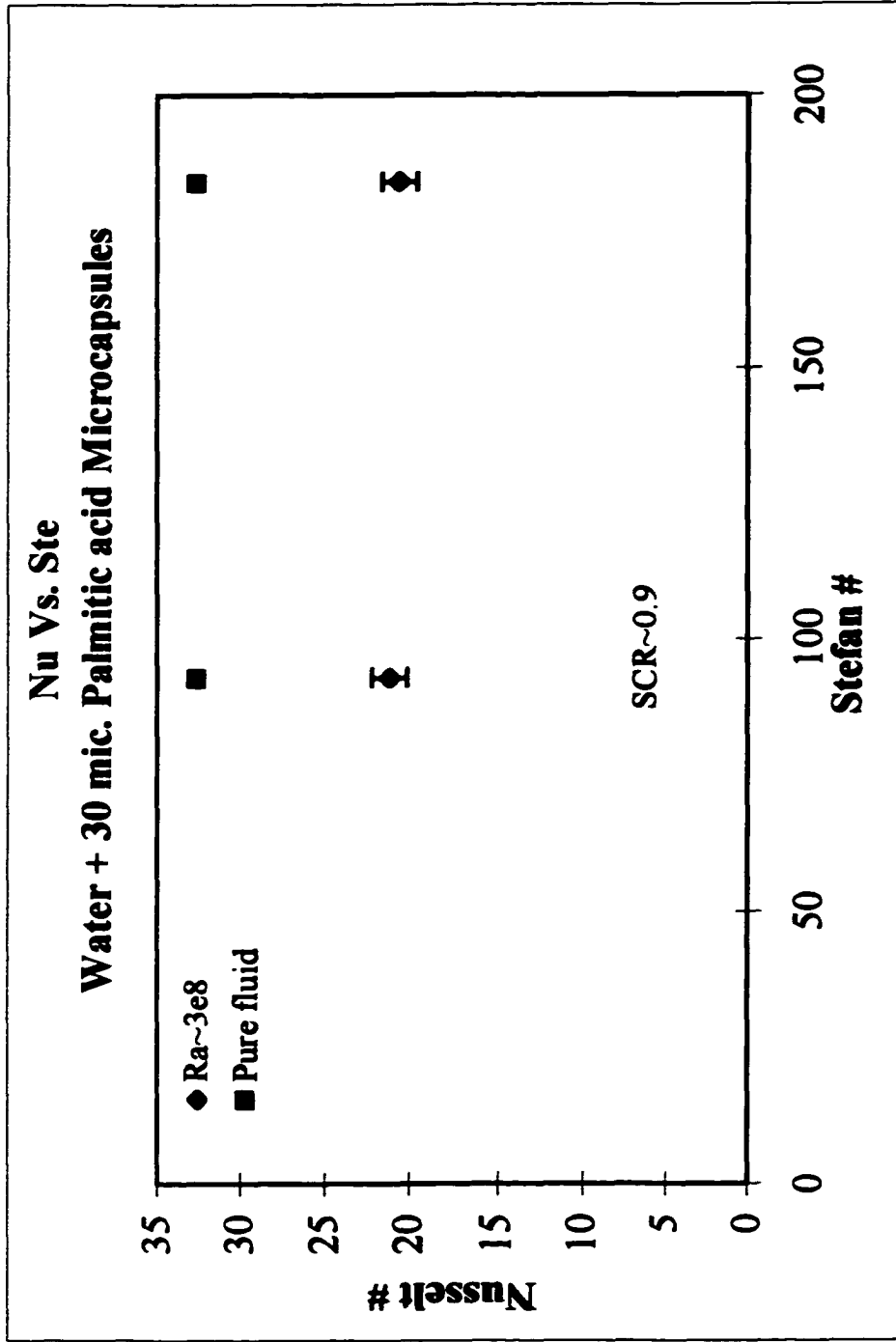


Fig 5.9 Variation of the Nusselt number with the Stefan number

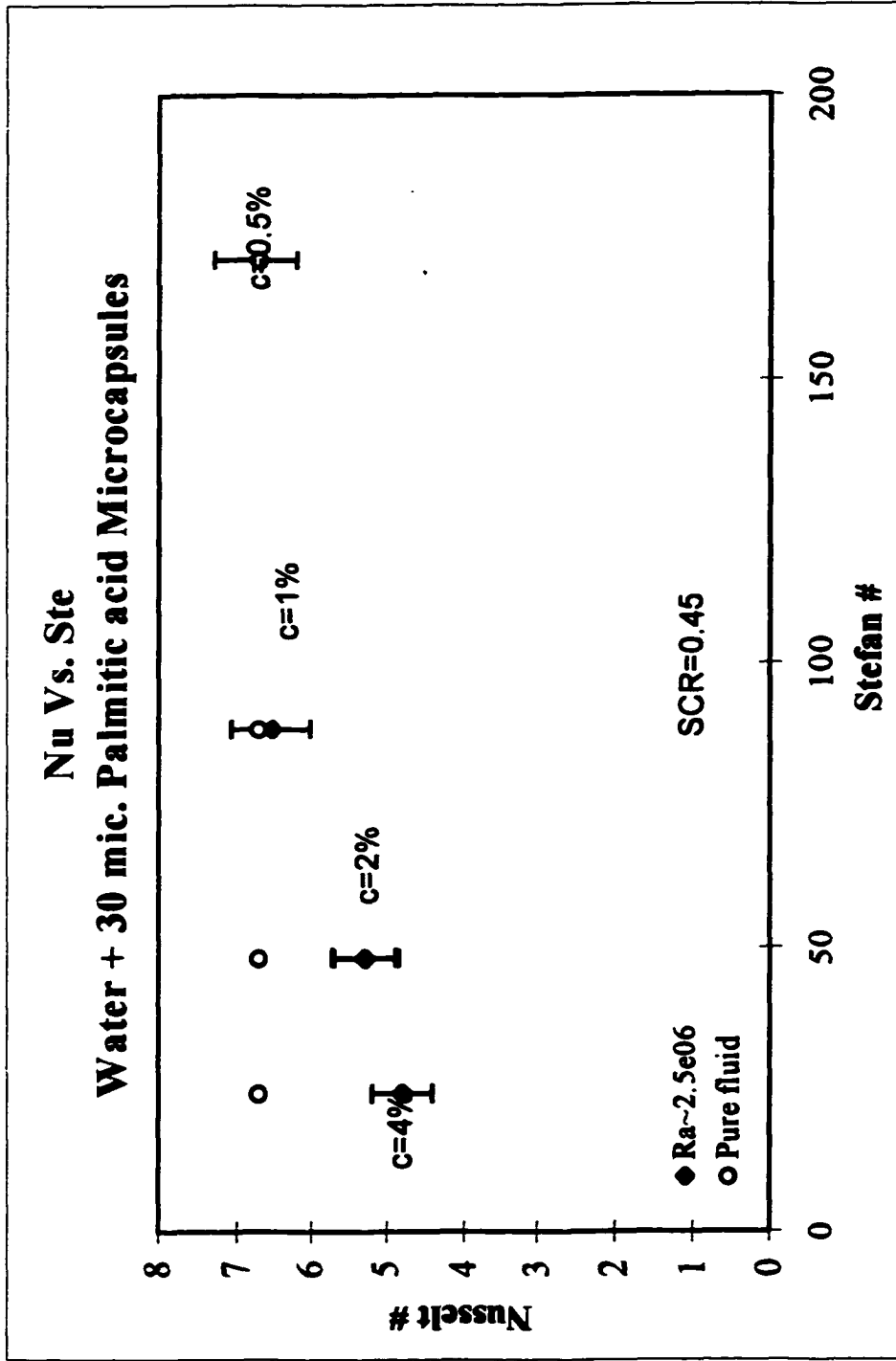


Fig 5.10 Variation of the Nusselt number with the Stefan number

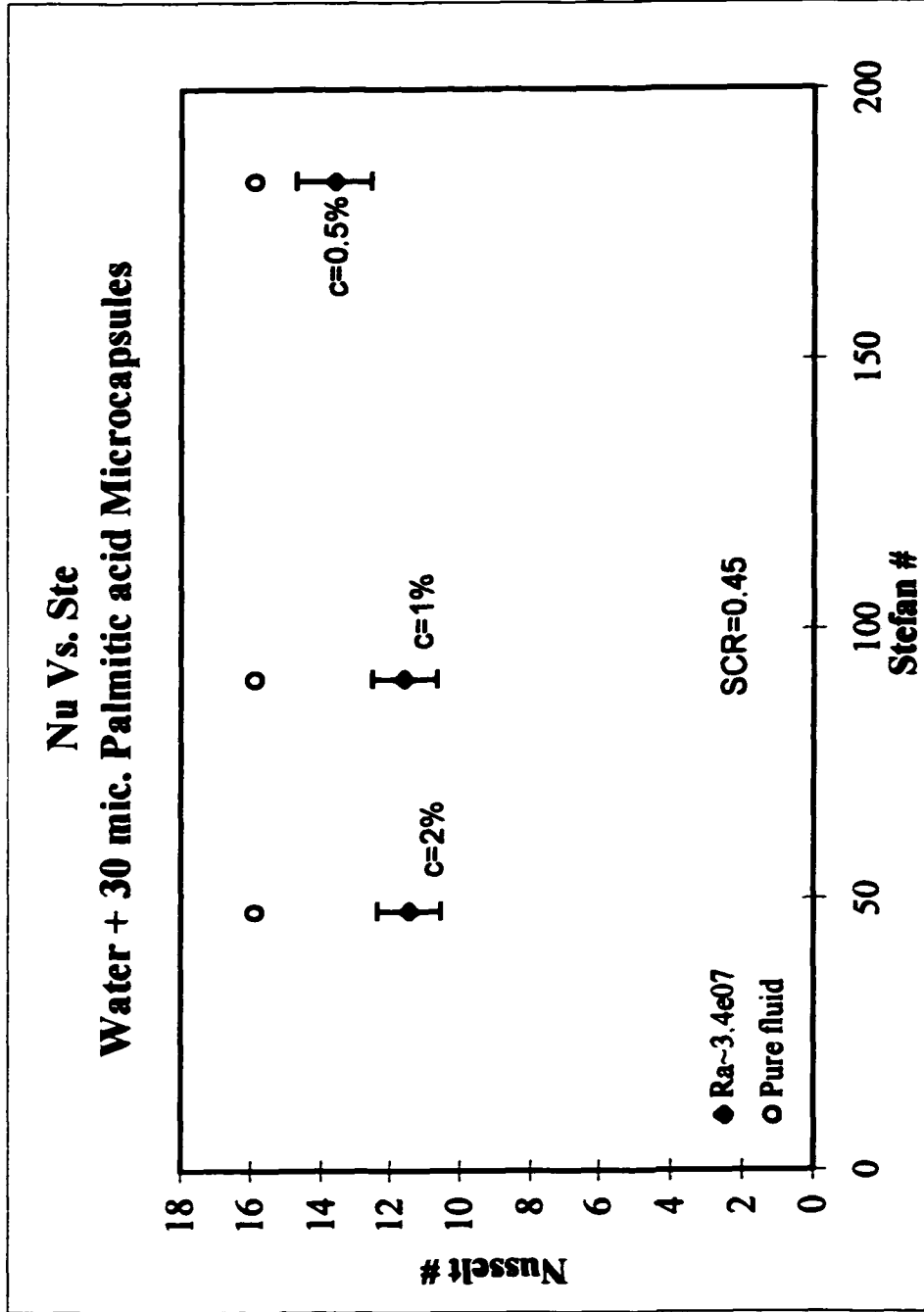


Fig 5.11 Variation of the Nusselt number with the Stefan number

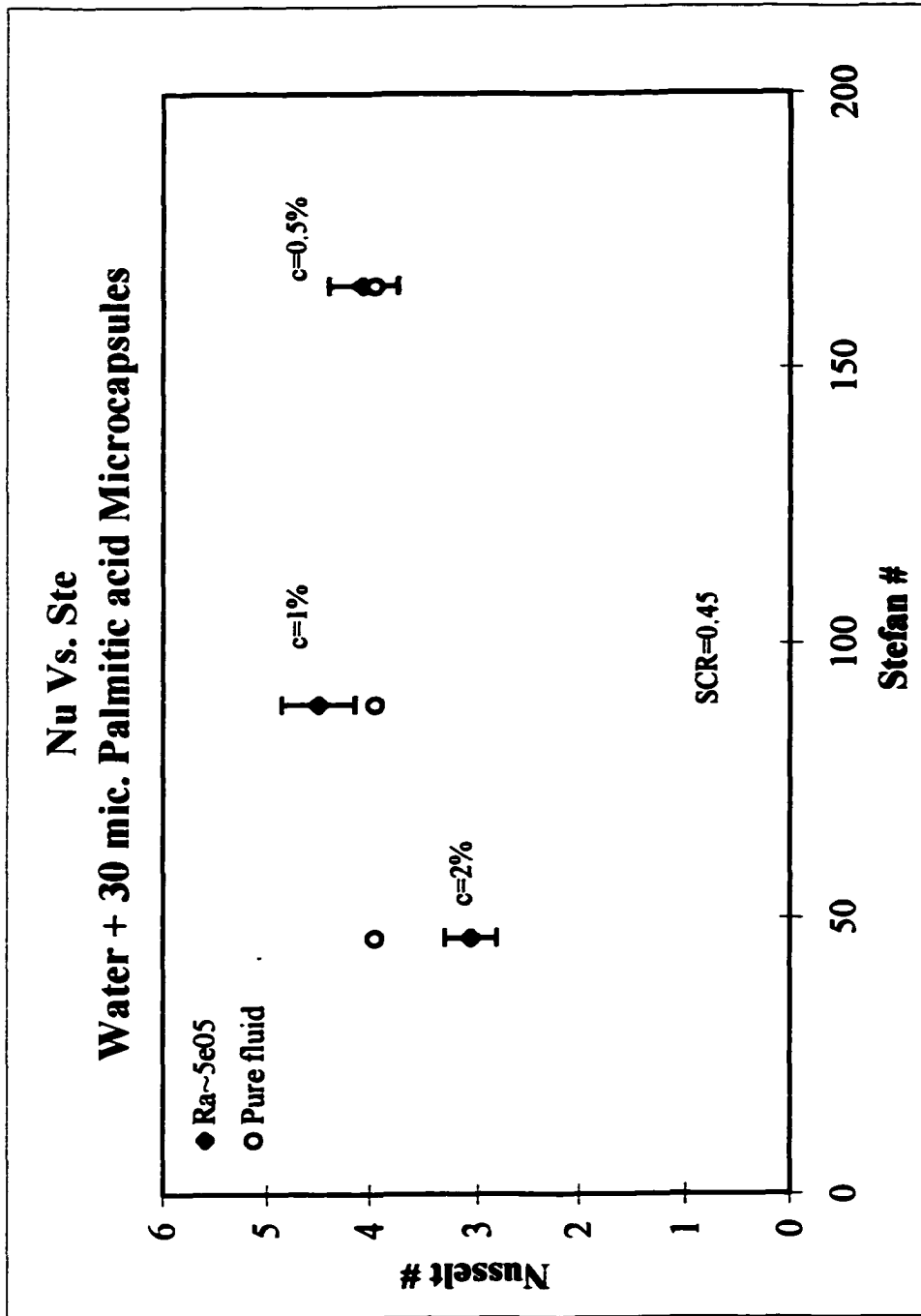


Fig 5.12 Variation of the Nusselt number with the Stefan number

5.1.2.2 Experiments with Silicone oil as the suspending fluid

The next set of experiments were conducted with a slurry which was made of PolyDimethyl-Siloxane, a silicone oil as the suspending fluid and 100 micron capsules of Myristic acid. The properties of both these phases are listed in Appendix A. The silicone oil was not a choice based on its thermophysical properties but more by virtue of a good density match with the Myristic acid microcapsules.

The MELT ZONE

The part of the cavity wherein the temperature is above the melting point of the PCM is termed as the melt zone. For natural convection experiments, this can be estimated by calculating Ra_δ . Ra_δ is defined as

$$Ra_\delta = \frac{g\beta(T_h - T_c)\delta^3}{2\alpha\nu} < 1700$$

This is the thin layer of fluid, which has remained stable (energy transfer through this layer is by diffusion) because the Ra across it has stayed below the threshold value of 1700 (for horizontally heated layers heated from below).

5.1.2.2.1 Variation of Nu with Ra

As in earlier experiments (Datta(92)), this slurry was made up of a high Pr heat transfer oil and medium sized microcapsules. The results were also similar. The slurry showed an enhancement in the heat transfer. The results plotted as Nu Vs Ra plots are presented below (Figs 5.13 – 5.19). The slurry did exhibit slightly inhibited convective strengths as compared to the water-based slurries (lower convective velocities). That

is, the same height or cavity depth resulted in about an order of magnitude lower Rayleigh number.

At higher Rayleigh numbers, the percentage increase or enhancement in the heat transfer is lower. This is possibly explained by the fact that at very low Ra, the region inside the cavity wherein melting can occur, is much larger compared to the deeper enclosure cases.

As explained previously, the melt zone is simply the stable fluid layer just above the hot wall. The depth (or height) of the melt zone is not a function of the cavity depth. It is simply the height of the fluid layer in which the Rayleigh number has not reached the threshold where convection begins and which can sustain the energy transport simply by diffusion.

As an example, the calculated melt zone depth for the silicone oil slurry case, for cavities of depth 6.3 mm and 50 mm, is about 4.3 mm. Clearly, in the latter case the particle could skim and escape the melt zone before all of it can melt. Besides, fewer particles reside in the melt zone at any given instant. It is harder to completely penetrate a thin melt zone, especially because the velocity in the deeper cavities is higher and some of the capsules are swept along just skimming the melt zone.

During the experiments it was observed that many capsules never reached the bottom of the cavity (onto the hot plate). Clearly, this meant that they were being swept along with the fluid. This leads to the issue of the amount of phase change material, which actually participates in the experiments. Section 5.1.2.6 estimates this from the experimental data.

In view of the counterintuitive results that have been obtained from the two sets of phase change slurries, further investigation is warranted. An order of magnitude estimate has been conducted in sections 5.1.2.4. and 5.1.2.5 which explains why only one slurry shows an enhancement. Figs 5.13 – 5.19 overleaf show the results obtained as Nu Vs Ra plots.

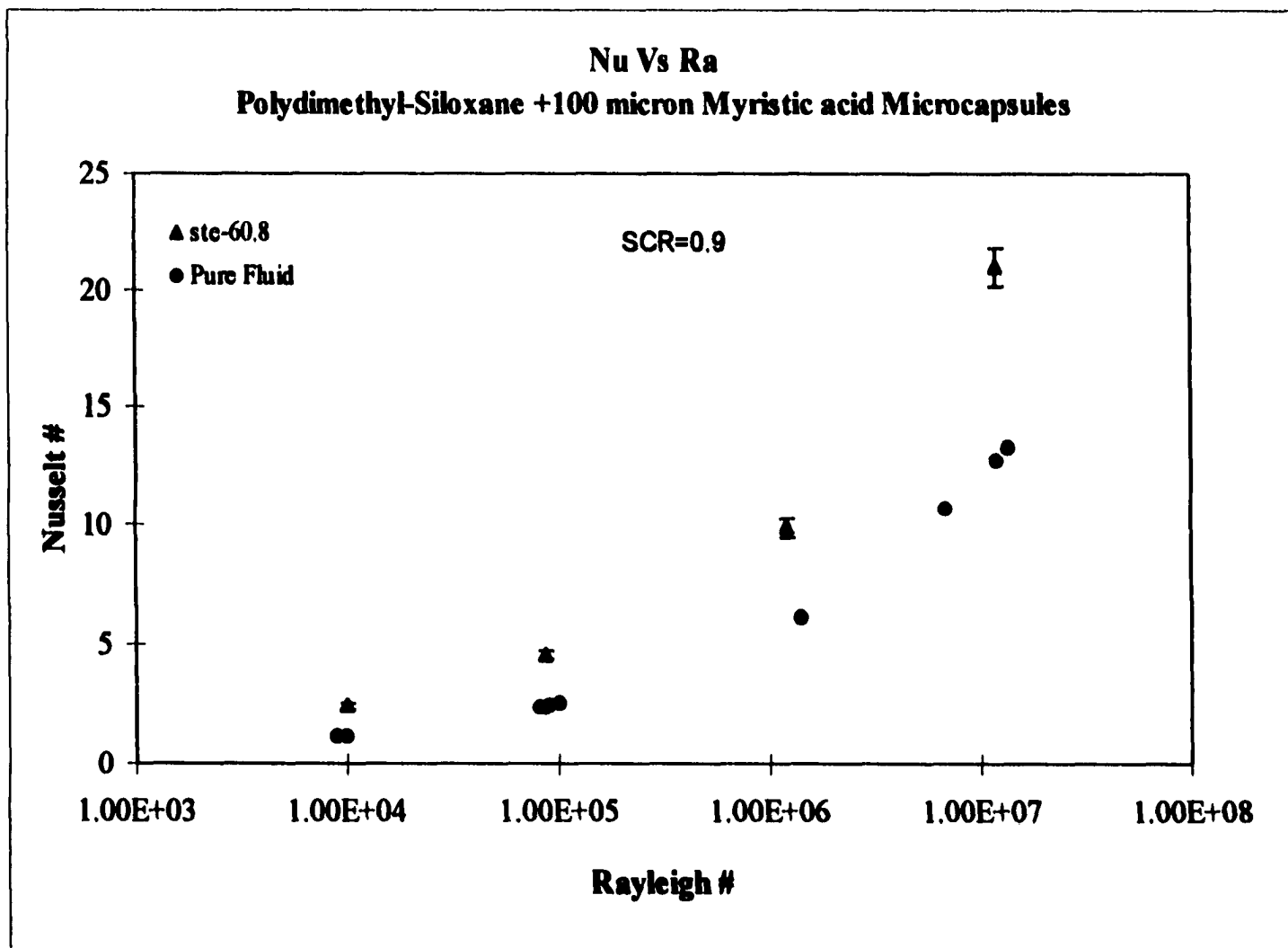


Fig. 5.13 Variation of the Nusselt number with the Rayleigh number for the silicone oil slurry.

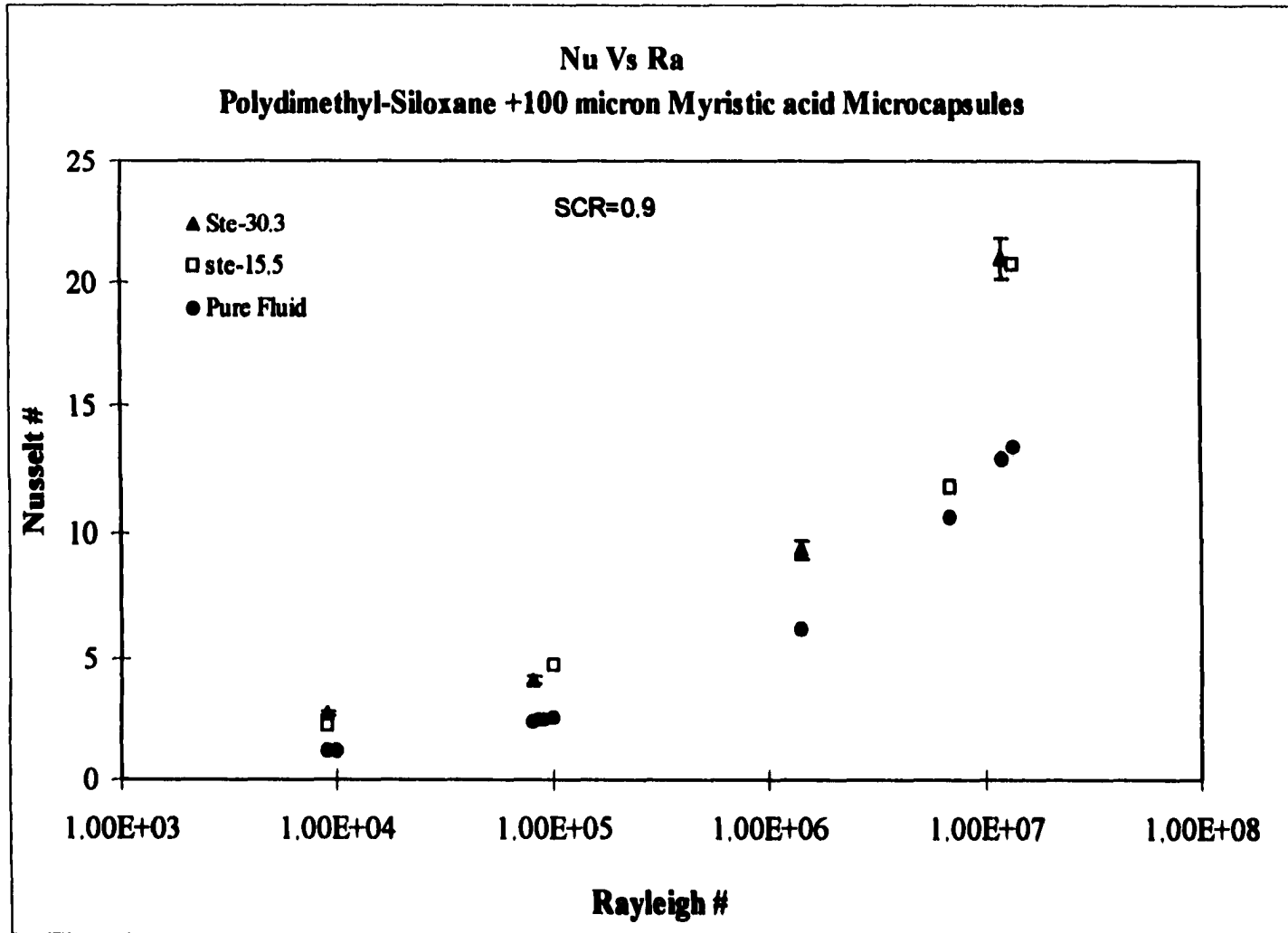


Fig 5.14 Variation of Nu Vs Ra showing heat transfer enhancement.

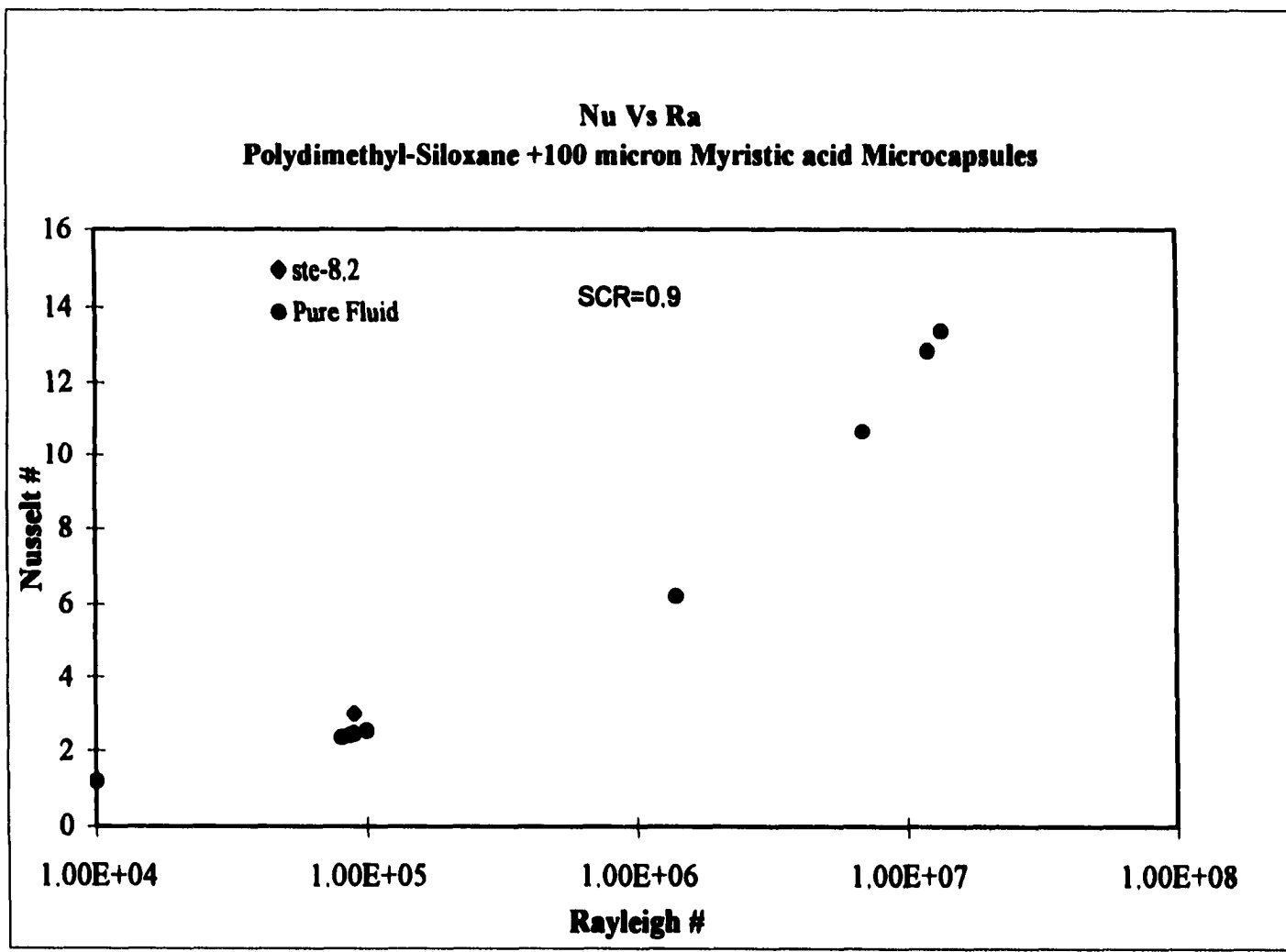


Fig 5.15 Variation of Nu Vs Ra for high concentration case.

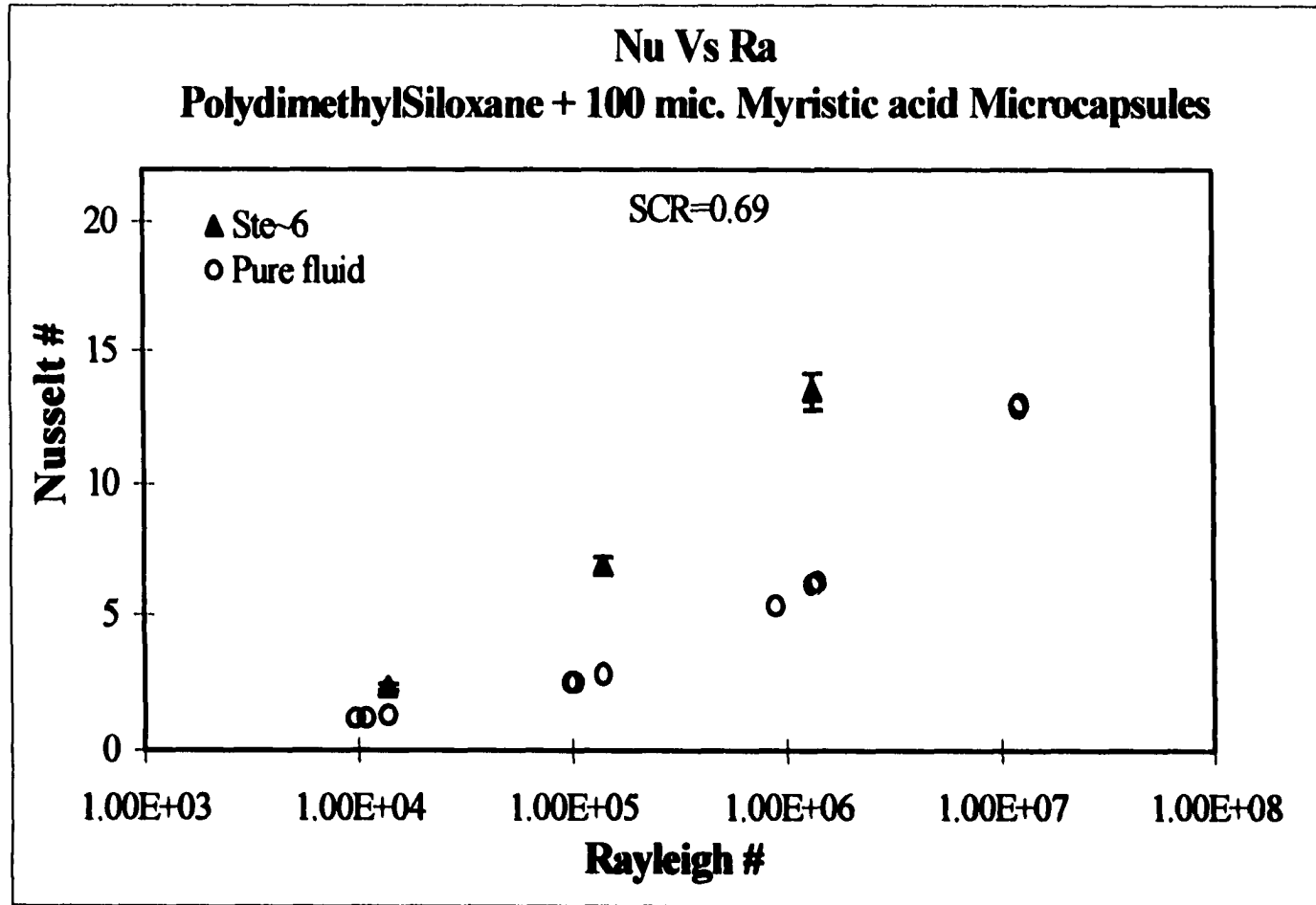


Fig 5.16 Variation of the Nusselt number with Rayleigh number.

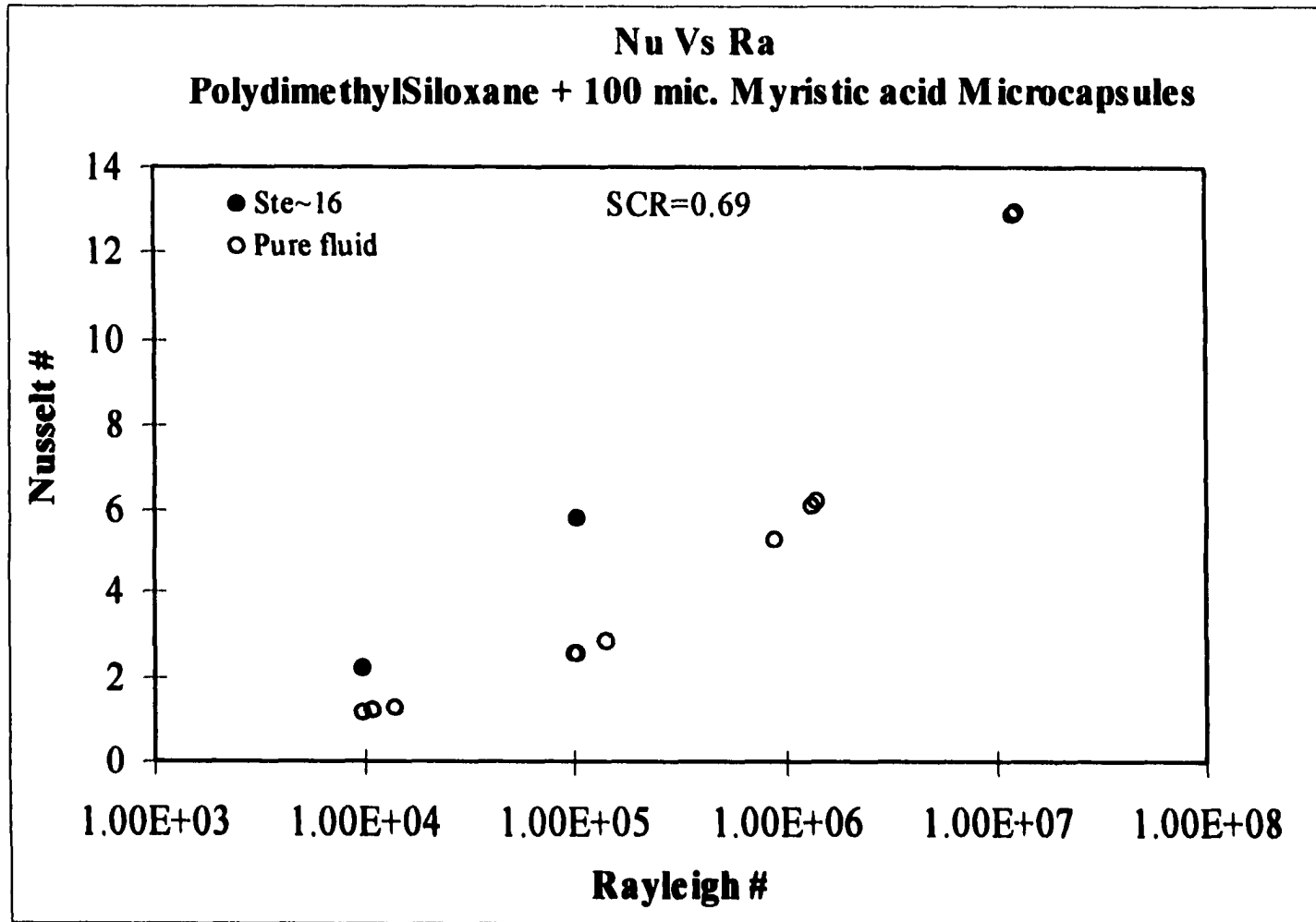


Fig 5.17 Variation of Nu Vs Ra for lower SCR and high concentrations.

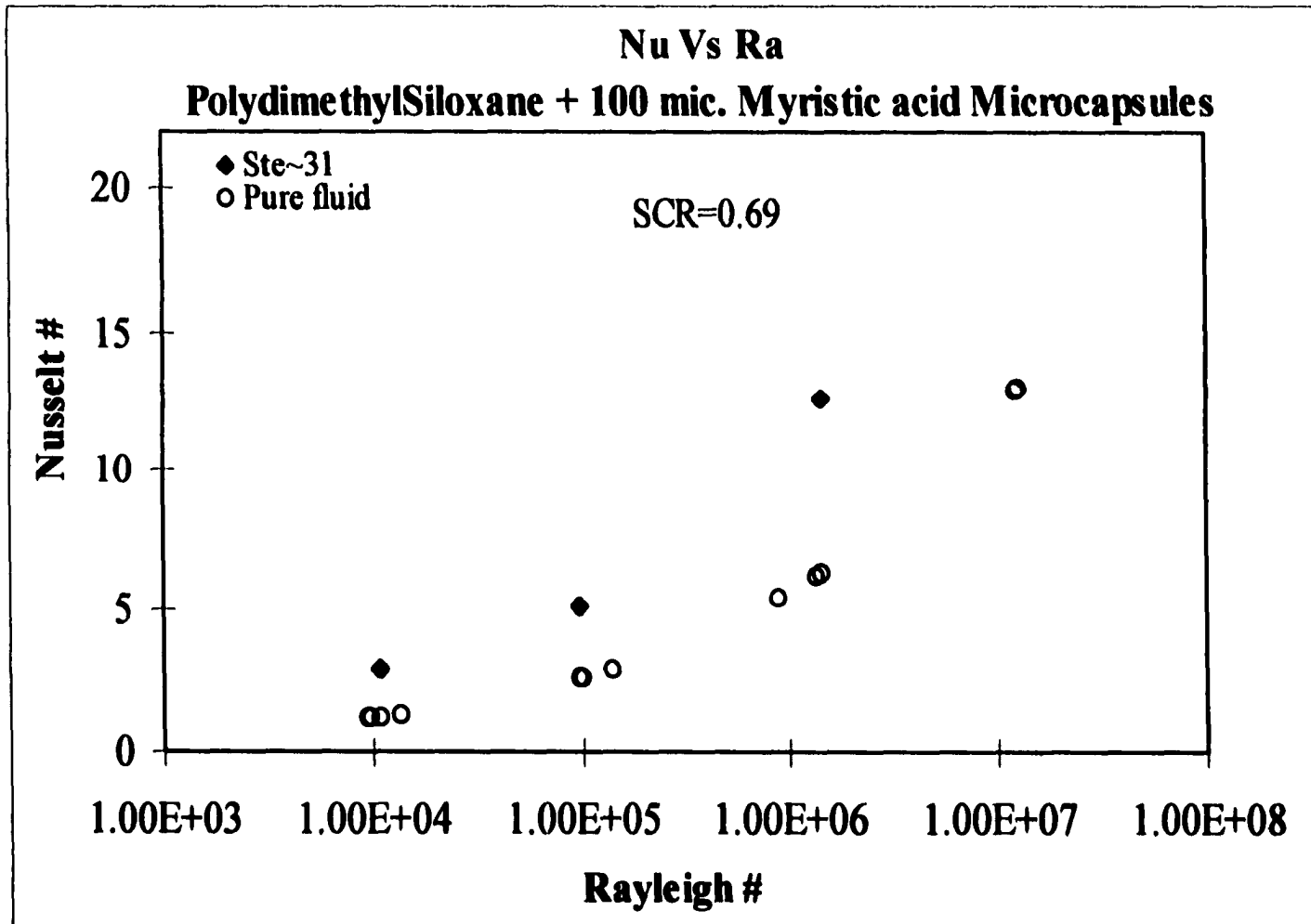


Fig 5.18 Nu Vs Ra plot for concentrations around 2%

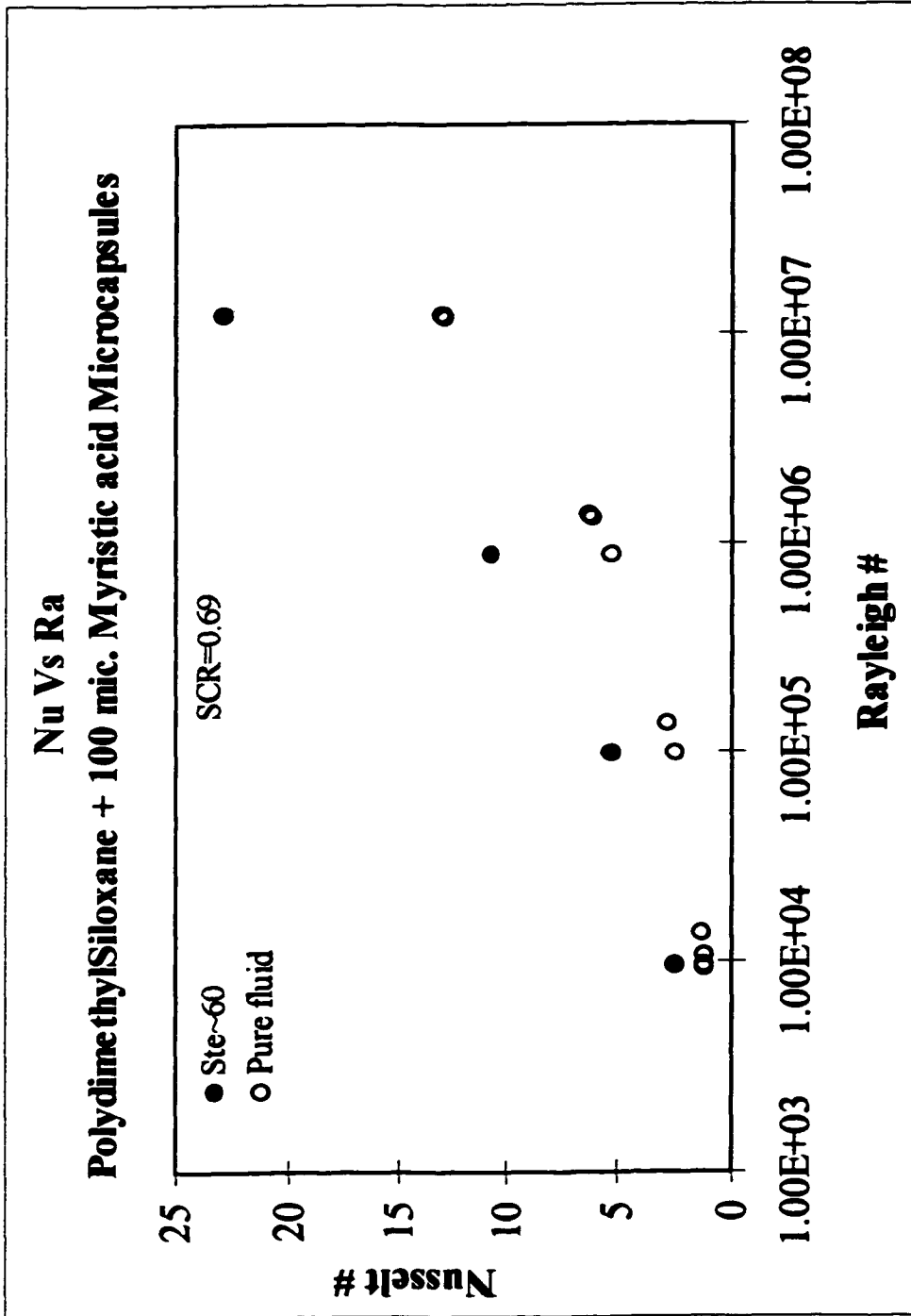


Fig 5.19 Variation of the Nusselt number with Rayleigh number at a SCR of 0.69

5.1.2.2.2 Variation of Nu with Ste

It was observed that higher concentrations did not result in equivalently high enhancements. In other words, doubling the concentration from 0.5%, to 1%, to 2%, did not cause a doubling in the heat transfer rate. Nor was there a definite trend indicating a corresponding increase in the heat transfer rate for every increase in concentration.

The Stefan number is the ratio of the sensible heat to the latent heat. Clearly, the enhancement results point to the fact that the latent heat is indeed a factor in the transport. It should be pointed out that the denominator in Ste, is the latent heat *available* in the slurry, not that which is actually used. Varying the latent heat does not in any way guarantee that the added PCM will participate in the heat transfer. In fact further analysis of the data reveals that a very small quantity of the available PCM actually ever changes phase! (Section 5.1.2.6)

The quality of the slurry is just as critical a factor as the level of concentration. That is, lower concentrations of the slurry (.5% and 1%) could have just as much of an enhancement. During the experiments it was observed that while the slurry was clearly homogeneous for the 1% and 0.5% concentration runs, the 4% concentration had a tendency to form clumps, albeit small ones. The 0.5-2% concentration range provided the best enhancements. Akino, et.al.(1994), observe that the enhancement is a strong function of the range of temperatures in which the PCM melts. PCMs, which do not have a sharp melting point, would form excellent candidates for phase change slurries. A wide range of melting temperatures implies that the PCM would be effective over a larger melt zone.

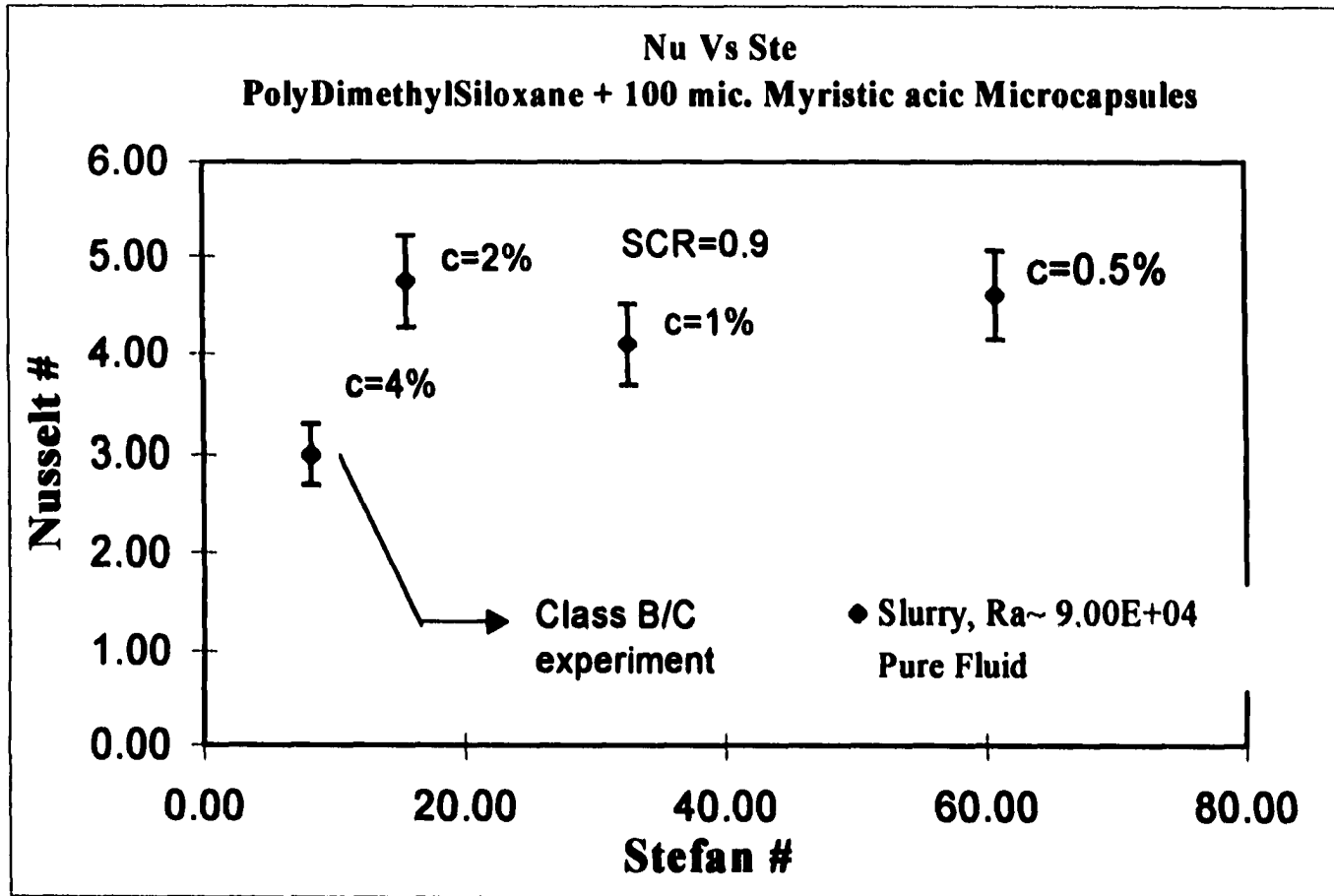


Fig 5.20 Variation of Nu with concentration (Stefan number).

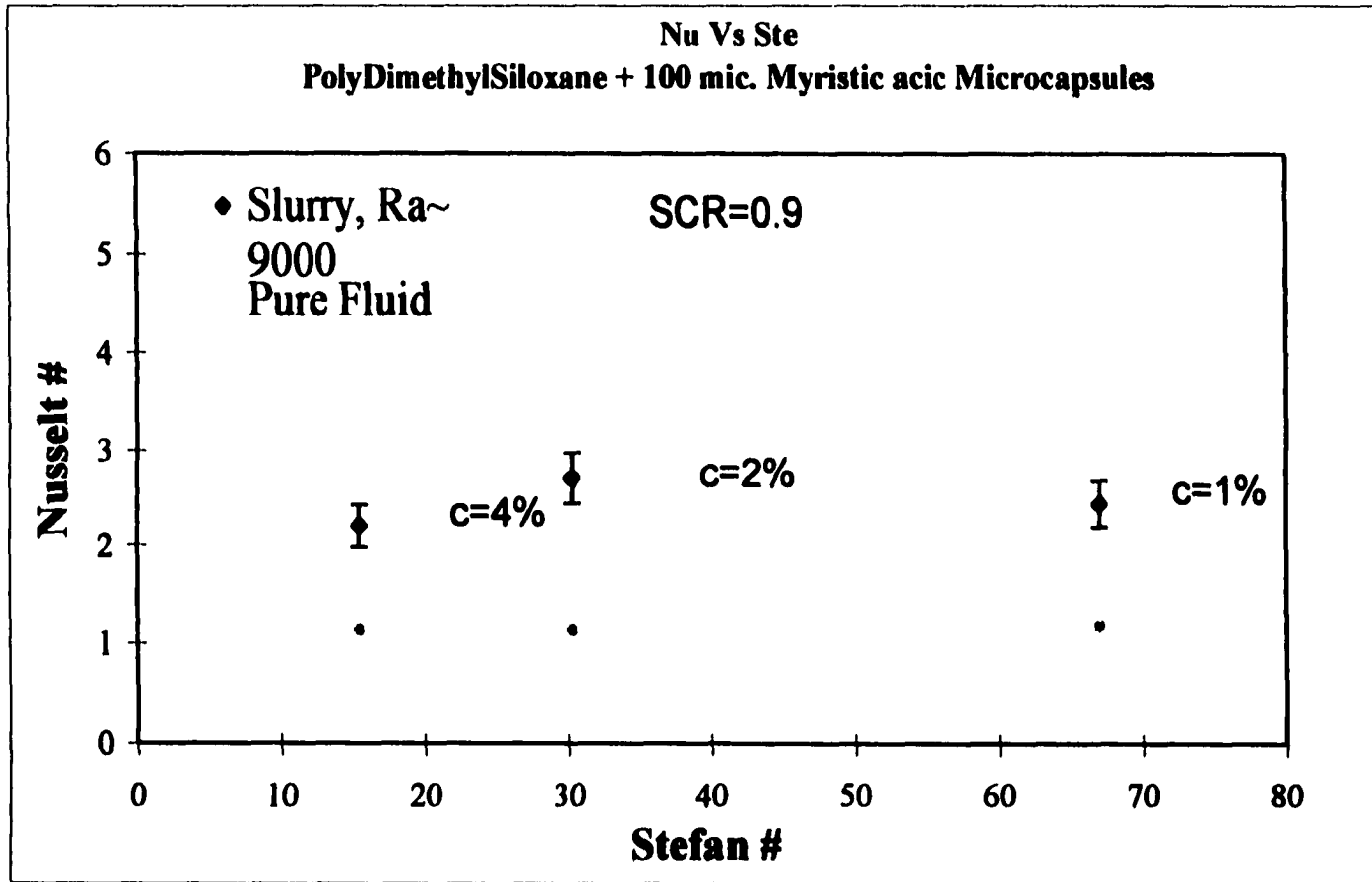


Fig 5.21 Variation of Nu with concentration (Stefan number)

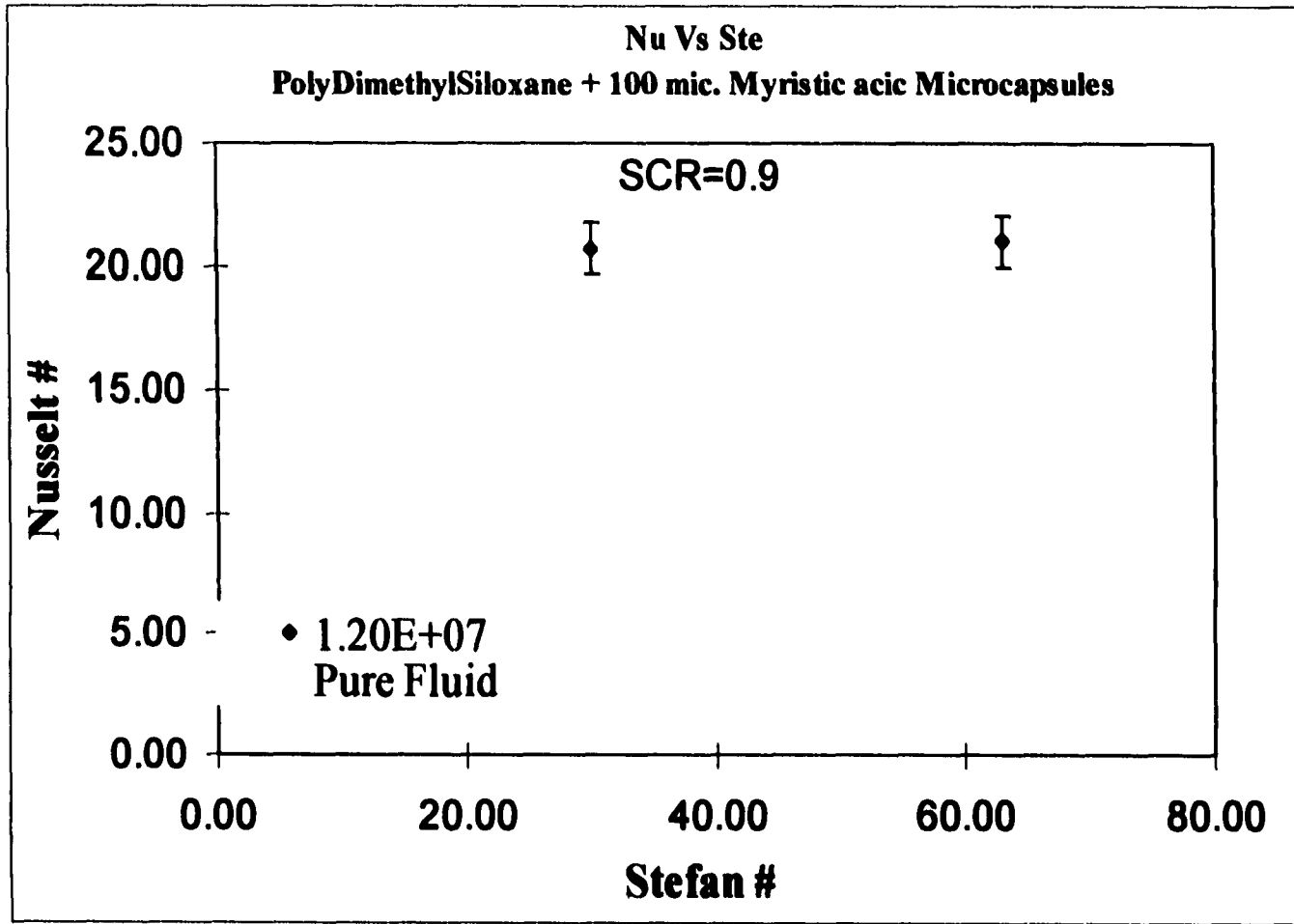


Fig 5.22 Variation of Nu with concentration (Stefan number)

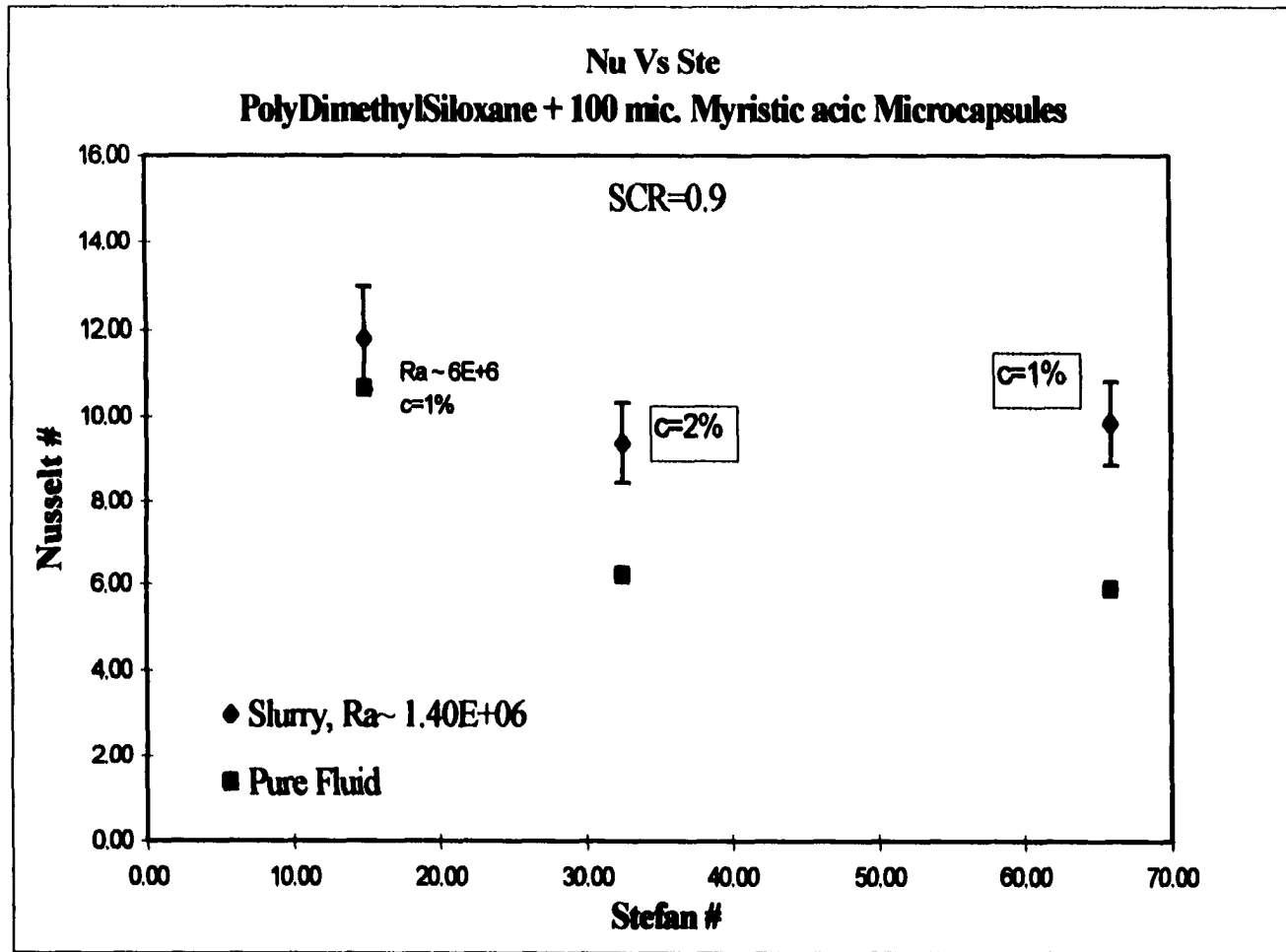


Fig 5.23 Variation of Nu with concentration (Stefan number)

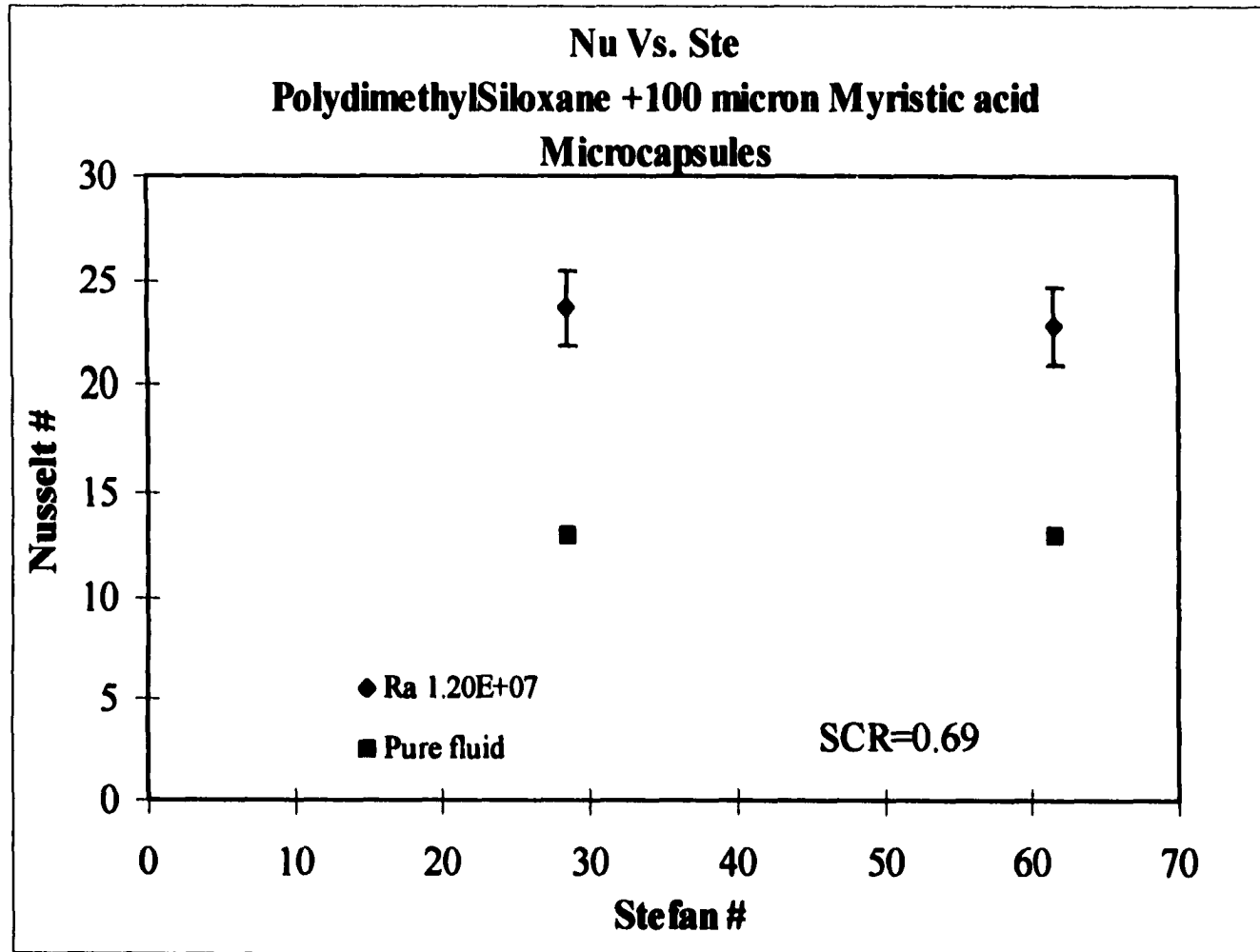


Fig 5.24 Variation of Nu with concentration (Stefan number)

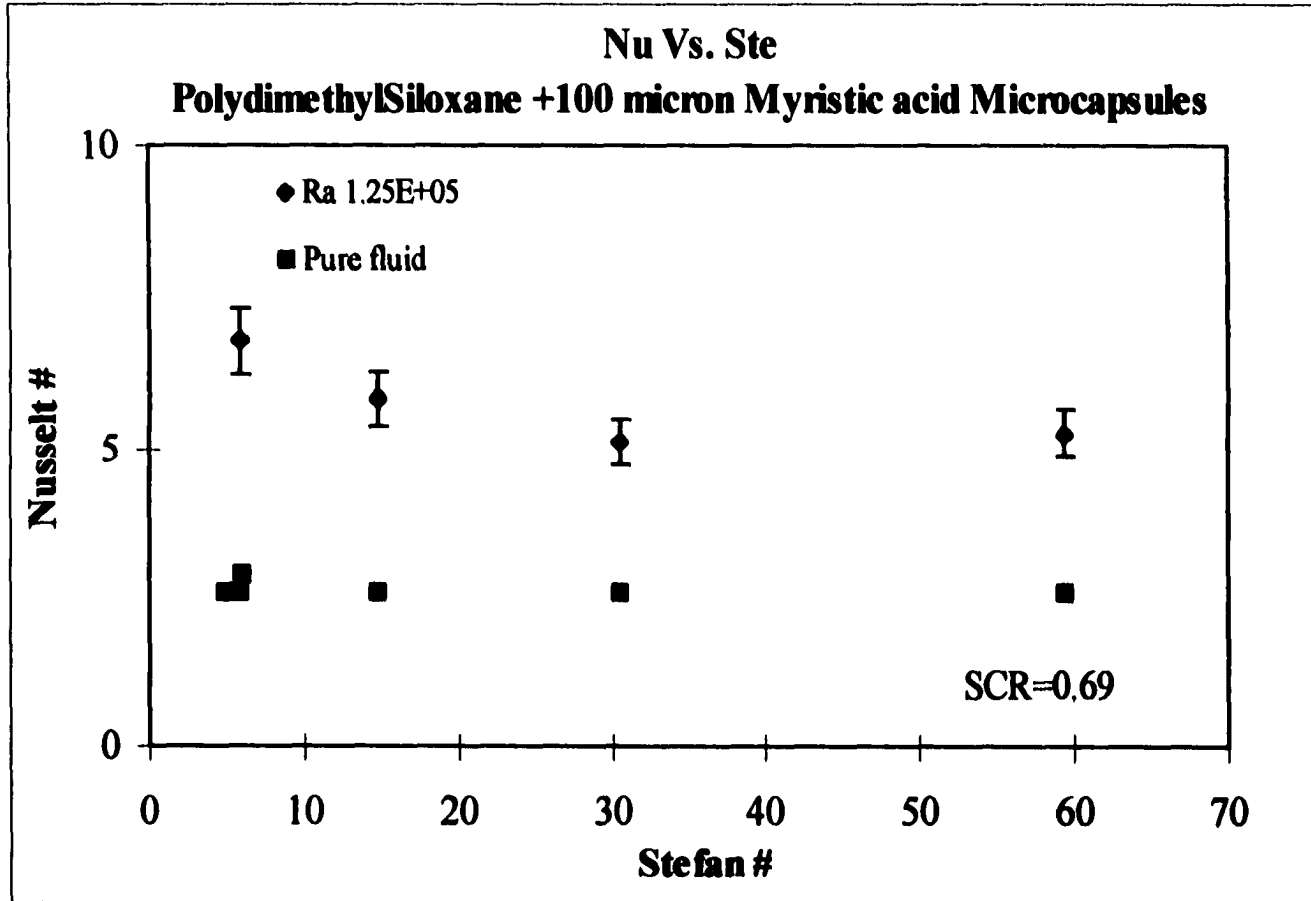


Fig 5.25 Variation of Nu with concentration (Stefan number)

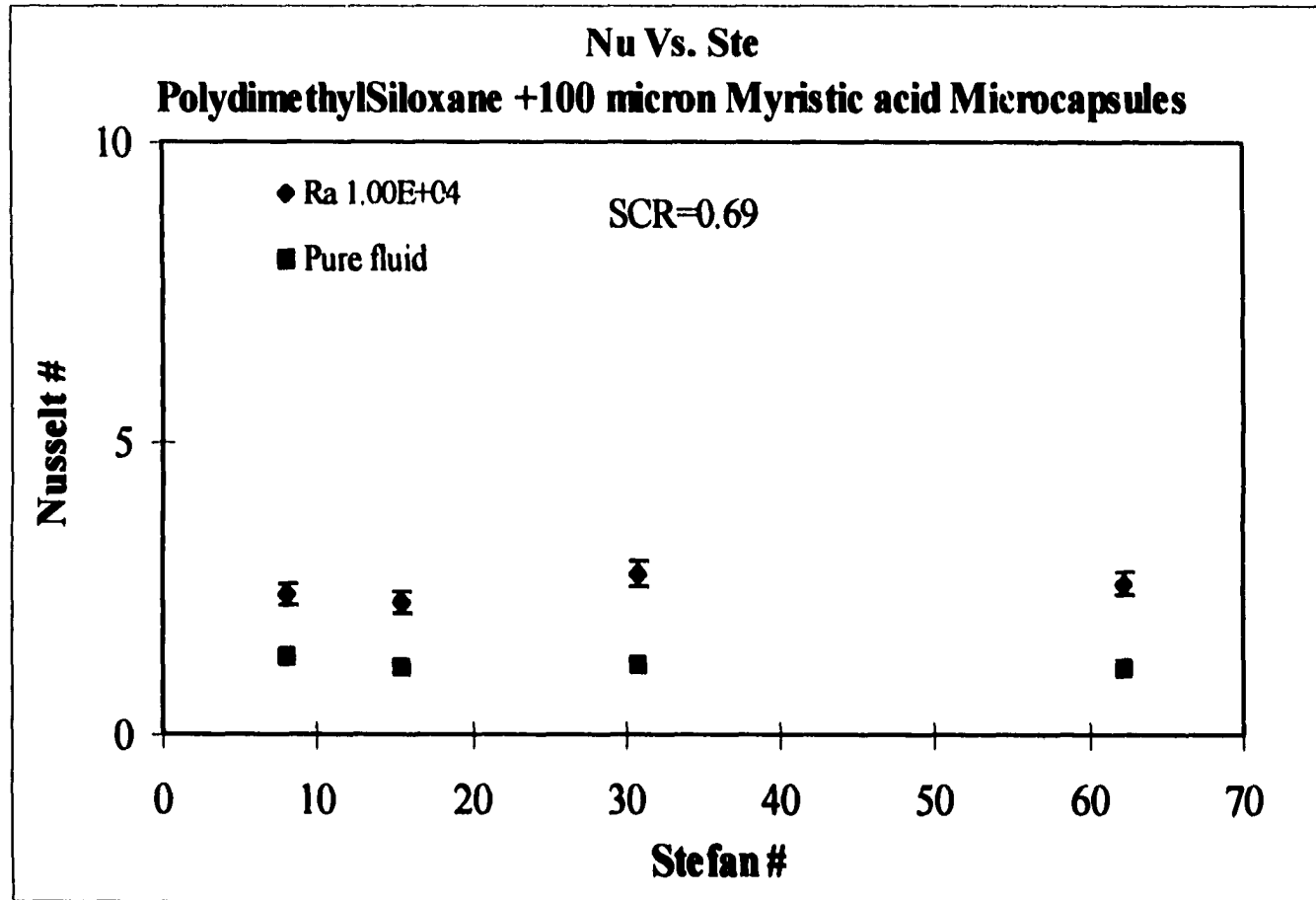


Fig 5.26 Variation of Nu with concentration (Stefan number)

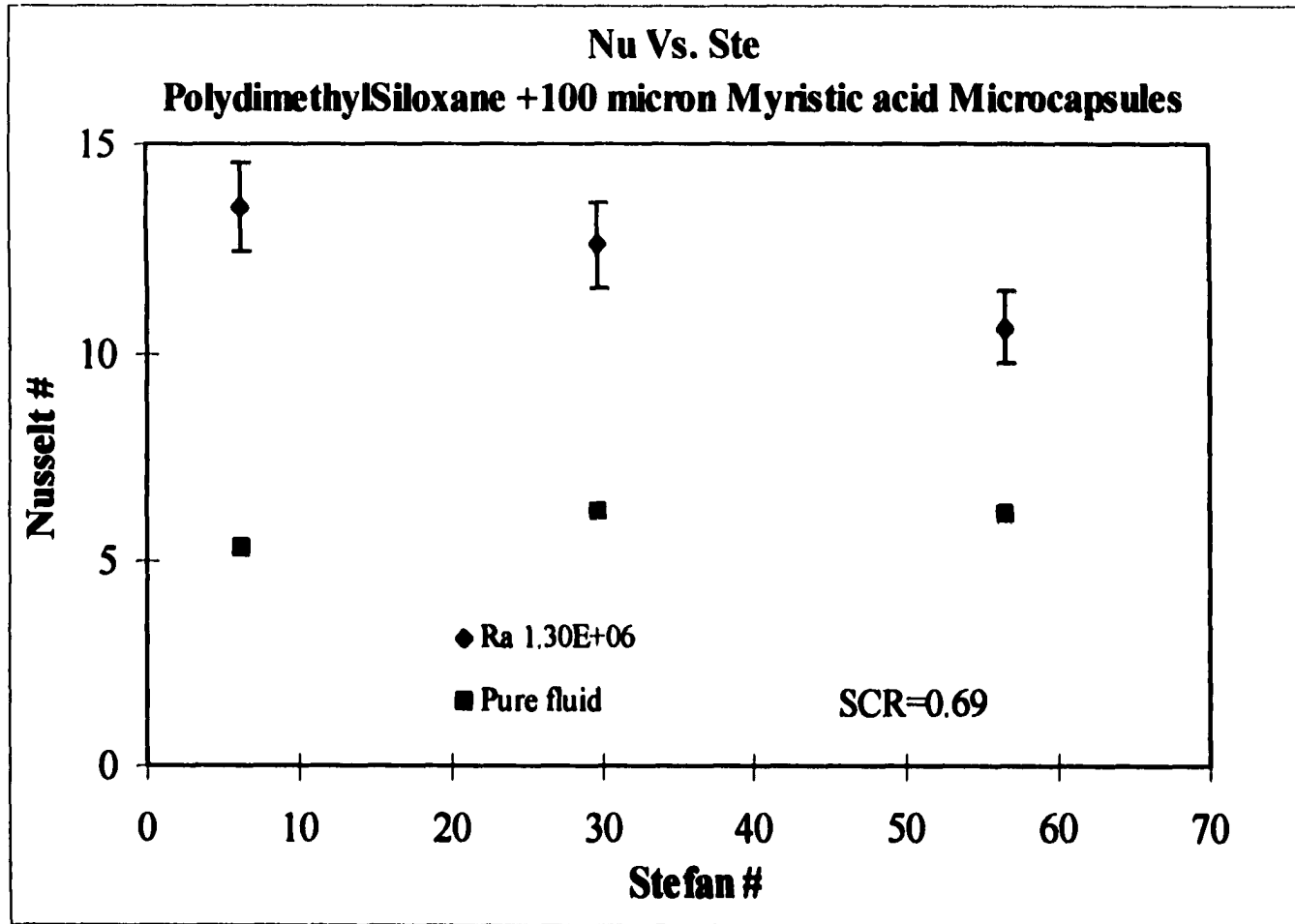


Fig 5.27 Variation of Nu with concentration (Stefan number)

5.1.2.3 The competing phases

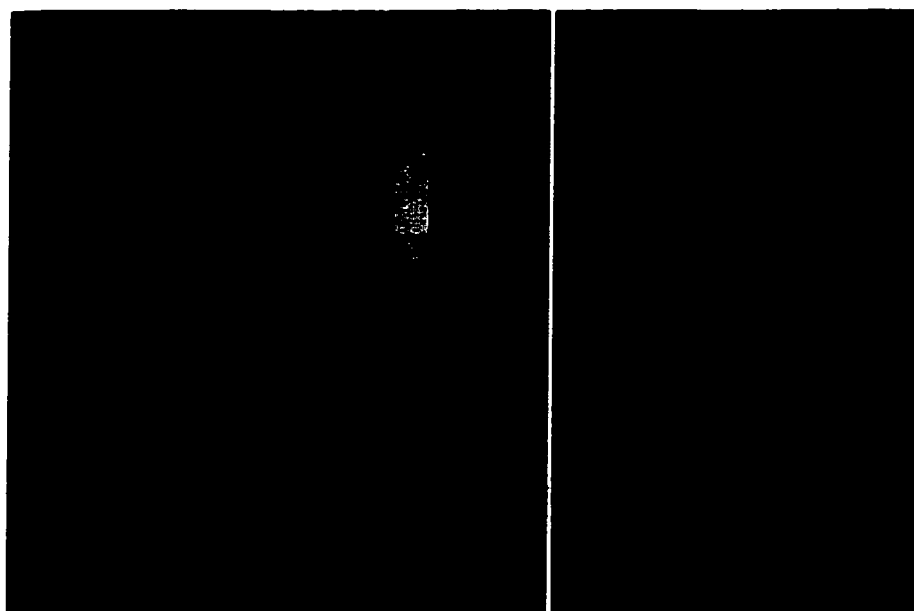
An order of magnitude analysis was performed to study if the particles were indeed undergoing phase change. The micro-capsules used in the study, are very small (30 and 100 microns) and have a density very close to that of water (the suspending fluid). This allows many of them to be swept along with the flow (typical relaxation¹ times are of the order of 10^{-3} s).

The energy transport in this problem occurs through the working fluid and the micro-capsules. The micro-capsules are therefore competing for the energy that passes through them with the coolant around them. The percentage of energy that passes through a phase would depend on the “thermal incentive” offered by that phase as compared to the other.

If “ ϵ ” is defined as the ratio of the heat flux entering the particle to the total heat flux transferring through the fluid layers, comparing ϵ % for different slurries would quantify the effectiveness of one slurry over another. An order of magnitude numerical estimate has been used to quantify the effectiveness of the particles when used with different suspending fluids. The figure below shows the computational domain used in this analysis.

The sphere shown is a single 100 μm micro-capsule (core + resin). Modeled around the sphere is a box of fluid. It has been assumed that the fluid around the capsule is frozen (the conduction limit) and that diffusion is the only mode of energy transport. The lower wall has been subject to an iso-flux (50000 w/m^2) boundary

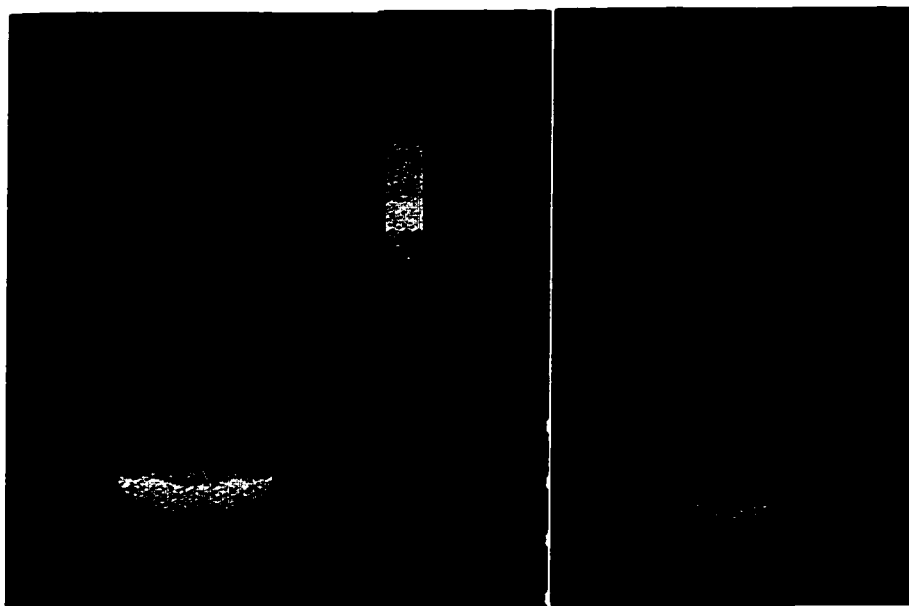
¹ If a particle is released into a freely flowing stream of fluid, *Relaxation Time* may be defined as the time it would take the velocity of the particle to approach 99% of the background fluid stream.



Myristic acid + silicone oil

Myristic acid + water

Fig 5.28 Material property contours showing the thermal conductivity variation through the capsule and the fluid



Myristic acid + silicone oil

Myristic acid + water

Fig 5.29 Contour plots showing the heat flux (w/m^2) entering the capsule cores

condition, (the value was chosen to give the capsule a realistic temperature gradient as was observed in the experiments), while the upper boundary is isothermal (300K). The heat flux through the capsule is surmised in Table 1 below.

Clearly, a larger heat flux enters the capsule for the Siloxane slurry as compared to the water based slurry (the contours on the left plot show higher values on the lower hemisphere of the capsule).

Case	$K_{particle}/K_{fluid}$	Heat flux through the floor (W/m^2)	Heat flux entering the capsule core(W/m^2)	ϵ %
Water + capsule	.25	50000	70	0.14
S'Oil + capsule	1	50000	609	1.22
Fluid + capsule	10	50000	1279	2.56

Table 5.1 Heat flux values as capsule properties vary compared to the background fluid

The percentage of heat flux entering the capsule core is almost an order of magnitude greater in the oil based slurry compared to the water based slurry.

Clearly, the results with water show that the significantly reduced participation of the suspended phase results due to the suspended phase losing out in the transport race. This translates into a detriment in the heat transfer. Most of the energy transfers through the background fluid and relatively little diffuses into the particles. Thus, the particle cores do not melt and the suspended phase only contributes to an increase in viscosity. Indeed, in many of the experiments with water, it was observed that the particles had a tendency to sediment in the fluid and many of them resided in the lower layers of the slurry.

5.1.2.4 Idealized estimate of the phase change per capsule

For most of the experiments (except the lowest Ra cases), the melting process would occur only in the region of the fluid close to the lower wall. This is because it (the melt zone), is the only region at, or above the melting point of the PCM. In any event, the process is not instantaneous and has a time lag (a thermal inertia), which is a function of the thermal diffusivity of the microcapsule. Physically this is a measure of the time that it would take a heat front to reach the core of the particle from the ambient fluid, which surrounds it.

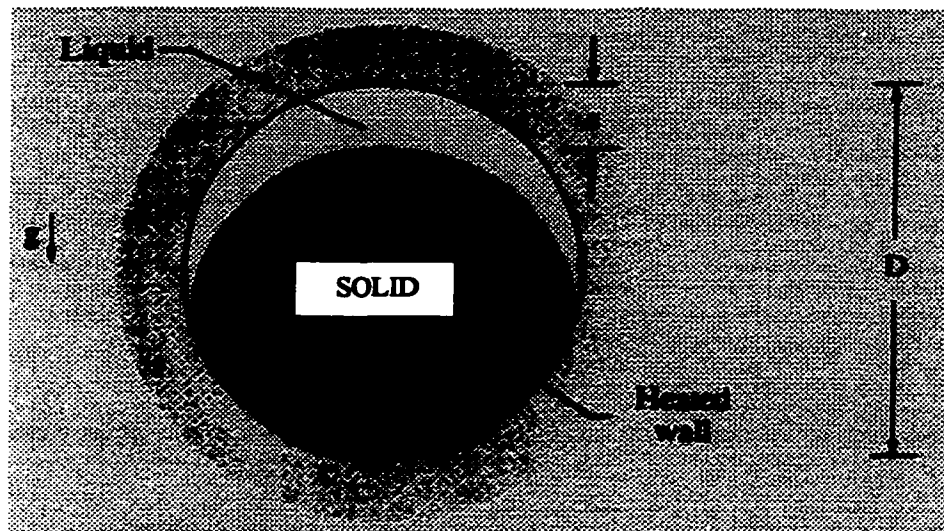


Figure 5.30 Schematic of a microcapsule melting (Bejan 1995)

The analysis shown below estimates the percentage of phase change material that is actively participating in the transport. Considering a single particle, and assuming that conduction was the only mode of energy transport, the diffusive time for a particle to completely melt could be written as follows :

$$t_{diffusive} = \frac{t_{wall}^2}{\alpha_{wall}} + \frac{(D - 2t_{wall})^2}{\alpha_{core}}$$

Where, “t” is the thickness of the resinous shell and “D” is the diameter of the particle. Figure 5.1 shows the schematic of a partially molten particle. The reason for using “D” as the length scale can be clearly understood from this schematic.

The above equation does not take into account the effect of the actual phase change. While a material undergoes phase change, the thermal lag increases due to the extra time taken to break the inter-molecular bonds in the solid (the situation is also observed during freezing). In addition to the time lag due to phase change, the particle is in relative motion with the suspending fluid due to the buoyancy effect (as more of the core melts, the particle becomes lighter than the suspending fluid).

Using a (2D) scaling analysis, assuming axisymmetry, a relationship can be developed for the phase change diffusive time. For the first step only the core of the capsule is considered. If “ δ ” is the film thickness between the solid and the wall and “D” is the diameter of the particle core, u and v are the tangential velocity components, then using the mass, momentum and energy equations one could obtain:

$$u\delta \approx vD \quad \text{from the mass balance}$$

$$\frac{\Delta P}{D} \approx \mu \frac{u}{\delta^2} \quad \text{from the momentum balance,}$$

$$k \frac{\Delta T}{\delta} \approx \rho_s L V m \quad \text{The energy balance at the melt front}$$

Where, ΔT is the temperature difference between the heated capsule wall and the film.

where the LHS can also be written as

$$\frac{\Delta P}{D} = \frac{g \Delta \rho^2 D / 3}{D} \quad (\text{in the case of a sphere})$$

On eliminating u and δ , and non-dimensionalizing with respect to the core diameter D (Bejan 1995), the above relations yield:

$$\frac{vD}{\alpha} = \left(\frac{\rho}{\rho_s} Ste_p \right)^{\frac{3}{4}} \left(\frac{\Delta P D^2}{\mu \alpha} \right)^{\frac{1}{4}}$$

Where Ste_p is defined as:

$$Ste_p = \frac{C_p (T_{\text{ambientfluid}} - T_{\text{melting}})}{L}$$

The particle stefan number, is a measure of the sensible to latent heat stored in the particle. In addition, the effect of gravity inside the sphere (the solid core sinks to the bottom, as shown in Fig 5.30), can be quantified by a particle Archimedis number Ar_p ,

$$Ar_p = \left(1 - \frac{\rho}{\rho_{PCM\text{solid}}} \right) \frac{gR^3}{v^2}$$

and a particle Prandtl number Pr_p defined as: $Pr_p = \frac{v_{\text{liquidPCM}}}{\alpha_{\text{liquidPCM}}}$

Using these quantities and the equation for $t_{\text{diffusive}}$ the melt time can be written as :

$$t_f \sim \underbrace{\frac{d^2}{\alpha_{\text{resin}}}}_{\text{Wall}} + \underbrace{\frac{D^2}{\alpha_{\text{PCM}}}}_{\text{Particle}} \underbrace{\left(\frac{\rho}{\rho_s} Ste_p \right)^{\frac{3}{4}}}_{\text{Melt lag}} \underbrace{\left(Ar_p \cdot Pr_p \right)^{\frac{1}{4}}}_{\text{Nat conv effect}}$$

In addition to the above (order of magnitude) estimate derived for the melt front to advance a distance “d” it is also possible to estimate the time the particle would reside in the actual “melt zone” of the PCM core.

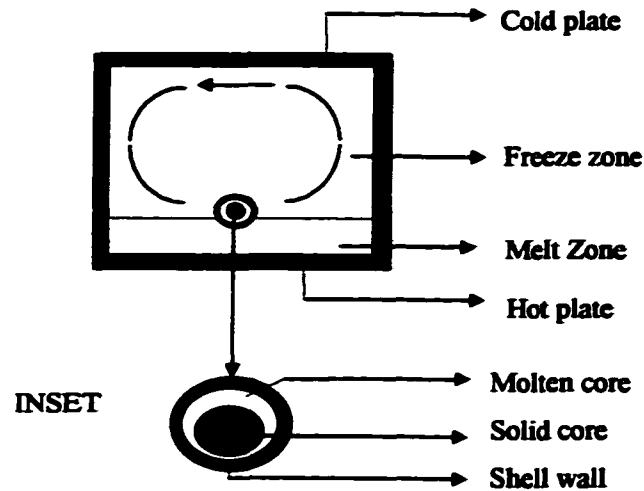


Fig 5.31 Schematic of the test section showing the melt and freeze zones.

Typical convective velocities observed during the experiments were about 1-5 mm/sec ($Ra \sim 10^6$) to 1cm/sec ($Ra > 10^8$). Using the estimate of the diffusive time obtained above and simplified particle dynamics, the “*resident time*” of a **SINGLE** particle in the melt zone can be estimated. From this estimate, the amount of PCM that actually melts in each particle (and in the slurry) can be obtained.

Given below is a simplified free body diagram of a single capsule. A force balance at any point yields the following :

Resultant force on the particle = (Effective Buoyancy force – weight of the particle)

Where the Effective buoyancy force is the resultant of two forces:

- (a) Buoyancy force on the particle due to the change in the particle's density
- (b) Drag on the particle due to the slip between itself and the background fluid

For the limiting case where there is no slip between the two phases, the effective buoyancy force is simply the buoyancy induced by the change in phase. For this particular case, the expression for the acceleration of the particle is:

$$a = g \left(\frac{\rho_{fluid} / \rho_{pccm,eq}}{\left(\rho_{pccm,fluid} / \rho_{pccm,eq} - 1 \right) \left(\frac{r_i}{r_p} \right)^3 + 1} - 1 \right)$$

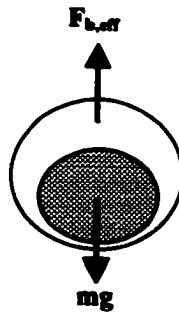


Fig 5.32 Free body diagram showing the forces acting on the particle

The radius r_i is a function of "s". for the purpose of this approximate estimate

$$r_i \approx r_p - \frac{s}{2}$$

the value of r_i is defined as:

Using the above equations for “ t_f ” and the acceleration “ a ” the amount of PCM that actually melts can be. A plot for the “no-slip” case is presented in Fig. 5.33

Clearly from the above plot, the capsule cores never melt entirely. This is quite coincidentally unavoidable. Since the particle density (wall+core) has to be greater than that of the background fluid density with a solid core and less than with a liquid core. Once enough of the particle has melted, it begins to shoot out of the lower fluid layers till enough of it begins to freeze again and it slows down and falls back. There is an upper limit to the amount of the capsule core that actually changes phase.

The melt zone never advances beyond a value of 50% of the capsule diameter, (even for very low background fluid velocities, when the particle residence time is at its maximum), for the Myristic acid capsules. Thus roughly 50% of the PCM in the core never melts. This is neglecting all microconvective effects around the particles and their influence on the heat transfer.

The phase change in the particles occurs at a certain rate. This can be obtained from the order of magnitude estimate presented above by calculating the total PCM that melts and the time that it takes for this phase change. Presented overleaf are plots showing the time taken by the melt front to advance as far as it would (for both the slurries tested), before the particles escape the melt zone.

The time estimate is essential to obtain an estimate of the heat transfer rate into the capsule due to the phase change process.

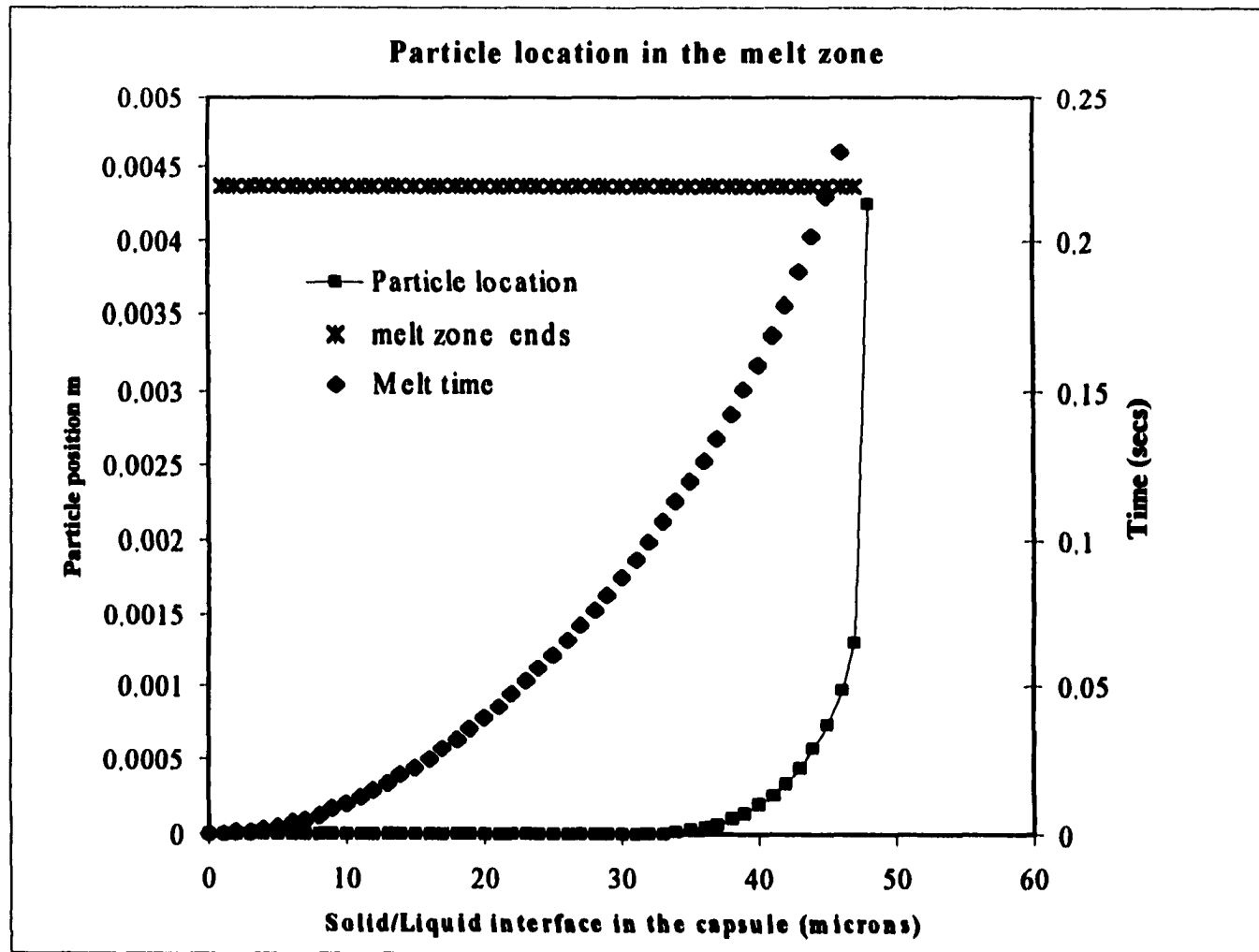


Fig5.33 Plot showing rise of the capsule as PCM core melts (100 μ m Myristic acid capsule in Siloxane)

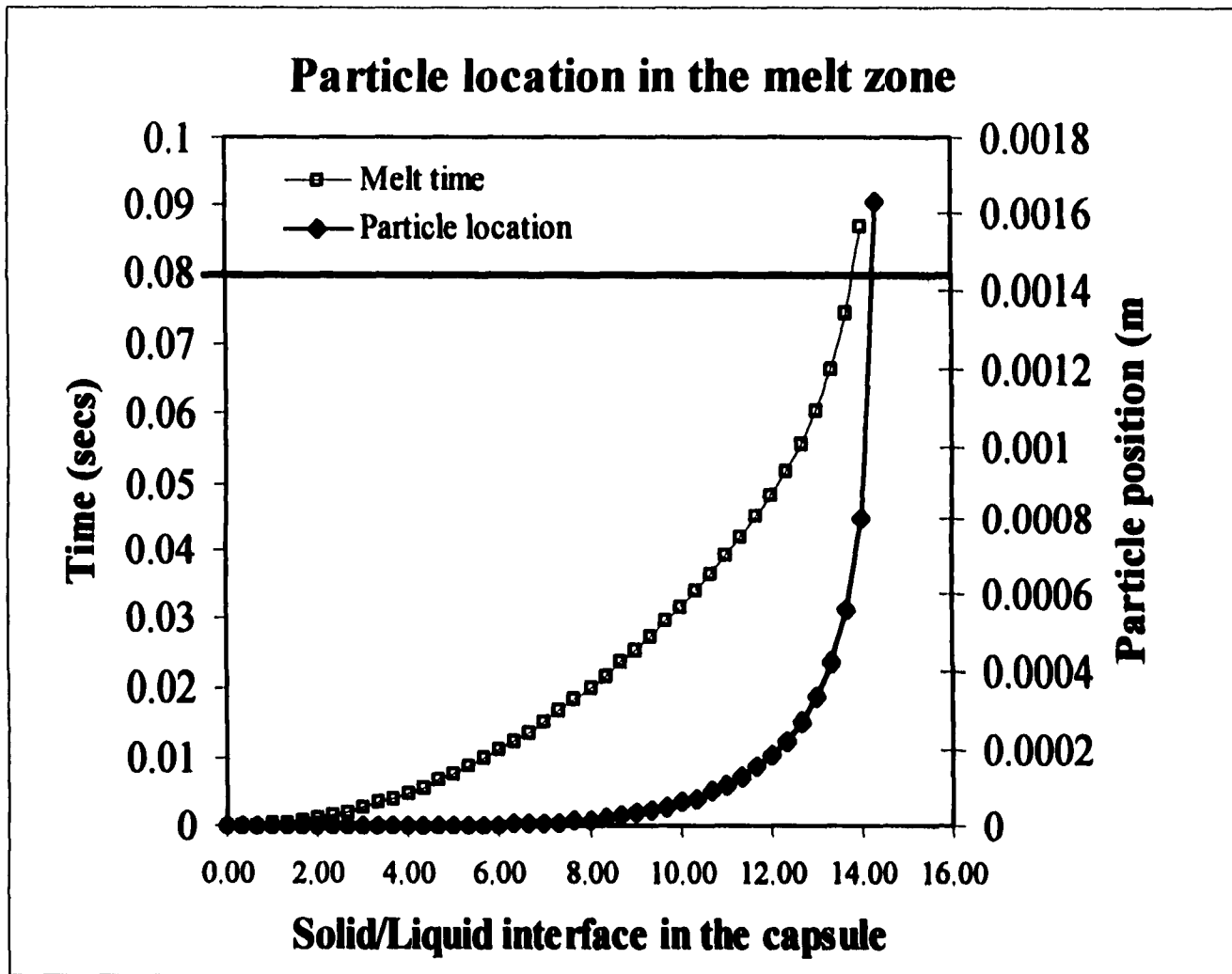


Fig 5.34 Plot showing rise of the capsule as PCM core melts (30 μ m Palmitic acid capsule in water)

5.1.2.5 Estimating the actual phase change in the experiments

Neglecting all other augmentation processes (microconvection, etc.), the enhancement in the heat transfer is primarily due to phase change. The difference between the heat transfer rate of the slurry and the pure fluid is known from experiment. This is the enhancement due to phase change.

Since the volume of PCM in the slurry is a known volume (the volumetric concentration) and so is the particle diameter, the number of particles in the slurry “n” can be calculated using ,

$$n = \frac{6 L^2 D C}{\pi d_p^3}$$

Assuming each particle to be a perfect sphere of known diameter (core diameter), the volume of the PCM in each capsule can be calculated. Using

$$\dot{Q}_{PCM} = -\rho_{solid} L 4\pi r^2 \frac{dr}{dt} \approx -\rho_{solid} L 4\pi r_i^2 \frac{(r_p - r_i)}{t_f}$$

The enhancement in the heat transfer due to phase change, can now be obtained by taking the product of the effective number of particles which melt “n_{melt}” (a lumped parameter giving the effective amount of material which changes phase) and the heat transfer rate per particle. From here the effective number of particles that undergo phase change can be obtained. Calculations for the silicone oil experiments reveal that the maximum amount of PCM that participated in the experiments was 2.7% of that available in the slurry! In fact, in many experiments, about 1% of the available PCM actually changed phase.

This does not indicate that by putting in 2.7% of the volumetric concentration, one could expect a similar enhancement in the heat transfer. Nor does it mean that 2.7% of each particle that was in the slurry underwent phase change. The number simply says that, for the concentrations used, the transport does not allow for more than 2.7% of the total PCM to melt. Putting in a smaller amount may well mean that the enhancements would decrease because there are fewer particles to cycle. In view of this extremely low participation of the PCM, the enhancements are truly significant.

The rationale behind such a low participation in the energy transport, (while particles were clearly seen to be a part of the fluid mechanics), is twofold. Firstly, the medium to high Rayleigh number experiments have a relatively small melt zone to cavity depth (δ/D) ratio. In other words less of the PCM in the cavity resides inside the zone where it can melt. Idealized estimates for the melt zone dimension indicate that the zone makes up between 2% and 16% of the height of the enclosure for medium to high Rayleigh numbers. Actual dimensions may be even smaller due to the fact that these experiments are in the transition regime and there is indeed some (albeit minor) turbulent mixing in the cavity.

Secondly, for very low Ra ($\sim 10^4$) it is quite possible that once the capsules became neutrally buoyant (after some portion of them had melted and the capsule began to rise), many of them were simply carried around by the fluid in the core of the cavity. Many did not break into the melt zone and those that did come close, were carried around by the fluid faster than the melt front could advance deep into the PCM.

5.1.2.6 The Effective thermal conductivity

It might be argued that there is a possibility of slip between the two phases and this could contribute to increased mixing due to the microconvective effects around the particles and therefore an increase in the effective thermal conductivity between the two phases. Clearly, if this were the case, the increased thermal conductivity would show up in both sets of experiments - since the velocity ranges and the particle sizes, are of the same order of magnitude.

The particle Peclet number - for natural convection experiments using particles in the vicinity of 50 μm - is roughly 1. No previous study has been conducted for such low Peclet numbers. To estimate the effect of the relative motion between the two phases as an enhancement in the thermal conductivity, the following expression by Chung and Leal has been used: $R=3\phi Pe^{3/2}$. Where R is defined as $(K_{\text{eff}}-K_b)/K_f$. While this expression is not really valid for such a low Pe range, it has been used here as an expression for an estimate. Clearly, for the very small concentrations used (~1%) K_{eff} is almost the same as K_b (the static ensemble thermal conductivity). In view of this estimate, clearly, there must be some phase change to account for the observed enhancements.

5.1.2.7 Correlations developed

The experimental set was designed to vary the variables in isolation. The data collected during the experimental work can be concisely put together through a regression analysis. The experiments with the two different slurries are presented here as correlations showing the Nu trend when Ra and Ste are varied.

Experiments with Silicone oil

The results of the experiments with different SCRs are presented as two surface plots. For an SCR of 0.69 the experiments predict the following trend in the data:

$$Nu = .135335 Ra^{.324924} Ste^{-0.0263294} \quad \text{For SCR} \sim 0.69$$

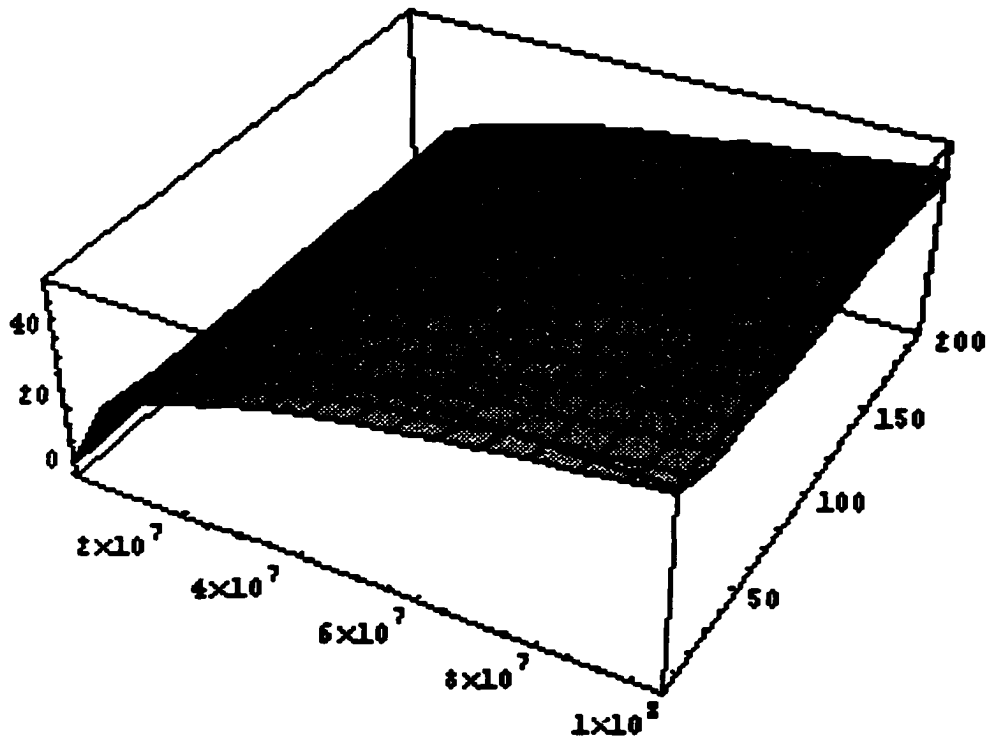


Fig 5.35 Curve fit for the data obtained using the silicone oil slurry.

For the cases run with an SCR of approximately 0.9, the correlation predicting the Nu trend is as follows:

$$Nu = .0988Ra^{.281587} Ste^{.171496} \text{ For SCR} \sim 0.95$$

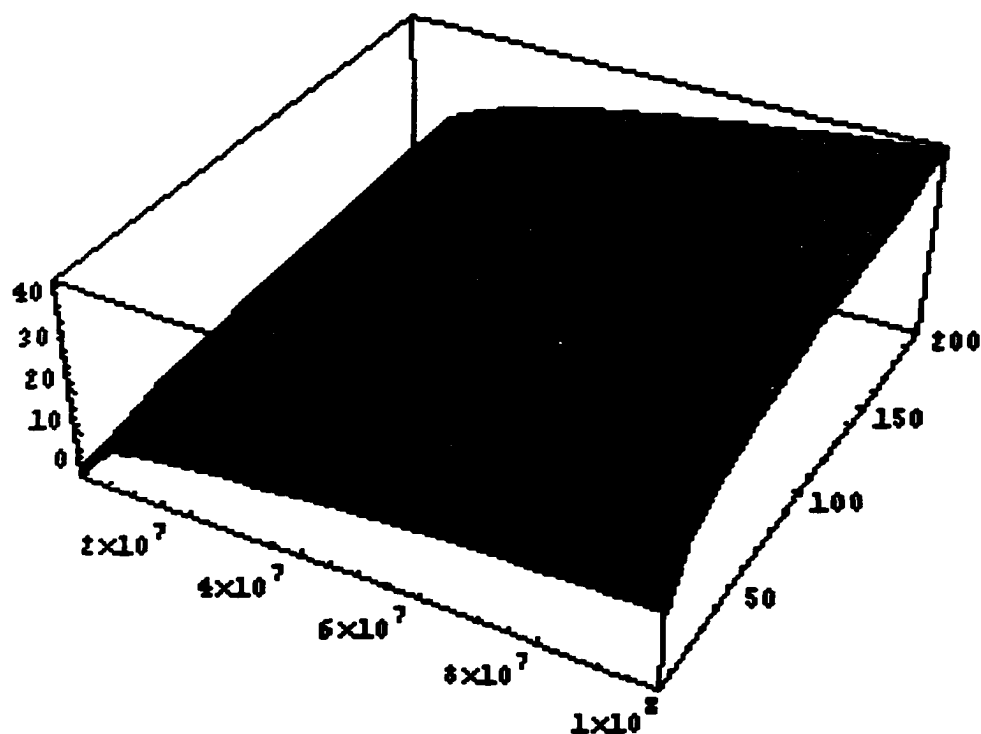


Fig 5.36 Curve fit for the data obtained using the silicone oil slurry (SCR ~ 0.95)

For the experiments with water

For the cases with water as the suspending fluid the correlation developed to predict Nu is as follows:

$$Nu = .0386592 Ra^{.273881} Ste^{.222089} \text{ For } SCR \sim 0.45$$

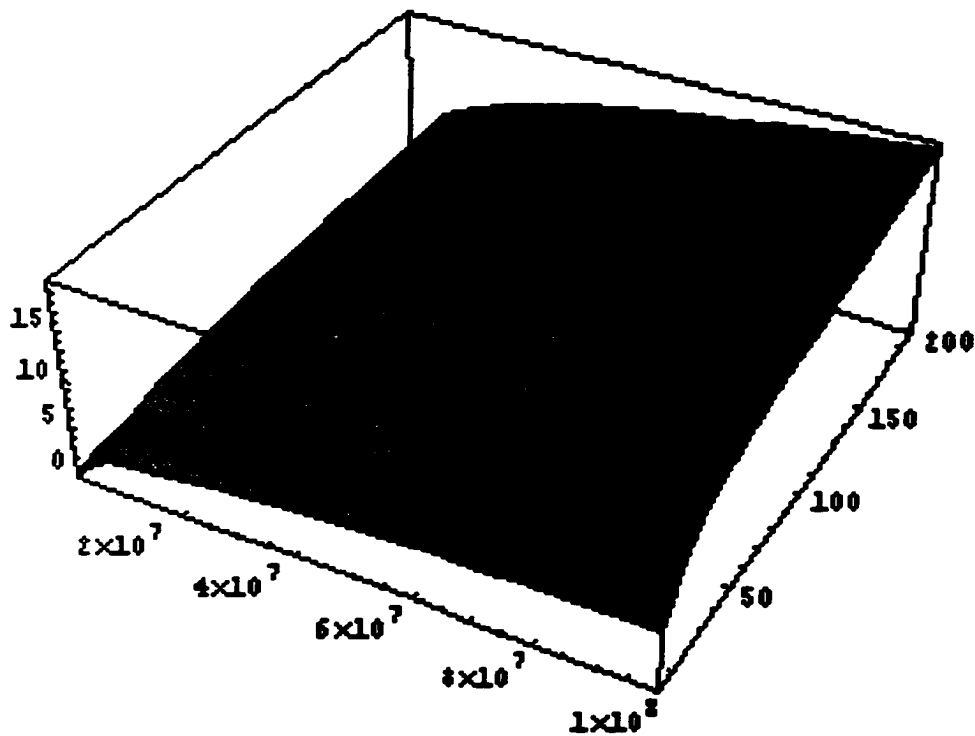


Fig 5.37 Curve fit for the data obtained using the water slurry (SCR ~ 0.45)

For the cases with water as the suspending fluid the correlation developed to predict Nu is as follows:

$$Nu = .0438921Ra^{.313316} Ste^{.0593848} \text{ For } SCR \sim 0.9$$

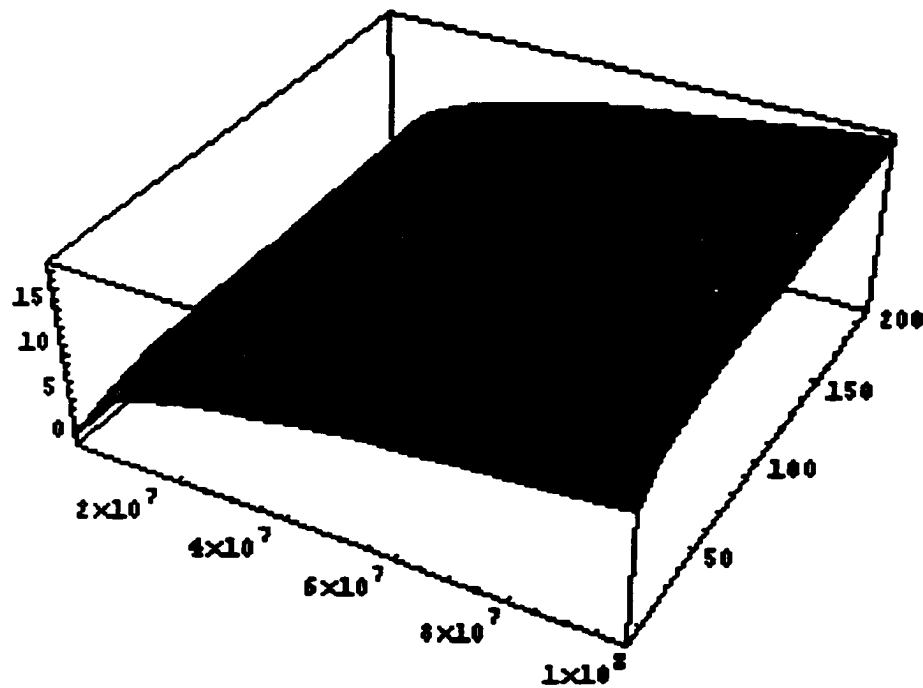


Fig 5.38 Curve fit for the data obtained using the water slurry (SCR ~ 0.9)

5.2 NUMERICAL WORK

The numerical work was done using FLUENT™ a commercial finite volume software. The results obtained are illustrated in the following sections. The results have been categorized under pure fluid flows and enhancement runs.

5.2.1 Assumptions

The simulations were conducted with the following underlying assumptions:

1. Steady state
2. Lateral walls are adiabatic (perfectly insulating)
3. Boussinesq approximation invoked (the fluid properties are considered constant at the bulk fluid temperature, except in the body force term)
4. Perfectly iso-flux and iso-thermal lower and upper horizontal walls respectively.

5.2.2 Validation (Pure fluid runs)

Results for the pure fluid cases were obtained for different depths of the enclosure corresponding to different Rayleigh numbers. The shallow cavity cases, where the depth of the enclosure was between 0.25 and 0.5 inches (Ra of the order of 10^4), yielded steady state results to a fair degree of accuracy (residuals were an order of magnitude, higher than expected for complete convergence). For larger enclosure depths (1-4 inches $10^7 < Ra < 10^8$), the flowfield converged to about 2 orders of magnitude for the velocities and about 4 orders of magnitude for the enthalpy. *A different approach was warranted.*

Most commercially available CFD solvers are (for the sake of general usage) “dimensional”. For some specific problems like natural convection heat transfer in cavities, dimensional codes have a distinct disadvantage. Typical natural convection velocities (for convection in cavities) are of the order of a few millimeters per second. Therefore, trying to reduce the residuals by 3 to 4 orders of magnitude, often results in a build up of round off error, which would continue to compound until the solution finally diverges or “wildly” oscillates.

One procedure to offset this problem, would be to develop a set of units which are less susceptible to round off. This can be accomplished by ensuring that the calculated velocities are normalized to output larger numbers, (they would be in millimeters/second instead of being in the usual SI units of m/s and therefore a 1000 times larger). Clearly, other physical properties would have to be accordingly modified so that the transport is not fundamentally altered (same Rayleigh and Prandtl numbers). The output however, would have to be interpreted in mm/sec.

It can be easily deduced that the following changes to the physical properties would keep the governing non-dimensional parameters (Ra & Pr) the same while scaling the velocities by a factor of 1000.

Density	$\rho_{new} = 10^{-6} \rho_{old}$
Thermal conductivity	$K_{new} = K_{old}$
Specific heat	$C_{P_{new}} = 10^3 C_{P_{old}}$
Dynamic viscosity	$\mu_{new} = 10^{-3} \mu_{old}$
Gravitational constant	$g_{new} = 10^6 g_{old}$

In other words, moving the experiment to a star with a million times the terrestrial gravitational pull, replacing the working fluid with one which is a million times less dense, a 1000 times less viscous and one which needs a 1000 times more heat to raise its temperature by a degree, will result in exactly the same transport mechanism, except scaling the velocities up by a factor of 1000.

Results quantifying the overall heat transfer through the cavity are presented as a set of Nu Vs Ra curves. Appendix C shows the contour plots for different variables for varying cavity depths (0.25 in, 0.5in, 1.0in, 2.0in and 4 in). Fig 5.39 shows the pure fluid case compared to predictions of previous investigators. As in the experimental studies, the numerical results confined themselves to the lower band of the predictions.

The use of an iso-flux lower boundary condition instead of an isothermal one is the only discernable difference between the present study and previous investigations. Hence, it seems the temperature variation¹, is a reason for the detriment in convective augmentation in the cavity.

¹ with the iso-flux boundary condition the temperature field on the lower surface of the cavity passively arranges itself to best augment the energy transport

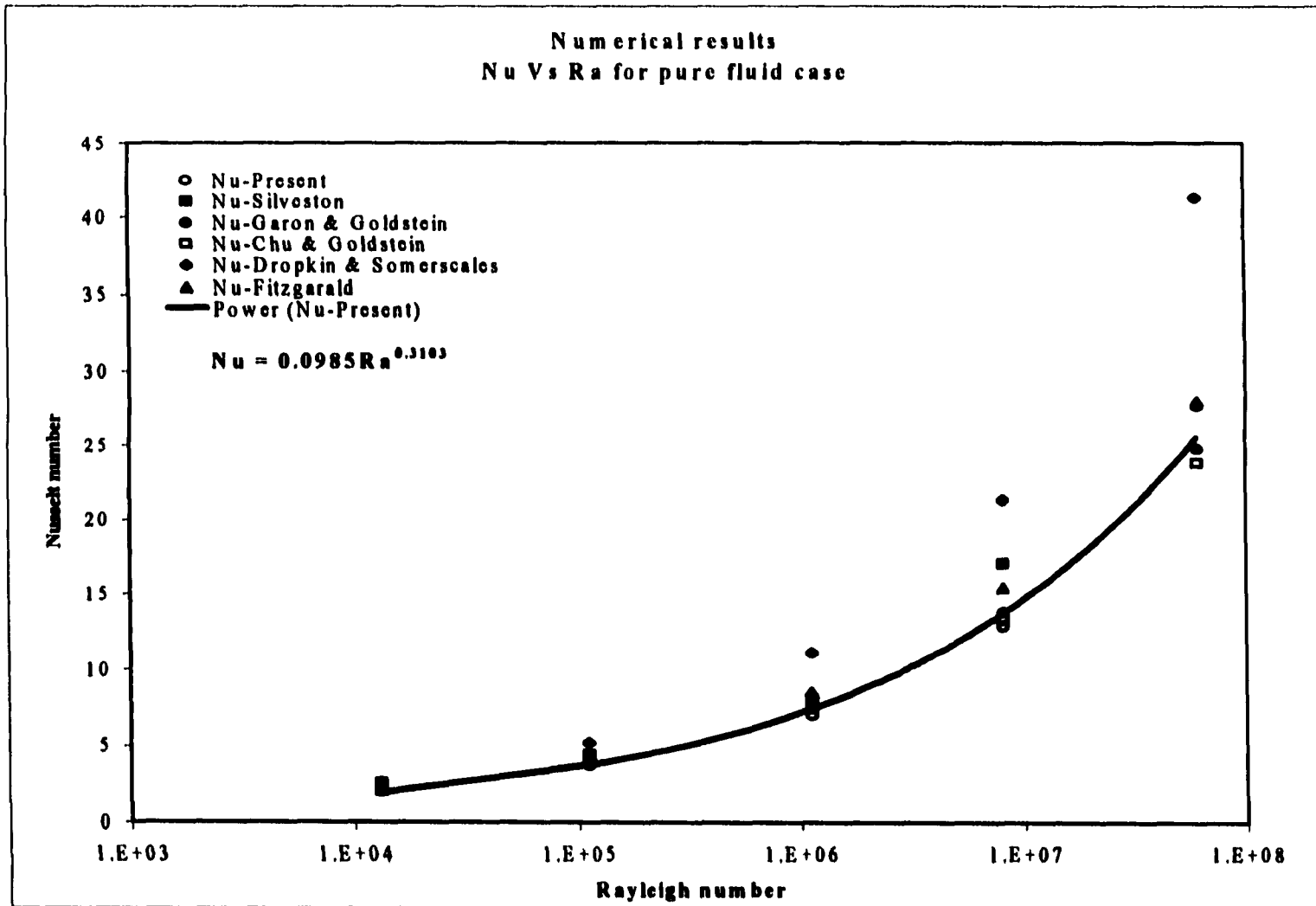


Fig 5.39 Steady state numerical results compared to those of previous investigators

5.2.2.3 ENHANCEMENT RUNS

The heat transfer augmentation runs were conducted using a commercially available Navier-Stokes solver FLUENT™ (block-structured version). A single phase fluid approach has been used wherein the suspension has been replaced by a fluid with the effective bulk properties of the suspension.

The change of phase within the capsules has been modeled as an increase in the specific heat C_p of the slurry. The following equations sum up the effective specific heat calculations. Over the range where the PCM melts, the energy is distributed into the sensible and latent components, as follows:

$$m_{total} C_{peffective} \Delta T = m_{total} C_{pbulk} \Delta T + m_{PCM} L$$

$$C_{peffective} \Delta T = \frac{m_{total}}{m_{total}} C_{pbulk} \Delta T + \frac{m_{PCM}}{m_{total}} L$$

$$C_{peffective} \Delta T = C_{pbulk} \Delta T + cL$$

$$C_{peffective} = C_{pbulk} + \frac{cL}{\Delta T}$$

Clearly, the temperature range over which the phase change occurs is of paramount importance. Melting or freezing never occur at a precise temperature but over a temperature range (albeit a short one).

With a stiff set of coupled governing equations for passive convection, it is virtually impossible to solve a system, where the working fluid has physical properties, which are a strong function (a pulse!) of the temperature. As a result, broadening the temperature range over which melting occurs is of paramount importance. Initial runs with a C_p spike over a 10 degree range yielded no results (the

solver diverged). After many numerical experiments it was observed that a 30 degree melting range was necessary to obtain satisfactorily converged results.

The latent heat modeled as an effective specific heat is shown in Fig. 5.40

The maximum C_p in the plot is :

$$C_{p \max} = \frac{2cL}{\Delta T_{\text{meltingrange}}}$$

A similar plot results for the Water + Palmitic acid slurry. A piecewise linear approach has been used for modeling the specific heat in FLUENT™. All properties have been modeled as bulk properties at the bulk fluid temperature. The Nusselt number Vs the Rayleigh number plot is shown in Fig 5.41.

Clearly the steady state results show no enhancement or detriment in the heat transfer. All values on the plot (the plot contains 20 numerical experiments), were within 2-3 percent of each other.

The results do not show any effect on the overall heat transfer through the cavity. Clearly, C_p does appear in the governing equations for natural convection through the thermal diffusivity. However, the heat transfer coefficient or Nu are only affected by the bulk fluid temperature. Since the hot cold wall temperatures do not change, the bulk fluid temperatures did not either.

Previous investigators have utilized effective C_p models to model phase change. However, this approach will clearly not work for the present problem. This is due to the fact that modeling the phase change through C_p excludes all the closely coupled physics between the two phases. A two phase multi component numerical solver seems to be the only way to model this phenomenon.

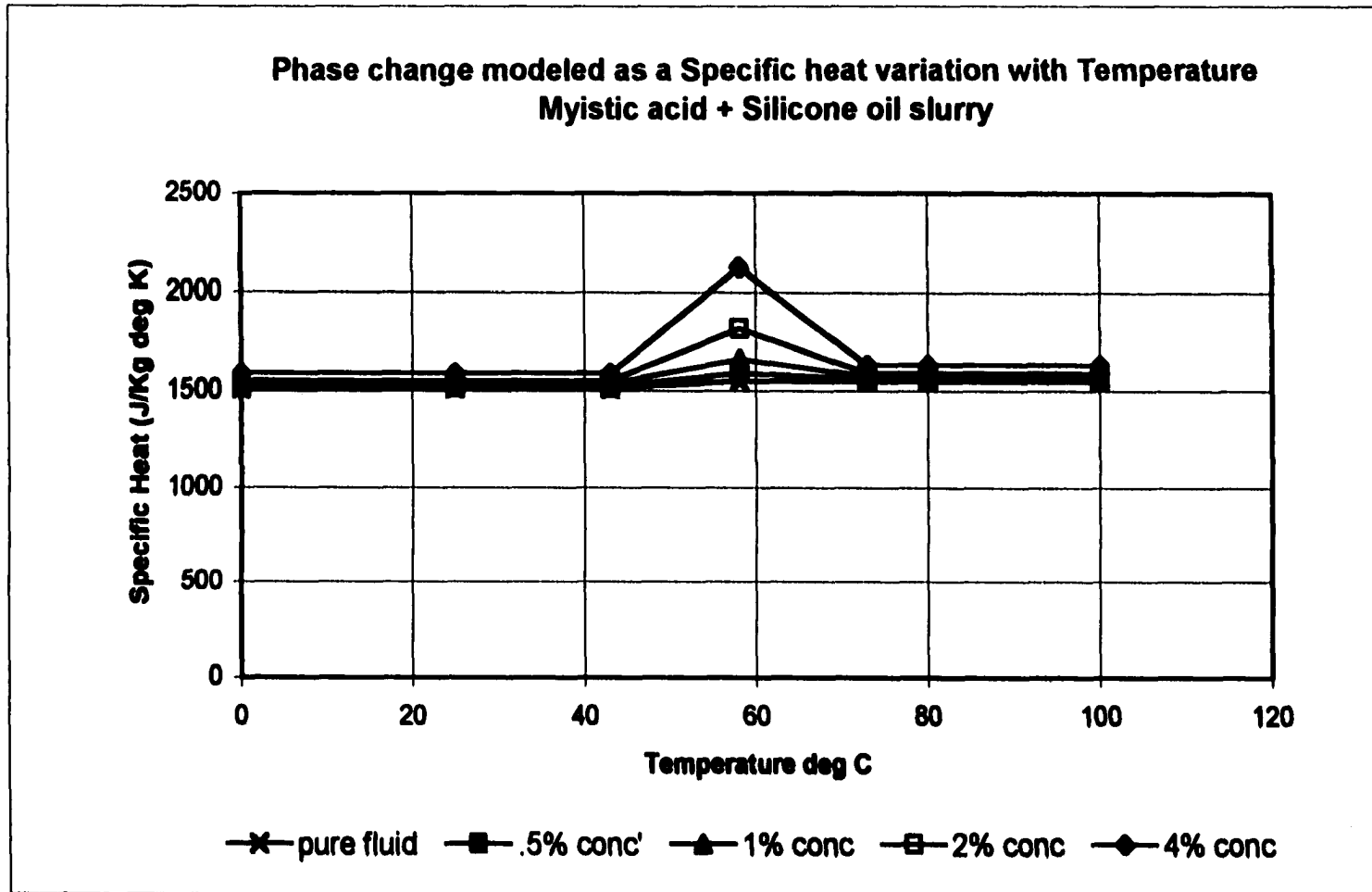


Fig 5.40 Plot showing the variation of C_p over the melting temperature for different concentrations

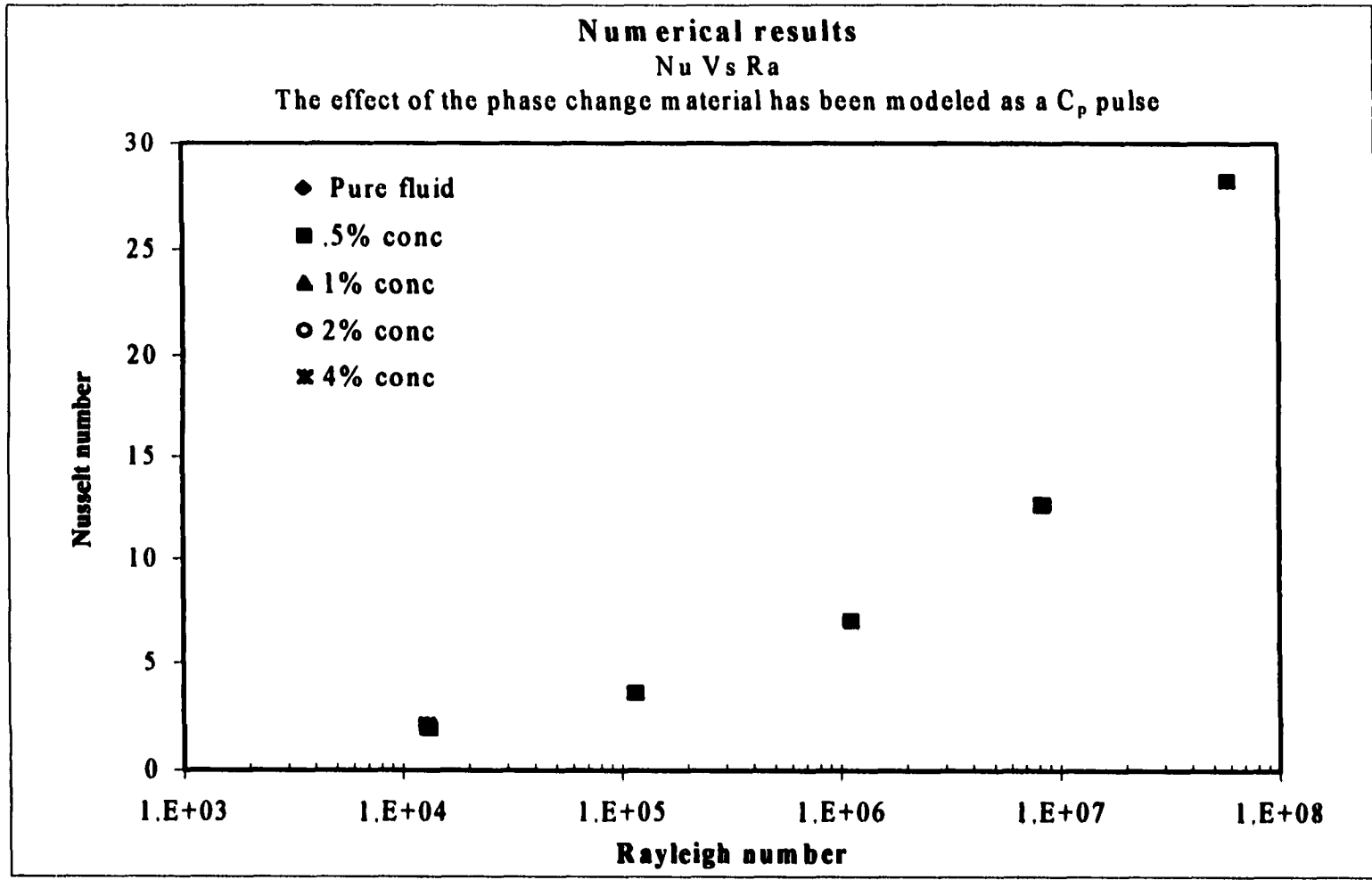


Fig. 5.41 Nu Vs Ra results for enhancement runs with the PCM effect modeled as a C_p pulse.

5.2.2.4 A NEW METRIC

Clearly the numerical approach to model the phase change as an effective C_p pulse will not work. Therefore a new metric which quantifies the phase change as an effective increase in the thermal conductivity is necessary. Such a metric will help quantify the thermal conductivity enhancement purely due to the phase change process. This would give the investigator a tool to simulate the thermal performance of a two-phase, phase change slurry, by running a single-phase steady state simulation.

From the analysis of the experimental data it is apparent that a known percentage of each particle in the melt zone actually melts. Assuming that,

- the fluid is homogeneous throughout the experiment,
- the particles are absolutely equidistant,

the total number of particles in the melt zone at a given instant (“ n ”) can be calculated.

$$n = \left(\frac{L}{d_p} \right)^3 \frac{6c\delta}{\pi D}$$

The heat transfer rate into a particle can also be calculated, since expressions for the total time taken for the particle to escape the melt zone and the distance the melt front advances into the particle are known.

$$\dot{Q}_{PCM} = \frac{\text{Mass of molten PCM}}{\text{Melting time}} = \rho_{solid} L \frac{dV_{molten}}{dt}$$

The heat transfer rate of the suspension in the special case of conduction (using the 1-D approximation) would be:

$$K_{effective} A \left(\frac{dT}{dz} \right)_{conduction} = K_{bulk} A \left(\frac{dT}{dz} \right)_{conduction} + n_1 \dot{Q}_{PCM}$$

$$\Rightarrow K_{effective} = K_{bulk} + \frac{n_1 \dot{Q}_{PCM}}{A \left(\frac{dT}{dz} \right)_{conduction}}$$

The above equation, states that in the limiting case of conduction heat transfer, the energy transfer rate from the hot plate is an ensemble of the bulk properties of the suspension and the rate at which the point sinks in the domain “soak up the energy”. Since there is no fluid motion, the sinks can be thought of as effectively increasing the fluid thermal conductivity.

For a known boundary condition where Q_c is the imposed energy transfer rate at the hot boundary, $\left(\frac{dT}{dz} \right)_{conduction}$ can be substituted with, $\left(\frac{dT}{dz} \right)_{conduction} = \frac{Q_c}{K_{bulk} A}$

Since the change of phase term will not manifest itself as a change in the conductive temperature gradient the above equation holds.

$$\Rightarrow K_{effective} = K_{bulk} + \frac{n_1 \dot{Q}_{PCM}}{Q_c} K_{bulk}$$

$$\Rightarrow K_{effective} = K_{bulk} \left(1 + n_1 \frac{\dot{Q}_{PCM}}{Q_c} \right)$$

Now, an expression for \dot{Q}_{PCM} it has already been established that,

$$t_f \sim \frac{d^2}{\alpha_{resin}} + \frac{s^2}{\alpha_{PCM}} \left(\frac{\rho}{\rho_s} Ste_p \right)^{\frac{3}{4}} (Ar_p \cdot Pr_p)^{\frac{1}{4}}$$

t_f can be written as a function of r_i . V_{molten} is the volume of the phase change material

$$\begin{aligned} V_{molten} &= \frac{4\pi(r_p^3 - r_i^3)}{3} \\ \Rightarrow \frac{dV_{molten}}{dt} &= -4\pi r^2 \frac{dr}{dt} \\ \Rightarrow \dot{Q}_{PCM} &= -\rho_{solid} L 4\pi r^2 \frac{dr}{dt} \approx \rho_{solid} L 4\pi r_i^2 \frac{(r_p - r_i)}{t_f} \end{aligned}$$

that undergoes phase change.

At any instant, therefore let there be “ n_1 ” particles that are undergoing phase change. The expression for effective thermal conductivity thus becomes

$$K_{effective} = K_{bulk} \left(1 + \frac{n \rho_{solid} L 4\pi r_i^2 \frac{(r_p - r_i)}{t_f}}{Q_c} \right)$$

Which can be further rearranged to the following expression

$$K_{effective} = K_{bulk} \left(1 + \frac{24c\rho_{solid}L}{Q_c} \left(\frac{l}{d_p} \right)^3 \frac{\delta_{BL}}{D} r_i^2 \frac{(r_p - r_i)}{t_f} \right)$$

From this expression, a number of parameters, which effect the enhancement function become evident. The concentration which determines the amount of phase change material crammed into the melt zone, the aspect ratio, the diffusive time scales of the wall and the core materials (through t_f) and the particle diameter to name a few.

The above expression could be used to obtain values for the effective thermal conductivity. However, it should be noted that, the single biggest assumption is in the number of particles " n_1 " undergoing phase change and being at the same level of phase change.

There is no simple analytical procedure to obtain a parameter (even a lumped parameter), which quantifies n_1 . As such if n_1 is substituted with n , the above expression would represent an idealized upper limit to the enhancement in heat transfer if each and every particle in the "melt zone" undergoes phase change.

The working fluid in the cavity could be treated as an anisotropic medium, with the effective thermal conductivity of the layers of the fluid within the melt (and freeze) zone being given by

$$K_{effective} = K_{bulk} \left(1 + n_1 \frac{\dot{Q}_{PCM}}{Q_c} \right)$$

While the rest of the cavity would have a thermal conductivity equal to K_{bulk} Future investigations utilizing, a statistical approach to quantify the factor n_1 , could improve on the expression for $K_{effective}$ given above.

CHAPTER

6

CONCLUSIONS

The present study is one of **THREE** ever conducted in natural convection heat transfer in rectangular cavities where the working fluid is a phase change suspension.

At the outset, it was observed that most studies in phase change suspensions have been in forced convection heat transfer and in energy storage. Hardly any study has been conducted where the cyclic phase change property of the slurry has been utilized as a heat transfer enhancing mechanism for passive convection in cavities.

The preliminary study by Datta (1992), showed that there was a significant heat transfer enhancement (up to 80%) when a slurry of n-Eicosane capsules and a heat transfer oil (Mobiltherm 100) was used. This study further explored the finding. A considerable amount of information has been collected both by experimental work and in attempts to numerically model the phenomenon. Clearly, the earlier findings while exciting were incomplete. Many new mechanisms and misunderstood facts are now better understood.

- *Enhancement in the heat transfer rate up to 110% have been documented with relatively low concentrations (0.5% - 2% by volume) of phase change microcapsules.*
- *Following experimental correlations developed for the Nusselt number as a function of the Rayleigh and Stefan numbers,*

For the oil based slurry ($k_p/K_f \sim 1$)

$$Nu = .0988Ra^{.281587} Ste^{.171496} \text{ For SCR} \sim 0.95$$

$$Nu = .0386592Ra^{.273881} Ste^{.222089} \text{ For SCR} \sim 0.45$$

For the water based slurry ($k_p/K_f \sim 0.25$)

$$Nu = .0438921Ra^{.313316} Ste^{.0593848} \text{ For SCR} \sim 0.9$$

$$Nu = .135335Ra^{.324924} Ste^{-0.0263294} \text{ For SCR} \sim 0.69$$

- *When designing a phase change slurry to enhance heat transfer, it is imperative that the ratio of conductivities of the two phases be close to 1.*

One of the most important findings from the present study was the importance of the **conductive contribution** in the transport. Clearly, for the suspended phase to contribute in the energy transport, the particles have to be able to compete for the energy transport. If this is not the case, the disproportionate time scales (with the suspended phase losing out), tilt the energy transfer in favor of the better conductive moving medium (the background fluid). Simply put, most of the energy evades the capsules.

- *A very small percentage of the phase change material available in the slurry actually melts. Data obtained from the present experiments shows that, a maximum of 2.7% of the PCM in the slurry was ever used.*
- *Even if the capsules could compete in the transport, the very design of a good slurry ensures that about 50% of the phase change material cannot be used.*

An order of magnitude estimate points to the fact that the very design of the slurry, wherein the particles have to be heavier than the background fluid when

solid and lighter when molten, ensures that by the time the melt front advances to about mid-particle, the capsule would have become light enough to escape the melt zone. Any attempt to tap more of the core by increasing temperature of the hot plate (i.e., the driving temperature difference), will result in the second instability point being reached. This is further discussed below.

- *If the bulk fluid temperature is above the melting point of the phase change material the second instability point will be reached.*

The most important mechanism for heat transfer enhancement in a phase change slurry, is the thermal cycling of the capsules. If the melt zone of the PCM is increased by increasing the hot plate temperature, the PCM will no longer cycle since the bulk of the working fluid will be above the melting point of the PCM. This is crucial in designing the phase change slurry and very important when choosing the phase change material to be used in a particular application.

- *An approximate expression for the effective thermal conductivity of the PCM slurry has been obtained which can be used to numerically simulate the two-phase phenomenon as an equivalent single-phase phenomenon with a comparable thermal performance at steady state.*

The numerical results obtained, point to the fact that using an effective C_p pulse to model the effect of the phase change as an equivalent single-phase phenomenon is not possible. The phenomenon has to be modeled with an effective thermal conductivity expression. The approximate expression developed in the present study is:

$$K_{effective} = K_{bulk} \left(1 + \frac{24c\rho_{solid}L}{Q_c} \left(\frac{l}{d_p} \right)^3 \frac{\delta_{BL}}{D} r_i^2 \frac{(r_p - r_i)}{t_f} \right)$$

It is possible to design a heat transfer enhancing phase change slurry, for many applications. Over the past five years, the science of Micro-encapsulation has matured to an extent where capsule durability (in thermal cycling) for passive heat transfer applications is no longer an issue. However, the challenge still lies in accurately modeling the physics of this extremely complex two-phase fluid system.

Recommendations for the design of PCM slurries

An ideal density match between the two phases is essential $\rho_p \sim \rho_f$. The capsule density should be greater than the suspending fluid's density when the core is solid and less than it with a molten core.

From the present work, it is imperative that the thermal conductivity match K_p/K_f be close to 1. To avoid the runaway heat flux (the second instability point) the melting temperature (T_{melt}) has to be lower than $(T_h+T_c)/2$.

Low concentration slurries ($\leq 2\%$) should be used to avoid agglomeration and the fact that increases in the slurry concentrations do not produce corresponding enhancements in the heat transfer rate.

Fillers (in the core) to increase capsule thermal conductivity can be used. These fillers can be chosen to bring the particle thermal conductivity to a par with that of the suspending fluid. Besides, not all the PCM in the core is useful anyway.

For low Ra, a mixture of phase change microcapsules, which are effective over a larger melt zone, can be used.

REFERENCES

Ahuja, A.S., 1957a, "Augmentation of heat transport in laminar flow of polystyrene suspension. I. Experiments and results," J. Appl. Phys., 46, pp 3408-3416.

Ahuja, A.S., 1957b, "Augmentation of heat transport in laminar flow of polystyrene suspension. II. Analysis of Data," J. Appl. Phys., 46, pp 3417-3425.

Anderson, A., Tannehill, C.J., Pletcher, H.R., 1984, "Computational fluid dynamics and heat transfer," Hemisphere publishing corporation, McGraw Hill Book company.

Bailey, J.A., et al., 1975, "Research on Solar Energy Storage Subsystems Utilizing the Latent Heat of Phase Change of Paraffin Hydrocarbons for the Heating and Cooling of Buildings," National Science Foundation, Grant GI-44381.

Bar-Cohen, A., and Kraus, A. D., 1988, "Advances in Thermal Modeling of Electronic components and systems," Volume-1, Hemisphere Publishing Corporation, N.Y.

Bar-Cohen, A., and Kraus, A. D., 1988, "Thermal Analysis and Control of Electronic Equipment," Hemisphere Publishing Corporation, McGraw Hill Book company.

Bart, G. C. J., and Van der Laag, P.C., 1990, "Modeling of Arbitrary-Shaped Specific Heat Curves in Phase Change Storage Simulation Routines", Journal of Solar Energy Engineering, Vol. 112, pp. 29-33.

Bejan, A., 1995, "Convective Heat Transfer," Wiley Interscience publication, John Wiley and Sons.

Catton, I., and Edwards, D.K., 1967, "Effect of Side Walls On Natural Convection Between Horizontal Plates Heated From Below," J. of Heat Transfer, pp 295-299.

Charunyakorn, P.K., 1989, "Forced convection heat transfer in Microencapsulated phase change material slurries," Ph.D. Dissertation Dept. of Mech. Eng., University of Miami, Florida.

Charunyakorn, P.K., Sengupta, S., and Roy, S.K., 1990, "Forced convection heat transfer in Microencapsulated phase change material slurries: Flow in circular ducts," International Journal of Heat and Mass Transfer.

Charunyakorn, P.K., Sengupta, S., and Roy, S.K., 1990, "Forced convection heat transfer in Microencapsulated phase change material slurries: Flow between parallel plates," AIAA/ASME Thermophysics and Heat Transfer Conference.

Chatree, M., and Sengupta, S., 1986, "Effect of bottom slope on laminar natural convection in enclosures: A two dimensional time dependent numerical investigation," Presented at, The winter annual meeting of the ASME, Ed. R.S. Figliola, I. Catton, HTD-Vol. 63.

Choi, Eunsoo., Cho, Young, I., and Lorsch, Harold, G., 1991, "Effects of Emulsifier on Particle Size of a Phase Change Material in a Mixture With Water ," International Communications in Heat and Mass Transfer, Vol. 18, pp. 759-766.

Choi, Eunsoo., Cho, Young, I., and Lorsch, Harold, G., 1992, "Enhancement of Convective Transfer with Phase Change Particles," ASME, Topics in Heat Transfer – Volume 2, HTD-Vol. 206-2, pp. 185-189.

Choi, Eunsoo., Cho, Young, I., and Lorsch, Harold, G., 1994, Forced Convection Heat Transfer with Phase Change Material Slurries: Turbulent Flow in a Circular Tube, International Journal of Heat and Mass Transfer, Vol. 37. No. 2. pp. 207-215

Chu, T.Y., and Goldstein, R.J., 1973, "Turbulent convection in a horizontal layer of water," J. Fluid Mech., 60, pp 141-159.

Colvin, D.P., and Mulligan, J.C., 1986, "Spacecraft Heat Rejection Methods: Active and Passive Heat Transfer for Electronic Systems-Phase-I," Air Force Wright Aeronautical Lab. Rept. No. AFWAL-TR-86-3074.

Datta, Partha., 1992, "Natural Convection Heat Transfer in an Enclosure With Suspensions of Micoencapsulated Phase Change Materials," Masters Thesis, University of Miami.

Datta, Partha., 1992, "Natural Convection Heat Transfer in an Enclosure With Suspensions of Micoencapsulated Phase Change Materials," 28th Annual Heat Transfer Conference, San Diego, General Papers in Heat Transfer, Vol. 205.

Datta, P., Sengupta, S., and Singh, T., 1996, "Rayleigh and Prandtl number effects in Natural Convection in Enclosures with Microencapsulated Phase Change Material Slurries," Proceedings of the 33 Japan Heat Transfer Conference, pp. 225-226.

Dropkin, D., and Somerscales, E., 1965, "Heat Transfer by Natural Convection in Liquids Confined by Two Parallel Plates Which Are Inclined at Various Angles With Respect To the Horizontal," J. of Heat Transfer, Trans. of the ASME., pp 77-84.

Fitzjarrald, D.E., 1976, "An Experimental Study of turbulent convection in air," J. of Fluid Mech. 73, pp 693-719.

Fukuda, Eiji., Saito, Natsukaze., Kimura, Isao., and Masato, Tanaka., 1996, "Encapsulation of PCM and Slurry Flow Characteristics," Proceedings of the 33 Japan Heat Transfer Conference, pp. 229-230.

Garon, A.M., and Goldstein, R.J., 1973, "Velocity and Heat Transfer measurements in thermal convection," *Physics of Fluids* 16, pp 1818-1825.

Globe, S., and Dropkin, D., 1959, "Natural Convection Heat Transfer in Liquids confined by two horizontal plates and heated from below," *J. of Heat Transfer, Trans. of ASME.*, 81, pp 24-28.

Goel, M., 1992, "Laminar Forced Convection Heat Transfer in Microencapsulated Phase Change Material Suspensions," Masters Thesis, University of Miami.

Goldstein, R.J., and Chu, T.Y., 1969, "Thermal Convection in a Horizontal Layer of Air," *Progress of Heat and Mass Transfer*, 2, pp 55-75.

Goldstein, R.J., Chiang, H.D., and Lee, S.D., 1990, "High Rayleigh number convection in a horizontal enclosure," *Journal of Fluid Mechanics*, Vol-213, pp 111-126.

Goldstein, R.J., Chiang, H.D., and See, D.L., 1989, "High Rayleigh Number Convection In a Horizontal Enclosure," *Journal of Fluid Mechanics*, Vol-213, pp 111-126.

Hale, D.V., Hoover, M.J., and O'Neill, M.J., 1971, "Phase Change Materials Handbook," NASA CR-61363 (NAS 1.26:61363).

Harhira, Miloud., 1993, "Natural Convection Heat Transfer from a Vertical Flat Plate to Suspensions of Microencapsulated Phase Change Materials," Masters Thesis, University of Miami.

Hart, R., and Thornton, F., 1959, "Microencapsulation of Phase Change Materials," Dept. of Energy, Ohio, Final Rept. Contract No. 82-80.

Heslot, F., Castaing, B., and Libchaber, A., 1987, "Transitions of Turbulence in Helium Gas," *Phys. Rev., A* 36, pp 5870-5873.

Hoshina, Hidehiro., Saitoh, S. Takeo., 1996, "Numerical Simulation on Combined Close Contact and Natural Convection Melting With Density Inversion in an Ice Storage Spherical Capsule," *Proceedings of the 33 Japan Heat Transfer Conference*, pp. 81-82.

Hwang, G.J., Chiou, K.C., and Kao, P.J., 1988, "An Experimental Study of Heat Transfer in Inclined Rectangular Cells," *Cooling Technology for Electronic Equipment*, Wing Aung, Ed., pp 3-13.

Inaba, H. and Morita, S., 1995, "Flow and Cold Heat Storage Characteristics of Phase-Change Emulsion in a Coiled Double-Tube Heat Exchanger," *Journal of Heat Transfer*, Vol. 117, pp. 440-446.

Inaba, H. and Morita, S., 1996, "Cold Heat Release Characteristics of Phase-Change Emulsion by Air-Emulsion Direct Contact Heat Exchanger Method," *Journal of Heat and Mass Transfer*, Vol. 39, No. 9, pp. 1797-1803.

Inaba, H. and Morita, S., Fujisaki, Masahiko., 1996, "Evaluation of Heat Transport Performance of Fine Latent Heat Storage Material and Water Mixture," *Proceedings of the 33 Japan Heat Transfer Conference*, pp. 227-228

Kasza, K., and Chen, M.M., 1985, "Improvement of the performance of solar energy or waste heat utilization systems by using phase change slurry as an enhanced heat transfer storage fluid," *Journal of solar energy engineering*, 108, 229-236.

Kishimoto, Akira., Chikazawa, Akio., Ishiguro, Mamuro., and Nakanishi, Yasunori., 1996 "Heat and Flow Characteristics of Heat Transportation Medium Containing Microencapsulated Phase Change Material," Proceedings of the 33 Japan Heat Transfer Conference, pp. 231-232

Leal, L.G., 1973, "On the effective conductivity of dilute suspension of spherical drops in the limits of low particle Peclet number," Chemical Engineering communication. 1, pp 21-31.

Maxwell, J.C., 1954, "A treatise on electricity and magnetism," Vol-1, 3rd Edition, Dover Publications Inc., New York, pp 440-441.

Muddawar, I.A., Incropera, T.A., and Incropera, F.P., 1988, "Microelectronic Cooling by Fluorocarbon Liquid Films," Cooling Technology for Electronic Equipment, Wing Aung, Ed., pp 417-434.

Mulligan, J.C., Bailey, J.A., Ozisik, MN, and Mayday, C.J., "A Demonstration and Evaluation of Phase-Change Thermal Energy Storage in Residential Heat Pump Systems," Final Report, North Carolina Energy Institute

Nakayama, W., 1986, "Thermal Management of Electronic Equipment: A Review of Technology and Research Topics," Appl. Mech. Rev., Vol-39, pp 1847-1868.

Newell, M.E., and Schmidt, F.W., 1970, "Heat Transfer by Laminar Natural convection within Rectangular Enclosures," Journal of Heat Transfer, pp 159-168.

Nir, A., and Acrivos, A., 1976, "The Effective Thermal conductivity of Sheared Suspensions," Journal of Fluid Mechanics, Vol-78, pp 33-48.

Oka, Mineo., 1996, "Effect of Heating Wall Shape of Contact Melting Process," Proceedings of the 33 Japan Heat Transfer Conference, pp. 91-92.

Oosthuizen, Patrick. H., 1997, "A Numerical Study of Three-Dimensional Natural Convection In A Horizontally Heated Enclosure", Proceedings of the Heat Transfer Division, HTD-Vol. 353, Vol. 3, pp.301-308.

Rossby, H.T., 1969, "A Study of Bénard Convection with and without Rotation," Journal of Heat Transfer, Vol-36, pp 309-335.

Roy, S.K., 1988, "Melting in Spherical Enclosures," Ph.D. Thesis, University of Miami.

Roy, S.K., and Sengupta, S., 1987, "The melting process within spherical enclosures," Journal of Heat Transfer, 109, pp 460-462.

Roy, S.K., and Sengupta, S., 1991, "An Evaluation of Phase Change Microcapsules for use in Enhanced Heat Transfer Fluids ," International Communications in Heat and Mass Transfer, Vol. 18, pp. 495-507

Rutgers, I.R., 1962, "Relative viscosity of suspensions of rigid spheres in Newtonian liquids," Rheologica Acta 2(4), pp. 305-348.

Sengupta, S., 1990, Microencapsulated phase change material slurries for the thermal management of electronic packages," Final Report, The Florida High Technology and Industrial Council.

Sohn, C.W., and Chen, M.M., 1981, "Microconvective thermal conductivity in a disperse two phase mixture as observed in a laminar flow," Journal of Heat Transfer, 103, pp47-51.

Sohn, C.W., and Chen, M.M., 1984, "Heat transfer enhancement in laminar slurry pipe flows with power law thermal conductivities," Journal of Heat Transfer, 106, pp 539-542.

Somerscales, E.F.C., and Gazda, L.W., 1968, "Thermal Convection in High Prandtl Number Liquids at High Rayleigh Numbers," Rensselaer Polytechnic Institute ME Rep. HT-5.

Takeuchi, Masanori., Kimura, Teruo., Niroh, Nagai., and Kawaguchi, Kazuhiro, 1996, "Natural Convection Between Inclined Parallel Plates," Proceedings of the 33 Japan Heat Transfer Conference, pp. 837-838.

Tanaka, H., and Hiyata, H., 1980, "Turbulent Natural Convection in a Horizontal Water Layer Heated From Below," International Journal of Heat and Mass Transfer, 23, pp 1273-1281.

Tao, L.C., 1967, "General numerical solutions of freezing a saturated liquid in cylinders and spheres," AIChE J. 13(1), pp 165-169.

Vand, V., 1945, "Theory of viscosity of concentrated suspensions," Nature 155, pp 364-365.

Yeh, L.T., 1987, "Future Thermal Design and Management of Electronic Equipment," Heat Transfer in High Technology and Power Engineering, W.J. Yang and Y. Mori, Ed., Hemisphere Publication, Washington DC, pp. 131-159.

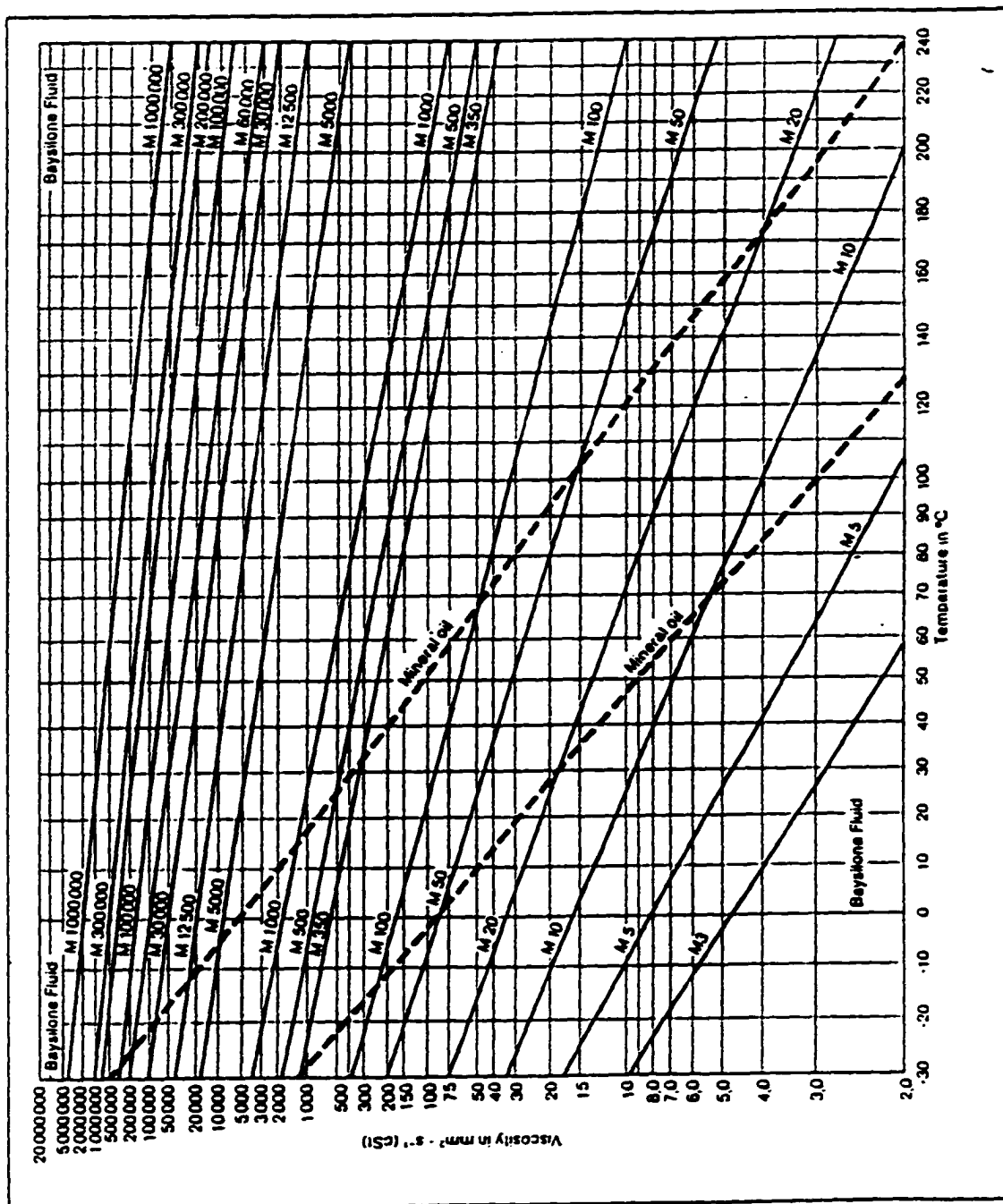
APPENDIX – A
PROPERTIES

PROPERTIES

	<i>Density Kg/cu-m</i>	<i>Viscosity mm²/s (40° C)</i>	<i>Thermal Cond W/mK</i>	<i>Specific Heat (J/KgK)</i>	<i>Melting point deg C</i>	<i>Latent Heat J/Kg</i>	<i>Beta (1/K)</i>
Water	999-977	0.66	0.63	4180	-	-	34.0 x 10 ⁻⁵
Silicone Oil*	970-940	75	0.16	1510	-	-	99 x 10 ⁻⁵
Palmitic acid	850	-	~0.165	1790 2415	62	163000	-
Myristic acid	858**	-	~0.16	1590 2260	58	199000	-
Stearic acid	847**	-	~0.16	~2000	69.4	199000	-
N-Eicosane	856 778***	-	~0.15	2210 2010	36.7	247000	-
Urea Formaldehyde	~1500***	-	~0.043	1669	decomposes >100 C	-	-

*PolyDimethyl Siloxane ** Liquid *** varies depending on the filler.

$$\alpha_{\text{water}}/\alpha_{\text{palmitic}} = 1.7 \quad \alpha_{\text{oil}}/\alpha_{\text{myristic}} = 1.2 \quad K_{\text{water}}/K_{\text{palmitic}} \approx 3.8 \quad K_{\text{oil}}/K_{\text{myristic}} \approx 1.0$$



Viscosity variation with temperature for Silicone oil M100.

Densilone Fluids M	Density in g · cm ⁻³						
	-40°C	0°C	25°C	50°C	100°C	175°C	
3	0.97	0.93	0.90	0.88			
5	0.99	0.95	0.92	0.90			
10	1.02	0.97	0.94	0.92			
20	1.02	0.98	0.95	0.93			
50	1.03	0.99	0.96	0.94	0.90	0.84	
100	1.04	1.00	0.97	0.95	0.91	0.85	
350	1.04	1.00	0.97	0.95	0.91	0.85	
500	1.04	1.00	0.97	0.95	0.91	0.85	
1,000	1.04	1.00	0.97	0.95	0.91	0.85	
5,000	1.04	1.00	0.97	0.95	0.91	0.85	
12,500	1.04	1.00	0.97	0.95	0.91	0.85	
30,000			0.97	0.95	0.91	0.85	
60,000			0.97	0.95	0.91	0.85	
100,000			0.97	0.95	0.91	0.85	
200,000			0.97	0.95	0.91	0.85	
300,000			0.97	0.95	0.91	0.85	
1,000,000			0.97	0.95	0.91	0.85	

Density variation with temperature for Silicone oil M100.

t in °C	c in $J \cdot g^{-1} \cdot K^{-1}$	W_{10} in $J \cdot g^{-1}$
20	1.51	0
40	1.51	30.6
60	1.55	62.0
80	1.55	93.4
100	1.55	123.5
120	1.59	157.8
140	1.59	192.2
160	1.63	229.0
180	1.67	267.5
200	1.73	309.0

Specific Heat variation with temperature for Silicone oil M100.

Baysilone-Fluids M	$W \cdot K^{-1} \cdot m^{-1}$
3	0.105
5	0.116
10	0.140
20	0.140
100	0.163
1,000	0.174
12,500	0.174
100,000	0.174

Thermal conductivity variation with temperature for Silicone oil M100.

APPENDIX – B
UNCERTAINTY ANALYSIS

UNCERTAINTY ANALYSIS

The thermocouples coupled with the Data acquisition system were calibrated initially. The uncertainties in the thermocouple readings were then transmitted through to the Nusselt number readings, which are displayed in the plots. A compendium of the uncertainty analysis is presented below. As an example, for the uncertainty in upper plate temperature :

$$\delta(T_{upper}) = \sum_{i=1}^n \left| \delta T_i \frac{\partial T_{upper}}{\partial T_i} \right|$$

$$\delta(T_{upper}) = \frac{1}{n} \sum_{i=1}^n \delta T_i$$

$$\Rightarrow \delta(\Delta T) = |\delta T_{upper}| + |\delta T_{lower}|$$

For the uncertainty in “h”, the heat transfer coefficient:

$$h_{exp} = \frac{Q}{A\Delta T}$$

$$\delta(h_{exp}) = \left| \delta\Delta T \frac{\partial h_{exp}}{\partial \Delta T} \right|$$

$$\delta(h_{exp}) = \left| h_{exp} \frac{\delta(\Delta T)}{\Delta T} \right|$$

Which in turn infects the Nusselt number as follows:

$$Nu = \frac{h_{exp} D}{K}$$

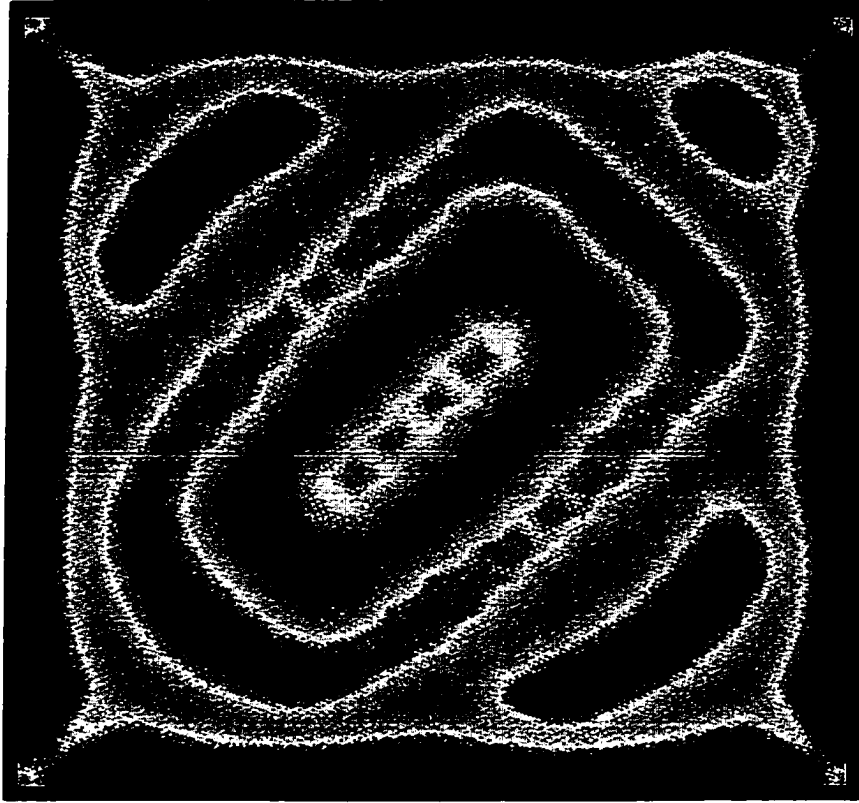
$$\delta(Nu) = \left| \delta h_{exp} \frac{\partial Nu}{\partial h_{exp}} \right|$$

$$\delta(Nu) = \left| \delta h_{exp} \frac{D}{K} \right|$$

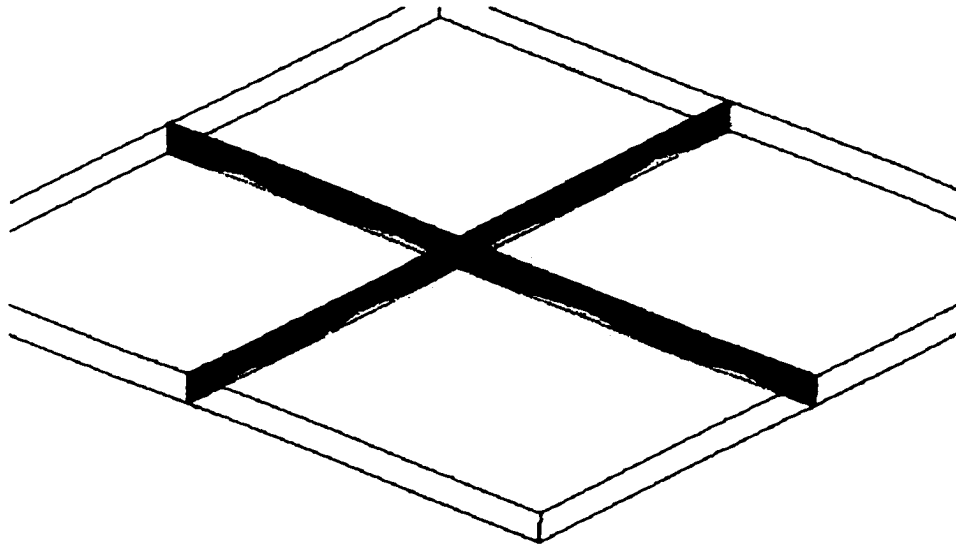
APPENDIX – C
NUMERICAL RESULTS

Cavity Depth 0.25 in

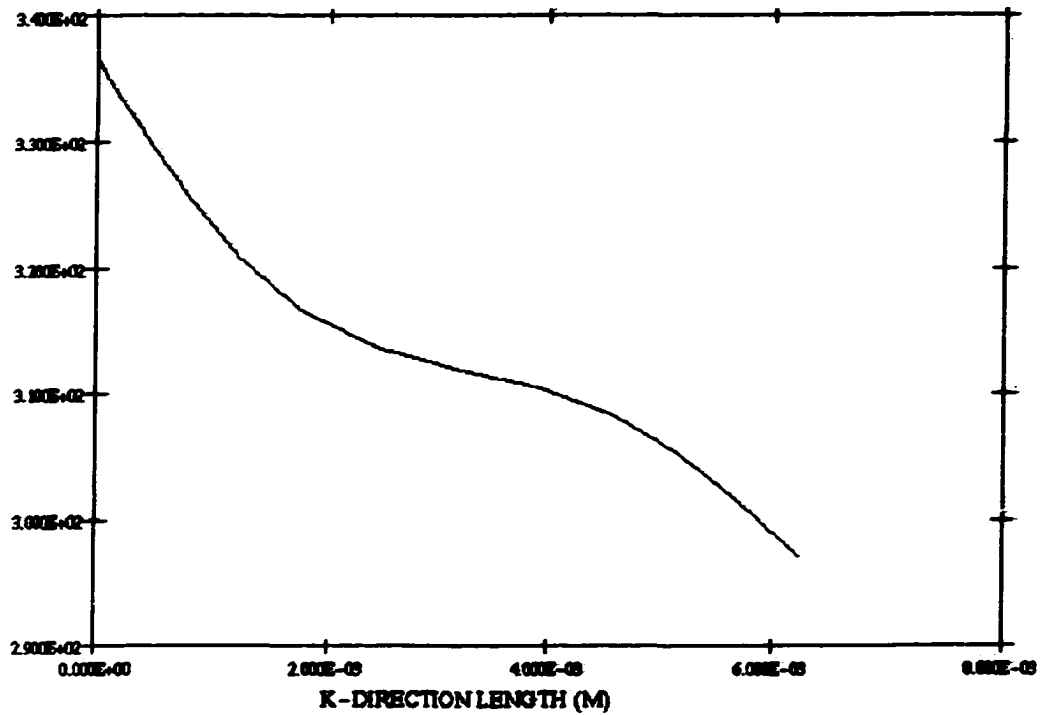
Rayleigh No $\sim 10^4$



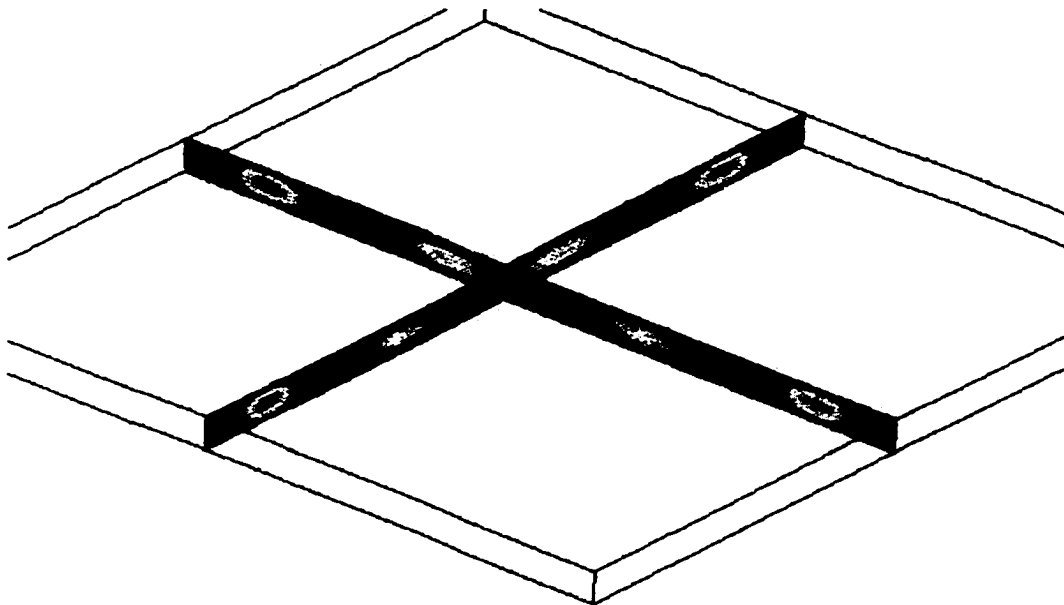
Temperature contours on the lower surface of the cavity. Since the boundary condition is Iso-flux, the temperature on the surface arranges itself to best transport the energy.



Temperature contours along the midsection of the cavity. The instability in the fluid layer can be inferred from the thermals that can be clearly observed in the cavity ($Ra \sim 10^4$).



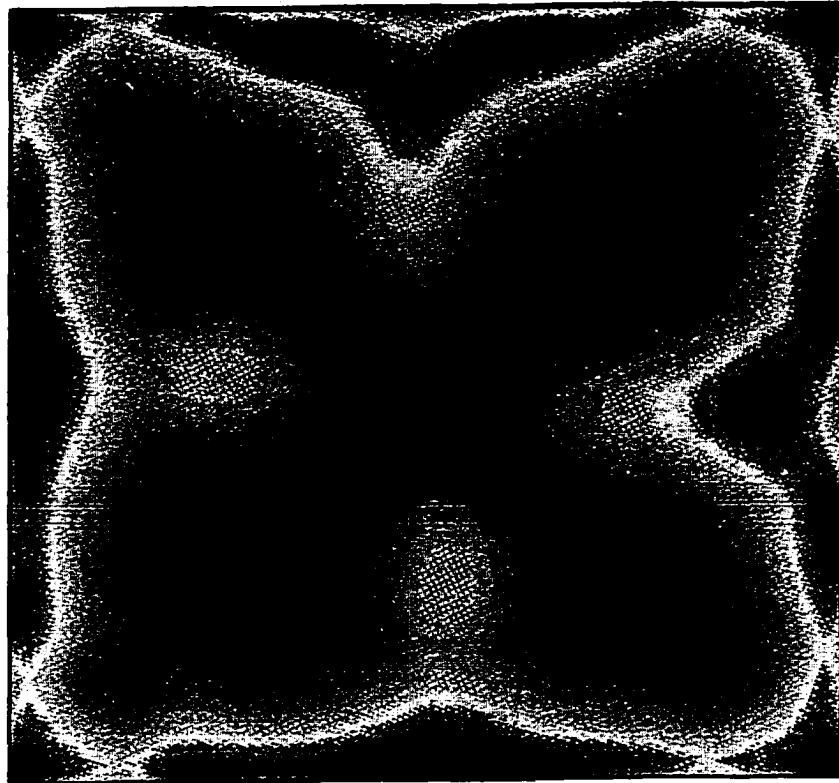
Temperature profile (deg K) through the midsection of the cavity.



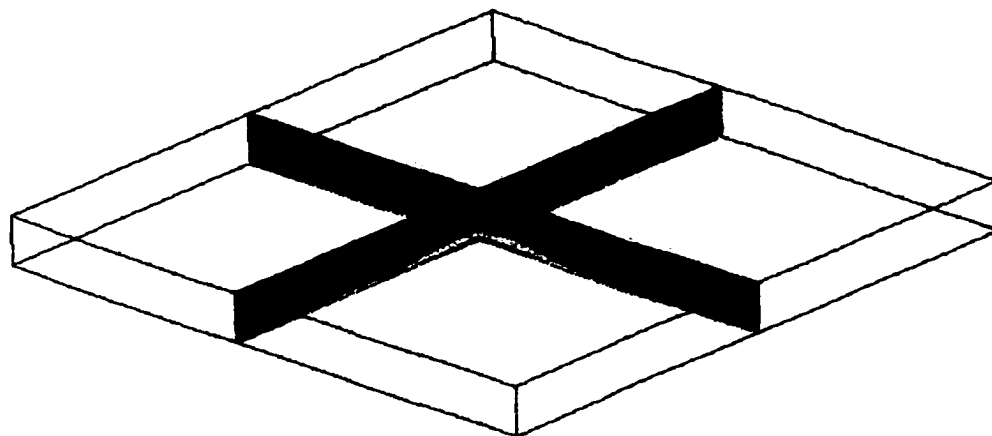
Contours of the vertical velocity (W component) in the cavity showing Beynard cells

Cavity Depth 0.5 in

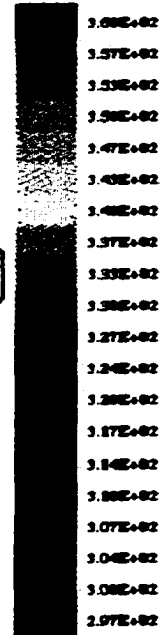
Rayleigh No $\sim 10^5$

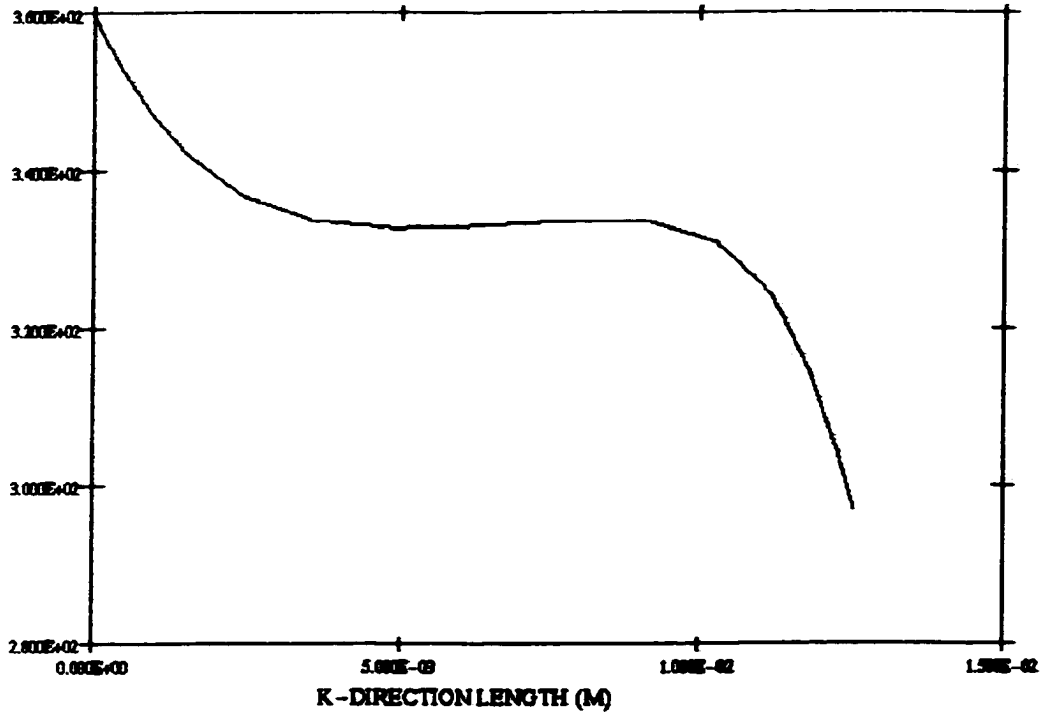


Temperature contours on the lower surface of the cavity.

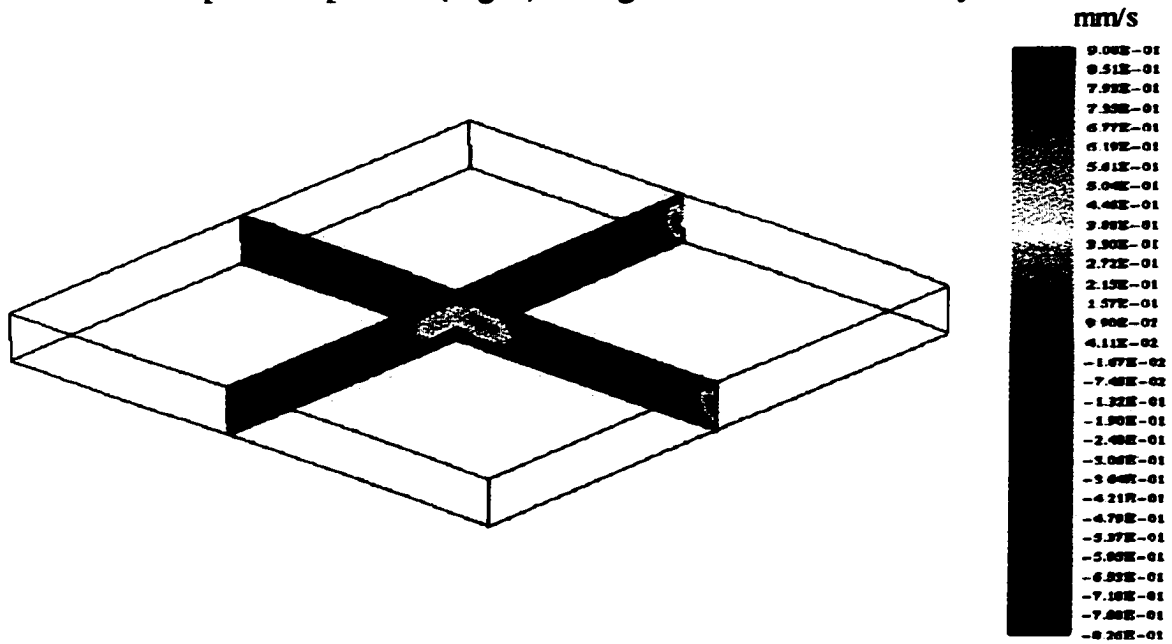


Temperature contours along the midsection of the cavity.





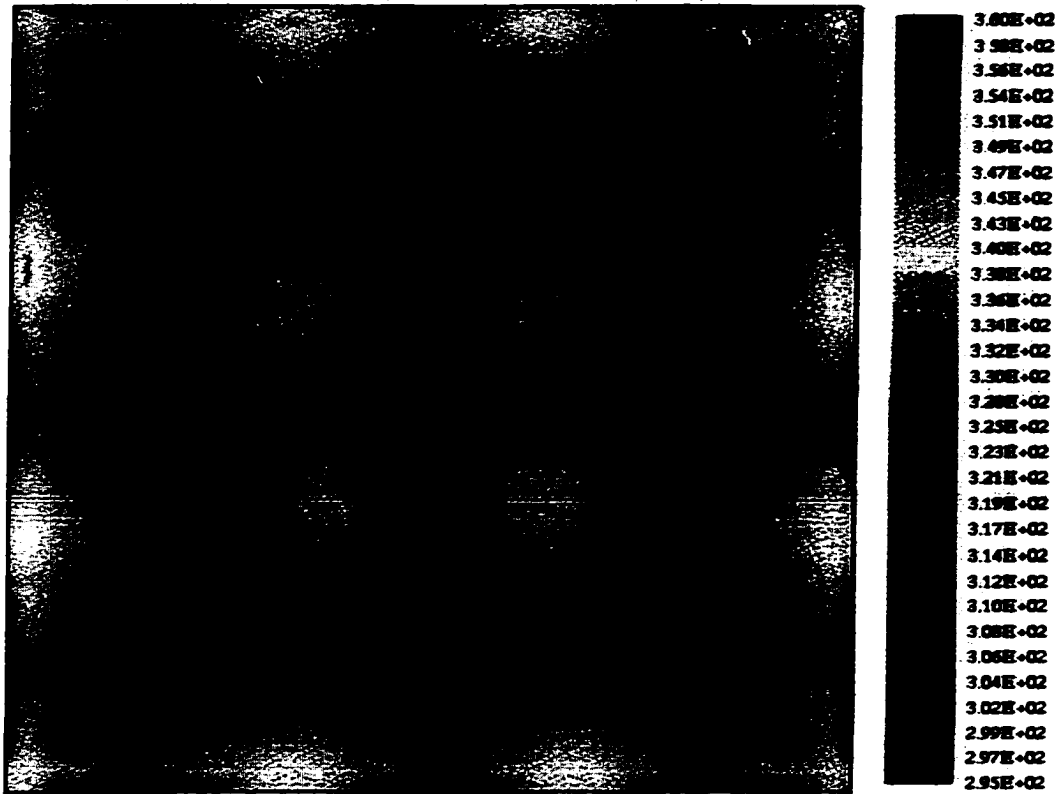
Temperature profiles (deg K) through the center of the cavity



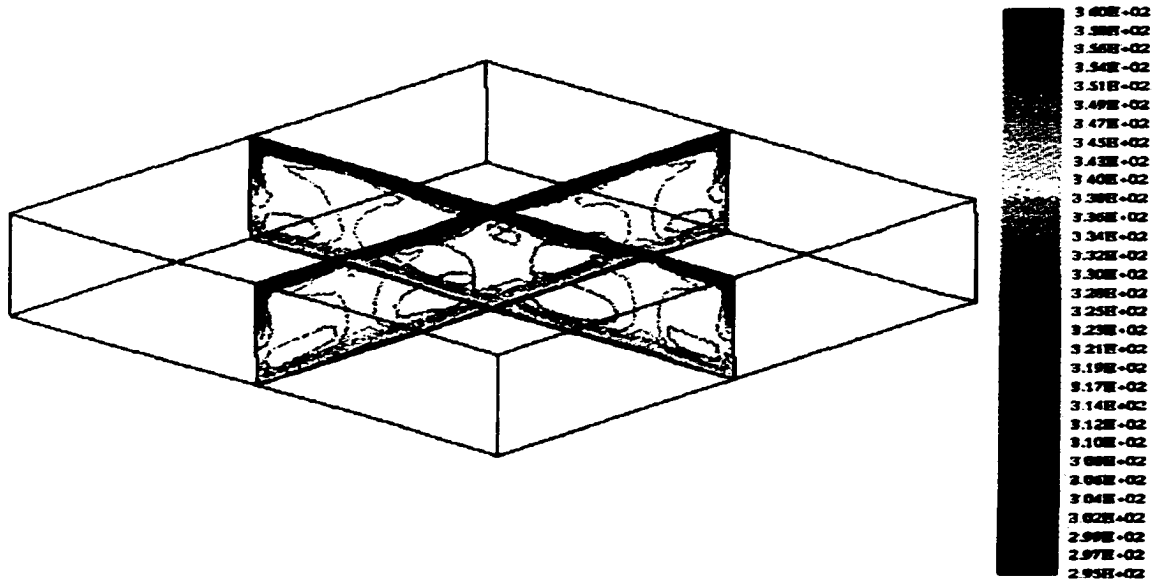
Contours of the vertical velocity (W component) in the cavity

Cavity Depth 1 in

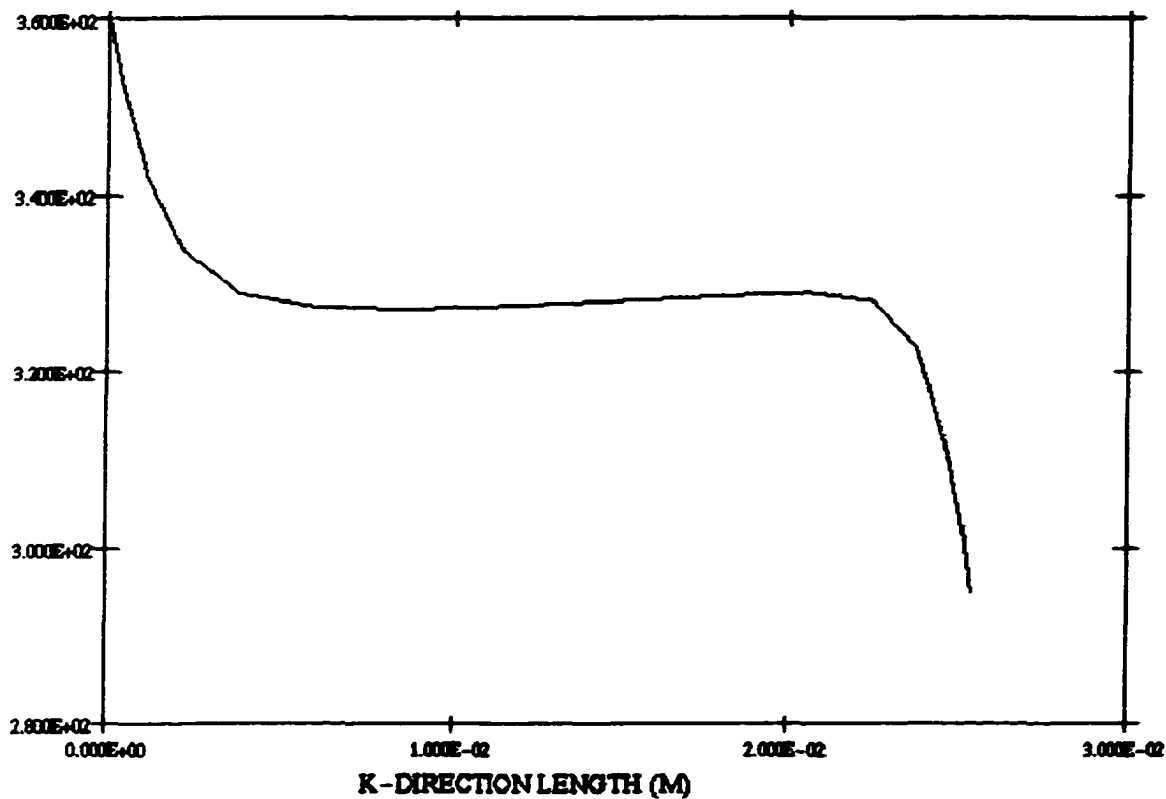
Rayleigh No $\sim 10^6$



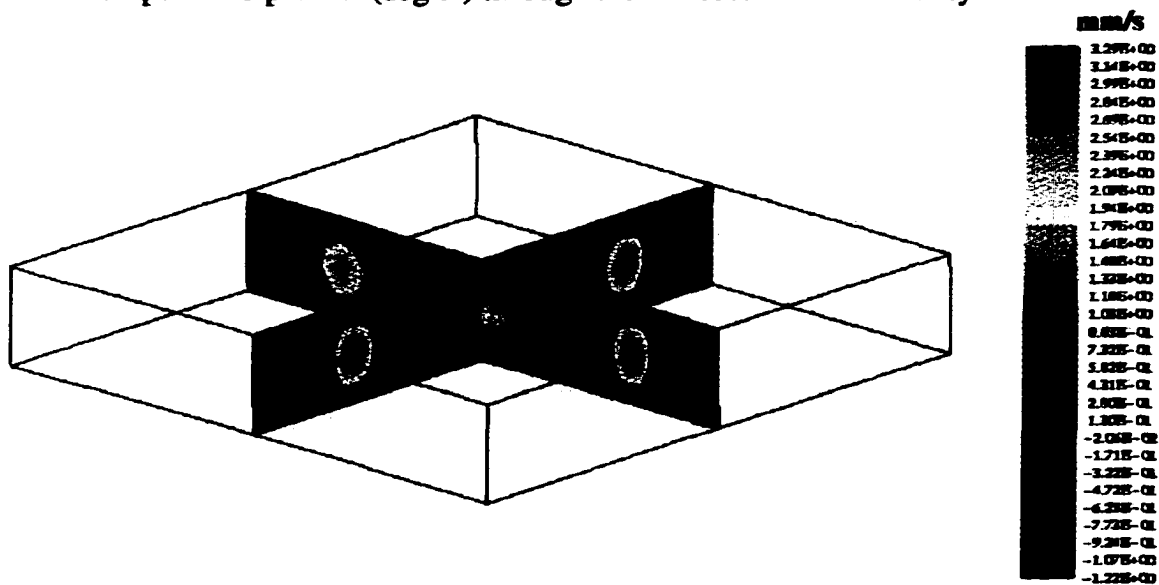
Temperature contours on the lower surface of the cavity.



Temperature contours along the midsection of the cavity. The rising thermals in the cavity can be seen as the mushroom shaped contours rising from the hot plate.



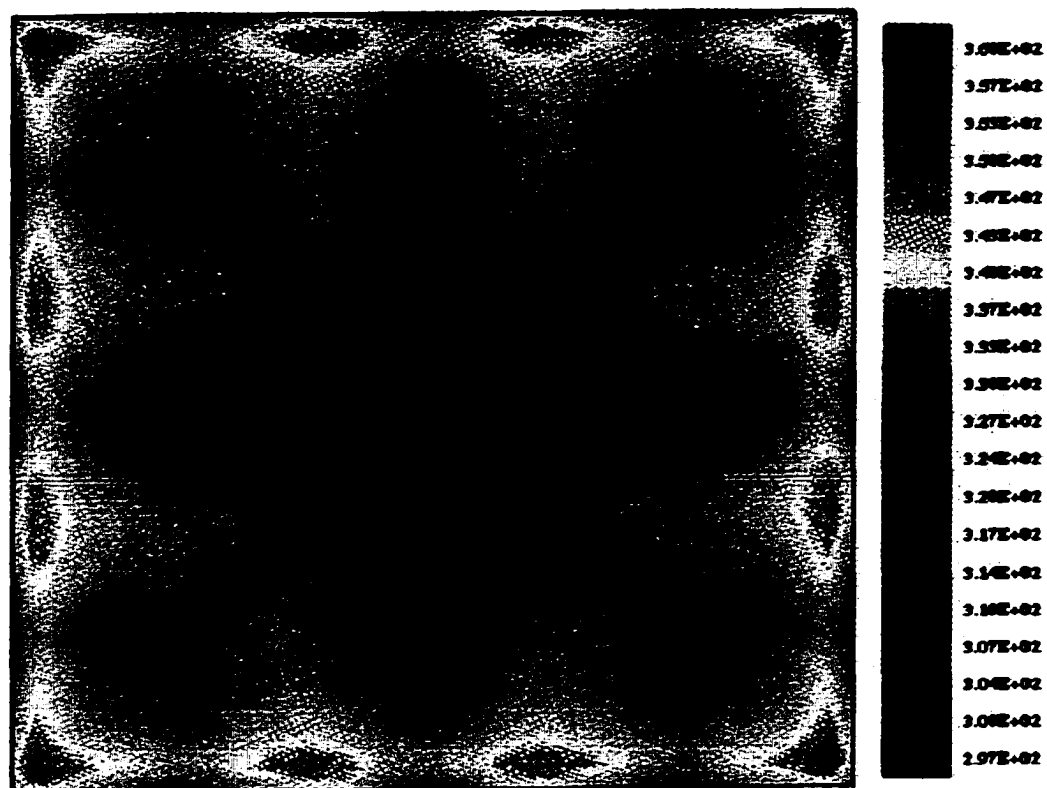
Temperature profile (deg K) through the midsection of the cavity.



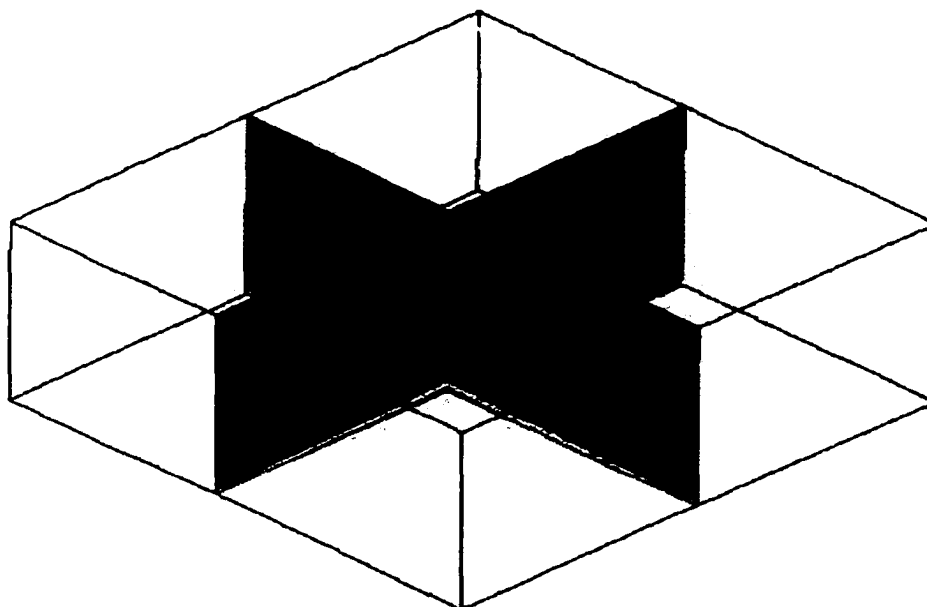
Contours of the vertical velocity (W component) in the cavity showing the cells formed. Notice the reduction in the number of cells formed.

Cavity depth 2 in

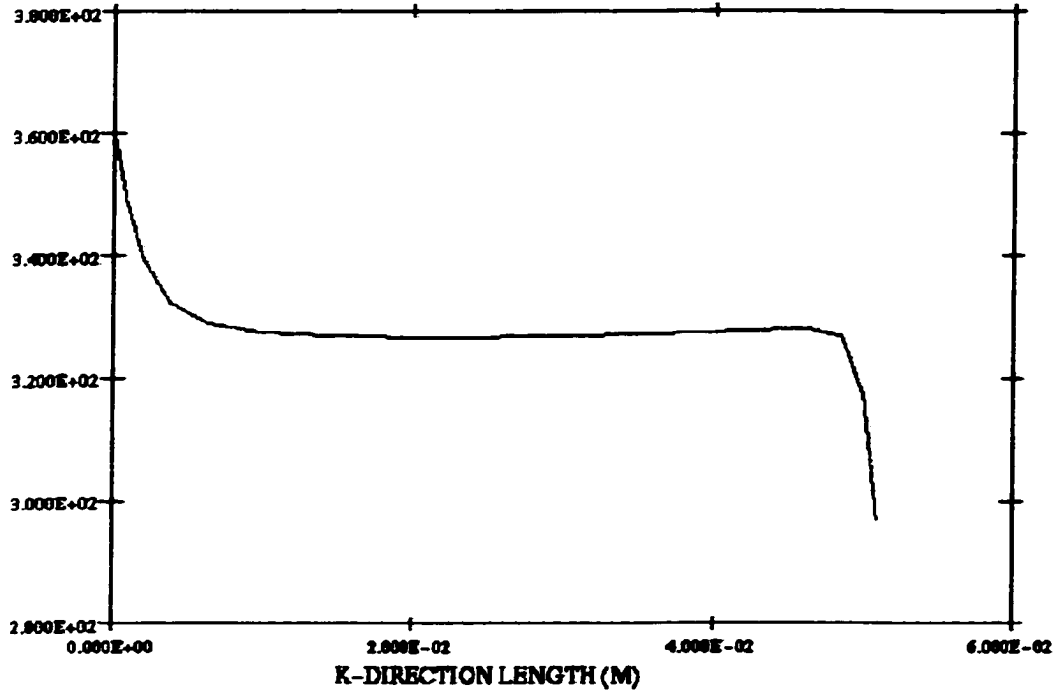
Rayleigh No $\sim 10^7$



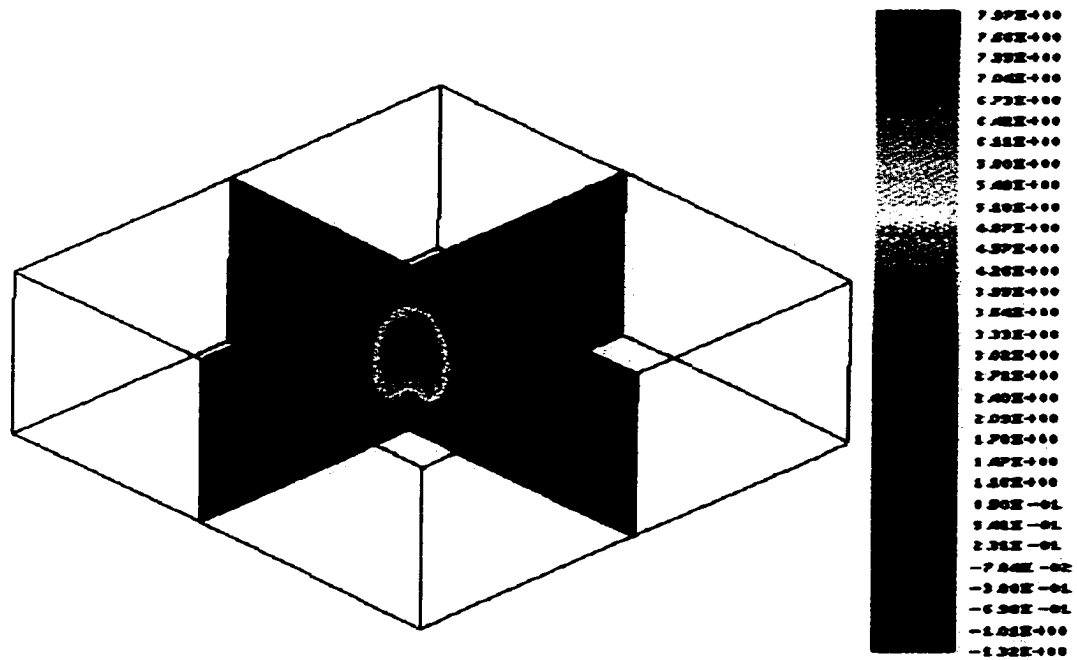
Temperature contours on the lower surface of the cavity



Temperature contours (filled and unfilled) along the midsection of the cavity.



Temperature profile (deg K) through the midsection of the cavity.

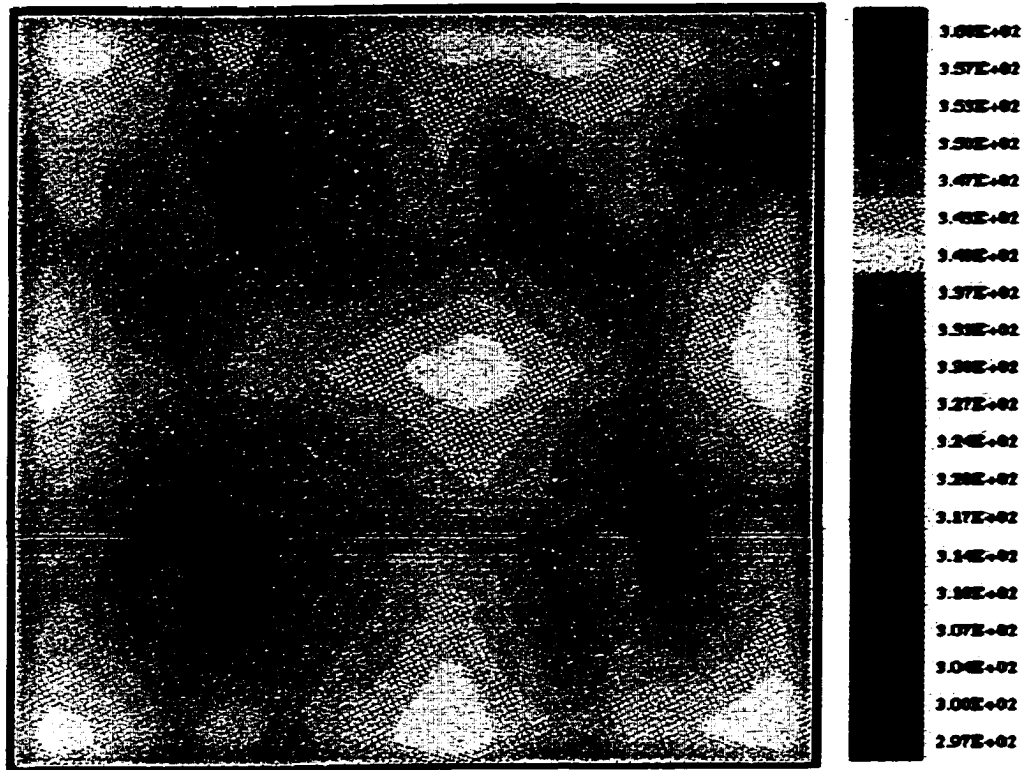


Contours of the vertical velocity (W component) in the cavity showing the cells formed.

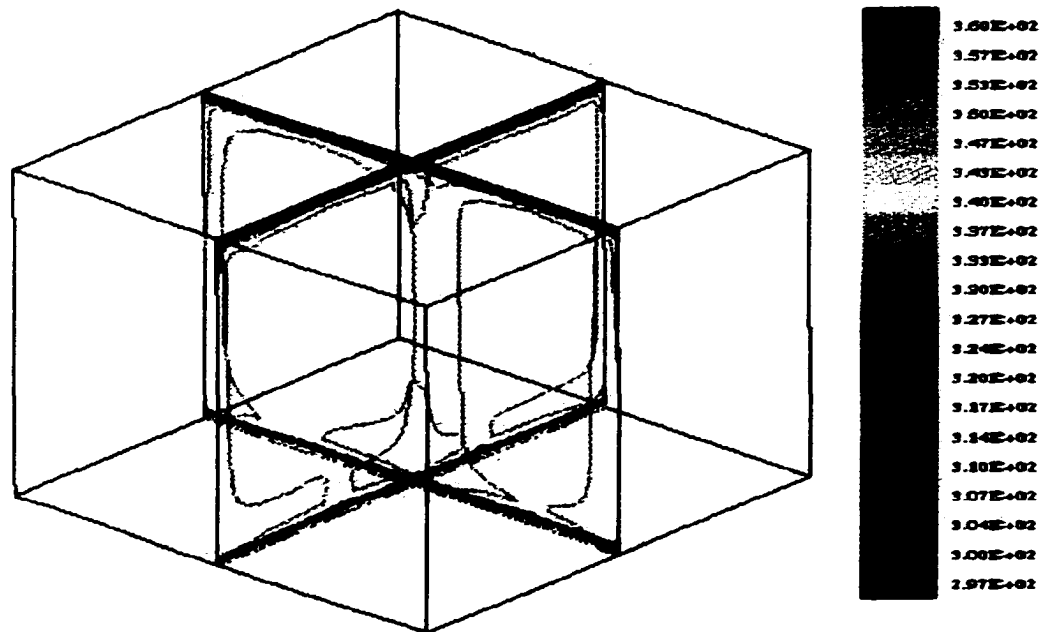
Notice the reduction in the number of cells formed

Cavity Depth 4 in

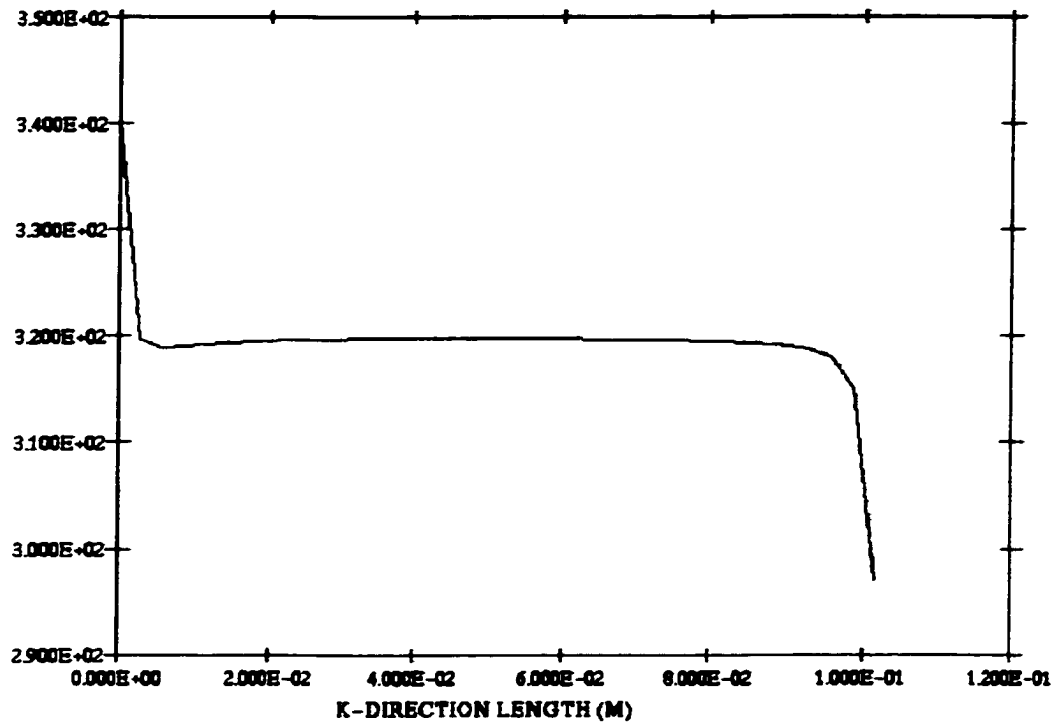
Rayleigh No $\sim 10^8$



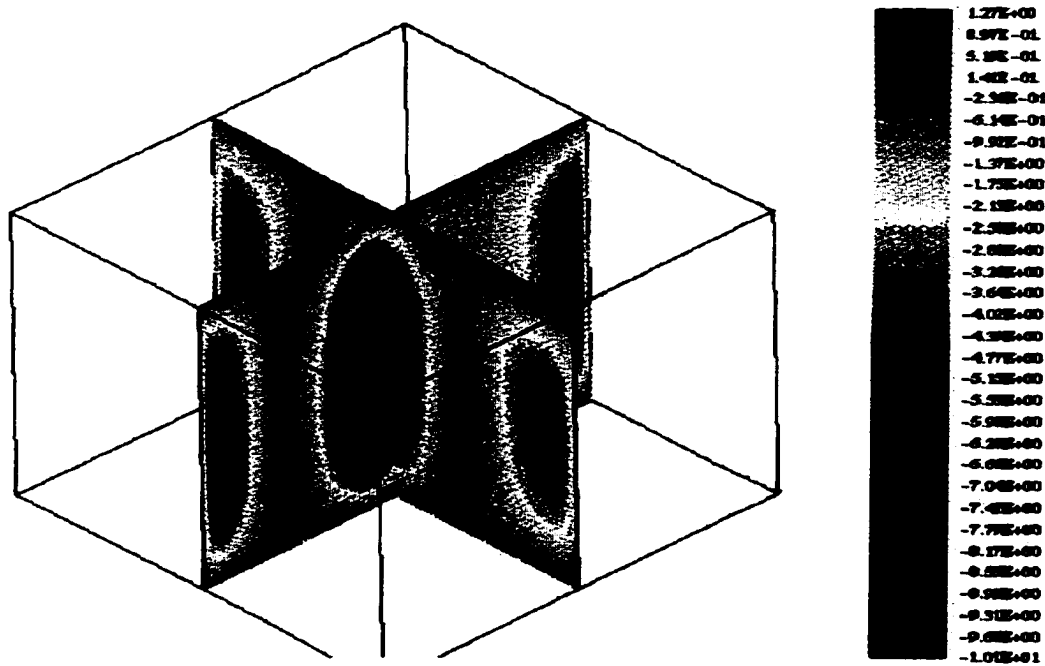
Temperature contours on the lower surface of the cavity.



Temperature contours along the midsection. Clearly, the core is at the bulk temperature



Temperature profile (deg K) through the midsection of the cavity.



Contours of the vertical velocity (W component) in the cavity

ABSTRACT

NATURAL CONVECTION HEAT TRANSFER IN A RECTANGULAR ENCLOSURE WITH SUSPENSIONS OF MICROENCAPSULATED PHASE CHANGE MATERIALS: A PARAMETRIC STUDY.

By

PARTHA DATTA

December 1999

Advisors: Dr. Subrata Sengupta
Dr. Trilochan Singh
Major: Mechanical Engineering
Degree: Doctor of Philosophy

The present work investigates the heat transfer enhancing capability of phase change slurries in natural convection, in rectangular enclosures heated from below. The working fluid used, was a suspension of phase change microcapsules. The vertical walls of the test section are insulated, the lower horizontal wall is a constant heat flux surface and the upper wall is isothermal. The work quantifies the heat transfer rate in parameter ranges hitherto not investigated ($\Delta Ra \sim 10^4$ and $\Delta Ste \sim 10^2$).

The results indicate a significant potential for enhancing the heat transfer rate using phase change slurries. Heat transfer rates increased by as much as 110% with low concentration slurries. The enhancement in heat transfer is strongly influenced by the conductivity ratio of the two phases, the quality of the suspension and the Rayleigh number range. Analysis also reveals that less than 3% of the total phase change material

in the slurry at any time actually melted. Idealized estimates indicate that even in the best designed slurries, the very design of the phase change slurry ensures that approximately half the phase change material in a capsule cannot be utilized. Correlations quantifying the Nu variation with Ra and Ste have been developed.

AUTOBIOGRAPHICAL STATEMENT

Partha Datta was born in Calcutta, India on November 4th 1967 to KumKum Datta. He received his elementary education in St. Aloysious Anglo Indian High School, Visakhapatnam, India. In June 1983, he entered Timpany School for his Higher Secondary Education. He earned his Indian Secondary Certificate in 1985.

In September of 1985 he joined the Gandhi Institute of Technology and Management, of Andhra University, from which he was conferred the degree of Bachelor of Engineering (B.E.) in Mechanical Engineering in May 1989.

In August 1989, he was admitted to the Graduate School at the College of Engineering, University of Miami - Coral Gables. He moved to Michigan in the Fall of 1990, where he continued to work on his research (located at the University of Michigan-Dearborn). He was awarded the Degree of Master of Science in Mechanical Engineering from University of Miami in the fall of 1992.

Partha joined the department of Mechanical Engineering at Wayne State University in Fall 1992 and became a Doctoral Candidate in 1994. He was awarded a Ph.D. in December 1999.

Married to Somlika Gill Datta on Jan 4th 1995, he now lives in Southfield, Michigan, with his wife and daughter Amisha.